KfK 3143
April 1981

An International Intercomparison of Results for the Reactivity Effect of Steam Ingress into the Core of a Gas-Cooled Fast Reactor

E. Kiefhaber, J. Braun
Institut für Neutronenphysik und Reaktortechnik
Projekt Schneller Brüter

Kernforschungszentrum Karlsruhe

KERNFORSCHUNGSZENTRUM KARLSRUHE
Institut für Neutronenphysik und Reaktortechnik
Projekt Schneller Brüter

KfK 3143

An International Intercomparison of Results for the Reactivity Effect of Steam Ingress into the Core of a Gas-Cooled Fast Reactor

E. Kiefhaber, J. Braun

Kernforschungszentrum Karlsruhe GmbH, Karlsruhe

Kernforschungszentrum Karlsruhe GmbH
ISSN 0303-4003

Abstract

Steam ingress into a GCFR core may lead to reactivity effects which are undesirable from the point of view of reactor safety. The amount of reactivity increase caused by a certain steam concentration is usually subject to some uncertainty as has become evident by occasional comparisons between different laboratories for specific examples. The aim of the present intercomparison is to determine and compare on an international basis the influence of different nuclear data sets and various calculational methods on the predicted steam ingress reactivity by means of simple fundamental mode neutronic calculations, thus avoiding any ambiguity and complexity with respect to the geometric modelling of a given experimental or design arrangement. The material compositions chosen as some kind of benchmarks differ in: plutonium isotopic composition, fission product concentration, absorber material concentration, fuel temperature and size of the core. From previous experience these parameters are expected to have a significant influence on the calculated steam density reactivity coefficient. Other probably less important design parameters have not been varied in the present study.

The analysis of the results obtained from laboratories in France (Cadarache), Germany (KfK), Japan (JAERI), Switzerland (EIR Würenlingen), and USA (ANL) shows that there still exist considerable deviations in the predicted steam ingress reactivity effect essentially caused by differences in the nuclear data basis used. A detailed evaluation of the results of corresponding perturbation calculations reveals that the observed discrepancies may be considered as not too surprising because there is a large cancellation of positive and negative contributions to the degradation - or moderation - term coming from different energy regions. Since this term is usually the dominating individual term, especially at low steam densities, it is obvious that small changes of partial components may lead to large relative changes for the total value.

In order to explain in a quantitative way the most important discrepancies observed between the results of the various laboratories participating in the present study, a closer examination of the nuclear data sets involved in this intercomparison would be necessary probably supplemented by a careful evaluation or re-evaluation of the nuclear data forming the basis of the data sets involved. A somewhat restricted sensitivity study concerning the influence of nuclear data changes is presented in an appendix to the present report. A more refined treatment of that kind would give a better insight as to which nuclear data in which energy range are most significant for the steam ingress reactivity effect and which accuracy and reliability can be expected for or probably attributed to the prediction of this quantity if one assumes reasonable values for the presently existing nuclear data uncertainties. Furthermore an intercomparison activity like the present one could be repeated or continued with the emphasis of using more modern nuclear data, e.g. based on ENDF/B-V or KEDAK-4. If sufficient agreement has eventually been obtained for this kind of simple benchmarks, an extension to more complicated examples

including heterogeneity- and streaming-effects would be desirable. Finally it may be concluded from the present study that, due to existing uncertainties in predicting steam ingress reactivity, it may be adequate to measure this quantity in several critical assemblies if they are characterized by major differences in their material composition and/or geometric arrangement of their components. This may apply to GCFR criticals as well as to LMFBR criticals because the reactivity effect of an entry of lubricating oil into a LMFBR core is similar to that of a steam ingress into a GCFR core.

Ergebnisse eines internationalen Vergleichs der berechneten Reaktivitätseffekte für den Dampfeinbruch in den Kern eines gasgekühlten schnellen Reaktors

Zusammenfassung

Der Dampfeinbruch in das Core eines GCFR's (Gas Cooled Fast Reactor) kann zu Reaktivitätsänderungen führen, die im Hinblick auf die Reaktorsicherheit unerwünscht sind. Das Ausmaß der von einer bestimmten Dampfkonzentration verursachten Änderung kann im allgemeinen nur mit einer gewissen Unsicherheitsspanne angegeben werden, wie einige stichprobenartig vorgenommene Vergleiche in der Vergangenheit gezeigt haben. Durch den vorliegenden internationalen Vergleich der Dampfdichte-Reaktivitätskoeffizienten soll mit Hilfe nulldimensionaler Rechnungen festgestellt werden, welchen Einfluß eine unterschiedliche nukleare Datenbasis auf die vorherzusagenden Reaktivitätswerte hat. Durch die Wahl eines derart einfachen Rechenmodells können mögliche Komplikationen durch einen in der Realität komplizierten geometrischen Aufbau des Reaktors vermieden werden. Die für den Vergleich ausgewählten Materialzusammensetzungen können als eine Art Benchmarks angesehen werden. Die einzelnen Mischungen unterscheiden sich in folgenden wesentlichen Merkmalen: Plutonium-Isotopenzusammensetzung, Spaltproduktkonzentration, Absorbermaterialkonzentration, Brennstofftemperatur und Größe des Reaktors. Aufgrund früherer Erfahrungen ist zu erwarten, daß damit die Haupteinflußgrößen des Reaktorentwurfs erfaßt werden konnten. Mit Rücksicht auf den Umfang der Studie wurden keine weiteren Einflußgrößen berücksichtigt und die Zahl der Parameterkombinationen stark eingeschränkt.

Die von fünf verschiedenen Forschungseinrichtungen - Deutschland (KfK), Frankreich (Cadarache), Japan (JAERI), Schweiz (EIR Würenlingen), USA (ANL) - eingesandten Beiträge zeigen, daß zur Zeit aufgrund der unterschiedlichen nuklearen Datenbasis noch erhebliche Abweichungen in den vorhergesagten Reaktivitätseffekten vorhanden sind. Eine eingehendere Betrachtung der Ergebnisse zugehöriger Störungsrechnungen verdeutlicht, daß derartige Differenzen nicht als allzu überraschend angesehen werden sollten: der Degradations- oder Moderationsterm, der meist den Hauptbeitrag zur Reaktivitätsstörung liefert, setzt sich aus etwa gleich großen positiven und negativen Beiträgen (in verschiedenen Energiebereichen) zusammen. Daher können kleine Änderungen der Einzelbeiträge ziemlich große relative Änderungen des Gesamteffektes bewirken.

Die genaue Ursache für die beobachteten Unterschiede in den berechneten Dampfdichte-Koeffizienten könnte nur durch eine sorgfältige und langwierige Analyse der verwendeten nuklearen Datensätze festgestellt werden. Im Anhang werden die Ergebnisse einer Empfindlichkeitsstudie von beschränktem Umfang gezeigt, um einen ersten Eindruck von den Auswirkungen von Kerndatenänderungen zu vermitteln. Eine ausführlichere und verbesserte Behandlung würde genauere Hinweise darüber liefern, welche Kerndaten in welchem Energiebereich besondere Bedeutung für den berechneten Dampfdichtekoeffizienten besitzen und es erlauben, die aufgrund der gegenwärtig noch vorhandenen Kerndatenunsicherheiten zu

erwartende Genauigkeit und Zuverlässigkeit der Vorhersage dieser Werte abzuschätzen.

Eine Fortsetzung der vorliegenden Vergleichsuntersuchungen könnte stärkeres Gewicht legen auf die Benutzung modernerer Kerndaten-information, z. B. basierend auf ENDF/B-V und KEDAK-4. Schließlich könnten die Untersuchungen erweitert werden auf kompliziertere Beispiele, bei denen eine realistischere geometrische Modellierung und damit verbunden die Berücksichtigung von Heterogenitäts- und Streaming-Effekten angestrebt werden sollte.

Aufgrund der bei diesem internationalen Vergleich gefundenen Ergebnisse und der noch erstaunlich großen Unsicherheit in der Vorhersage des Dampfdichte-Koeffizienten für geometrisch einfache Rechenmodelle sollte der Aufwand und die Zweckmäßigkeit geprüft werden, diese Größe in mehreren kritischen Anordnungen zu messen, falls diese erhebliche Unterschiede in ihrer Materialzusammen-setzung und/oder ihrem geometrischen Aufbau aufweisen. Neben einem erweiterten Test der nuklearen Datenbasis und der verwendeten Rechenmethoden würde dies eine umfassendere Einschätzung der Unsicherheitsspannen ermöglichen, die bei Auslegungsrechnungen und Sicherheitsuntersuchungen in Betracht zu ziehen sind. Da der Reaktivitätseffekt des Eindringens von wasserstoffhaltigen Ölen in das Core eines schnellen natriumgekühlten Reaktors ähnlich ist demjenigen des Dampfeinbruchs in einen gasgekühlten schnellen Reaktor, betrifft die obige Schlußfolgerung kritische Anordnungen für beide Reaktortypen.

CONTENTS

I) Introduction

During the past years considerable effort was devoted to the study of the reactivity effect of a postulated, possibly hypothetical steam ingress into the cooling channels of a Gas Cooled Fast Reactor (GCFR). The problem associated with this safety-related reactivity variation caused by a possible steam ingress arises if one assumes that - due to a break in the heat exchanger or leak in the steam generator - considerable amounts of steam leak from the secondary (water) cooling circuit into the primary (gas) circuit of a GCFR. The work of Fortescue /1/ was probably among the earliest dealing with that subject. Later, Eisemann /2,3/ performed similar studies of this effect for the German design of a GCFR. Results of the continuing interest of General Atomic in that problem are reported e.g. in /4/. For those interested in a historical review, illustrative remarks concerning this topic can be found on p. 2 of /4a/, which also contains a useful list of references. The possible consequences caused by the reactivity effect due to steam entry into a GCFR core are indicated in the chapter "perspective on the safety impact of steam ingress" on pp. 14 of the same report /4a/. Just recently, Iijima et al. /5/ published a study for the Japanese 1000 MWe GCFR dealing especially with the influence of the heterogeneity effect on the calculated steam entry reactivity.

In addition to theoretical studies for specific power reactor designs, several experimental investigations in various countries provided information about the measured magnitude of equivalent effects and about the capability and reliability of calculational tools to accurately predict the corresponding reactivity changes. The investigations /6/ at EIR, Switzerland, in the PROTEUS mixed fast-thermal critical assembly were designed to give an early assessment of steam worth and to complement subsequent more extensive Argonne measurements. Steam was simulated in PROTEUS in the form of polystyrene beads, in the corresponding ANL experiments by slabs of polyethylene (CH_2) foam. Several publications during 1976 - 1977 (e.g. in Trans. Am. Nucl. Soc.)

deal with these experimental studies which were evaluated in a cooperation between ANL and GA. Some more detailed relevant information may be found e.g. in references /7/ to /12/.

A situation comparable to the steam entry into a GCFR core lattice can be imagined if one assumes as a hypothesis that hydrogenous material such as lubricating oil from the circulating pumps were accidentally introduced into the core region of a Liquid Metal Cooled Fast Breeder Reactor (LMFBR). According to the temperature and pressure of the coolant and the boiling point of the oil this material may enter the core region in liquid or gaseous form. An analysis of corresponding simulation experiments in ZEBRA cores has been published recently by Ingram and Sweet /13/. The density of the simulation material hydrocarbon, which was inserted in the form of polythene or polypropylene plates, ranged up to 200 g/l thus exceeding the densities of interest for a commercial fast reactor (CFR) where the maximum hydrogen worths have been found for a density of about 100 g/l. In /13/ calculations have been made for a 1200 MWe CFR assuming that three quantities of oil (8, 40 and 160 kg of hydrocarbon, equivalent to volumes of 10, 50 and 200 litres of oil which extend the examined range well beyond that likely to be achieved in practice) are replacing sodium at carefully selected sites in the reactor core chosen to maximize the reactivity increase. The corresponding reactivity worths have been determined to be + 0.4 %, + 1.7 % and + 4.2 % dk/k, respectively.

With respect to calculational methods used in the evaluation of experiments and subsequently in the prediction of the behavior of power reactor, Greenspan was possibly the first who indicated that the application of a few group structure, i.e. using a coarse subdivision of the neutron energy scale, could lead to appreciable discrepancies in calculated reactivity worths of predominantly scattering materials of light or medium mass. In his study /14/ for GODIVA, a small critical assembly with a hard neutron spectrum, he has shown that the application of the conventional flux-averaging scheme may lead to severe errors in the few group results for the material worth of hydrogen compared to reliable

results obtained when treating in appropriate detail the energy dependence of all quantities involved in the perturbation expression. This significant influence of the group structure, i.e. the subdivision of the energy or lethargy scale, called "in-group spectral effect" by Greenspan, is attributed to distortions of the few group adjoint spectrum if the usual flux weighting is used for group collapsing as has also been shown in a subsequent study by Kiefhaber /15/.

Both studies /14, /15/ were stimulated by the work of Pitterle /16/, who was probably the first to examine in detail the merits of bilinear averaging for multigroup diffusion theory calculations. Although this method was already described earlier in the literature, Pitterle's publication clearly demonstrated that such a procedure - besides other advantages - leads to adequate average few group constants to be used in perturbation calculations. Subsequently, several authors have investigated the influence of various weighting schemes and the effect of using different approximations to the weighting functions, e.g. regarding the conservation of the adjoint neutron spectrum or the conservation of perturbation theory results. Those readers interested in the development may find many useful references in the fairly recent publications of Greenspan /17/ and Wade and Bucher /18/. In addition to the preceding remarks concerning calculational methods it should be mentioned, that the heterogeneity effect and the related influence of the anisotropy of diffusion constants are often quite important for the realistic nuclear analyses of GCFR cores as e.g. shown in /5/ and /19/.

In 1976, the time when the present fundamental mode GCFR steam entry benchmark was originally suggested, there existed considerable uncertainty concerning the sign of the GCFR steam entry reactivity effect. Part of the uncertainty may have been caused by equivocal or disagreeing assumptions with respect to the type of reactor studied, as regards the size, the burn-up state, the plutonium isotopic composition (especially the relative concentrations of ^{240}Pu and ^{241}Pu), the fuel temperature, the presence of

control rod poison, the amount of steam introduced etc. Therefore it seemed quite helpful to define some simple fundamental mode benchmarks which could be used as a common uniform data reference for an international intercomparison. Since the material composition and the geometric buckling are specified as input data, this exercise should mainly reveal the influence of different nuclear data sets employed in the calculations. Quite naturally the conclusions to be drawn from the present intercomparison of fundamental mode results are of restricted validity. Primarily this is due to approximations (a) in treating the leakage term which is usually highly dependent on the modelling of the core (e.g. we kept constant the value of B^2 for simplicity reasons) and (b) in the methods of preparing group cross-sections including heterogeneity effects and anisotropic neutron diffusion constants. The deliberate acceptance of a simplified problem results in the advantage of having available analyses differing only in the nuclear data set used, thus avoiding ambiguities in the modelling of the geometric configuration and in the interpretation of particular results. Of course, more insight and confidence with regard to the ability of reliably predicting steam entry effects will be gained by corresponding analyses of actual experiments. However, this requires a much larger effort than that devoted to the present type of zero-dimensional benchmark calculations. Nevertheless, the present results are useful in demonstrating tendencies, i.e. the influence of the reactor size, the plutonium isotopic composition, the fuel temperature, the presence of absorber or fission product poison on the steam ingress reactivity. Moreover they could establish a better basis for advanced intercomparisons related to more realistic problems.

Besides the Kernforschungszentrum Karlsruhe, Germany, represented by the authors of this report, who were responsible for the benchmark proposal and the evaluation of the results, the following countries (laboratory / scientists in charge) contributed to the intercomparison:

France (Cadarache / J. Soulié, J. Courchinoux, J. Y. Barré)
Japan (JAERI Tokai-mura / J. Hirota)
Switzerland (EIR Würenlingen / C. McCombie, R. Richmond)
USA (ANL Chicago / L. LeSage, C. E. Till)

Unfortunately GA was not able to make a timely contribution to the benchmark which would have been especially valuable because recent GA steam worth calculations (e.g. /11/, /12/) compare favourably with measured results from ANL critical experiments thus verifying the adequacy of the calculational techniques applied in the GA analysis. To a certain extent a GA participation might have provided some kind of a reference solution. Due to the lack of such a firm basis, the present intercomparison can not assess the absolute quality of the solutions obtained from the various laboratories but only make evident the fairly big relative differences in the steam ingress reactivity calculated with different nuclear data sets.

Due to the late delivery of results of some participating laboratories, partially caused by a hindrance in data transmission, the evaluation could not be published as early as intended at the outset of the intercomparison.

IIa) Characterization and Specification of the Benchmark Compositions

It was the basic intention that the neutronic calculations for the present GCFR Steam Entry Benchmark should use a very simple model to avoid possible complications which may arise for space dependent problems with optional inclusion of heterogeneity and streaming effects. Therefore, a fundamental mode model is suggested using a buckling value B^2 which is kept constant during the variation of the steam density.

It is well known from previous publications, (some of them may be found in the references and in the literature mentioned there) that the reactivity effect to be determined is strongly influenced by several parameters. We tried to include the most important ones in the specifications of the present benchmark problems:

- o Plutonium isotopic composition
- o Fission product concentration
- o Fuel temperature
- o Absorber material concentration
- o Size of the core

Several other parameters influencing the reactivity effect to be considered are not varied at the present time to keep the number of benchmarks reasonably small. Such parameters could be: pitch to diameter ratio p/d of the lattice ($\hat{=}$ volume fraction of the coolant), type of structural and cladding material, etc.. For the same reason it is suggested that, for the present, the possible combinations of the parameters are kept small. The number of elements and isotopes taken into account is kept fairly small in order to facilitate intercomparison of the results of calculations with different nuclear data. The specificaitons of the 8 benchmark mixtures, labelled Bo - B7, which have been chosen for the present purpose are listed in Tables I and II. The reference case (Bo) of the benchmark-series is not too different from the hot core composition of the General Atomic 300 MWe demonstration plant

including fission products. Helium is omitted from the list of atomic number densities because its influence on neutronic characteristics is known to be fairly small. These characteristics are nearly identical with those of a completely voided reactor. The Pu-isotopic composition is varied twice (B1 and B2) to determine the influence of ^{240}Pu and ^{241}Pu separately. B3 represents a fresh core poisoned with ^{10}B in order to compensate for the reactivity gain obtained by removing the fission products when completely refueling the reactor. B4 shows the influence of a temperature variation. B5 represents a clean cold core mixture of a GCFR without absorber materials such as ^{10}B or fission products. Except possibly for the plutonium isotopic composition, B5 is not too different from mixtures used up to now in critical assemblies to study the characteristics of a GCFR. It is a modification of B4 obtained by replacing fission product pairs by ^{238}U. It is also similar to B3, the differences consisting in removing ^{10}B and in reducing the temperature. Compared to B0 the changes consist in substituting ^{238}U for the fission product pairs and reducing the temperature. Case B6 represents a clean, cold composition with a plutonium isotopic composition and a Pu/U ratio not too different from that used in the GCFR-Phase I ZPR-9-Assembly. The specifications for B6 therefore resemble fairly closely the corresponding experimental situations investigated so far. In agreement with the transition B0 → B5, Case B6 has been deduced from B1 by substituting ^{238}U for the fission products and reducing the fuel temperature. B7 is included to study the influence of halving the geometric buckling which may be considered as a crude approximation of a transition from a 300 MWe reactor to a 1000 MWe reactor.

In all cases B0 - B7 the number of heavy atoms has been kept constant (the fission product pairs (FFP) are comprised in the sum of heavy atoms). This means that the volume fractions of the various components of the composition are the same for all cases. Case B3, e.g., represents a fresh core with some absorber material inserted, whereas case B0 corresponds to a burn-up core in which the absorber material has been removed and replaced by coolant

which is neglected for the purpose of the present benchmark calculations.

The fission product pairs, which are equivalent to the number of fuel isotopes which have undergone fission, correspond to a fairly low average discharge burnup. This number may probably be representative only for the first few reactor cycles and will eventually increase later on.

The plutonium-isotopic composition chosen for the reference case roughly corresponds to plutonium reprocessed from PWR reactor fuel with fairly high burnup. It can be expected that mainly this kind of plutonium has to be used in the start-up phase of large fast breeder reactors before a characteristic fast reactor equilibrium plutonium isotopic composition has been established. The fuel temperature is chosen to be 1500 K. For all other materials the - admittedly unrealistic - temperature of 300 K should be applied for the sake of simplicity.

It was suggested to use a Maxwellian-type fission spectrum with an average energy of 2.115 MeV corresponding to the nuclear temperature Θ = 1.41 MeV. In case this specification leads to difficulties or complications of the calculations, the fission spectrum really applied in the calculations should be specified in the documentation of the results, which should also include a reference to the nuclear data basis or to the library of group constants and a description of the group structure used for the calculations.

The upper limit of the steam density to be considered for examining the effect of steam ingress into a GCFR core is taken to be about .05 g/cm^3 for the present evaluations. The number densities of Table II are proposed for the stepwise addition of hydrogen and oxygen to the core compositions, assuming a coolant volume fraction of about 50 % of the total core volume.

We have chosen a fairly large number of steam densities S0 - S19 which should be used in determining the reactivity effect of steam

Table I

Specifications of the Fundamental Mode GCFR-Steam Entry Benchmarks
(Atomic number densities given in atoms $\cdot$ cm^{-3} $\cdot$ 10^{-20})

	B0	B1	B2	B3	B4	B5	B6	B7
B10	0.	=	=	0.2	0.	0.	0.	0.
CR	30.	=	=	=	=	=	=	=
FE	140.	=	=	=	=	=	=	=
FPP *)	2.	=	=	0.	2.	0.	0.	2.
NI	3.	=	=	=	=	=	=	=
O	100.	=	=	=	=	=	=	=
Pu239	9.0	12.3	12.7	9.0	9.0	=	12.3	5.8
Pu240	3.5	1.7	0.	3.5	3.5	=	1.7	2.4
Pu241	2.3	0.	0.	2.3	2.3	=	0.	1.4
U238	33.2	34.0	35.3	35.2	33.2	35.2	36.	38.4
Temp. [K]	1500.	=	=	=	300.	=	=	1500.
B^2 [10^{-4} cm^{-2}]	12.	=	=	=	=	=	=	6.
Θ [MeV]	1.41	=	=	=	=	=	=	=

*) FPP $\hat{=}$ Fission Product Pairs

Table II

Number densities for steam ingress
(atoms $\cdot$ cm^{-3} $\cdot$ 10^{-20})

	S_0	S_1	S_2	S_3	S_4	S_5	S_6	S_7	S_8	S_9	S_{10}
H	0.	0.33	0.66	0.99	1.32	1.65	1.98	2.31	2.64	3.30	3.96
O	0.	0.165	0.33	0.495	0.66	0.825	0.99	1.155	1.32	1.65	1.98

	S_{11}	S_{12}	S_{13}	S_{14}	S_{15}	S_{16}	S_{17}	S_{18}	S_{19}
H	4.95	5.94	7.26	8.58	9.9	11.55	13.20	14.85	16.5
O	2.475	2.97	3.63	4.29	4.95	5.775	6.6	7.425	8.25

The number densities given in table II evidently have to be added to those given in table I.

ingress in a GCFR core. The reason for this probably somewhat excessive number of density values is that we want to be sure (a) to detect possible nonlinearities in $k_{eff}(\rho_{H_2O})$, (b) to determine corresponding changes in the reactivity worth per unit mass of steam (RUM) upon variation of the steam density, an effect which has been reported e.g. for experiments in the ZPR-9 assembly mentioned before, (c) to easily derive the relative extrema of $k_{eff}(\rho_{H_2O})$ or $RUM(\rho_{H_2O})$, (d) to determine those values of $\rho^*_{H_2O}$ where $k_{eff}(\rho^*_{H_2O}) = k_{eff}(\rho_{H_2O} = 0)$, i.e. the zeros of $\Delta k_{eff}(\rho_{H_2O})$.

Participants only interested in the first part of the reactivity curve $k_{eff}(\rho_{H_2O})$ could omit those steam densities which they are not interested in and provide only the results for the remaining steam densities.

Although a complete treatment of all cases B0 - B7 would have been favourable, participants interested only in some specific examples appearing in B0 - B7 have been asked to take their own choice and to provide the corresponding results for this restricted number of cases in order to include as much as possible of the presently existing experience into the intercomparison.

Several intercomparisons had shown up to 1976 that the predicted criticality values for GCFR designs are reasonably close to each other when using different, recently established nuclear data sets. Therefore it did not seem very meaningful to adjust the enrichment or the buckling at the various laboratories participating in this benchmark activity. The deviations which will eventually result between the different criticality values obtained at various laboratories for the completely voided cases most probably will not influence the conclusions with respect to the test of the predicted reactivity effect of steam entry, i.e. $k_{eff}(\rho_{H_2O})$. It was therefore suggested that the criticality adjustment should be omitted at present. The most interesting results are primarily the values showing the criticality differences as a function of the hydrogen-concentration $k_{eff}(N_H)$. It was proposed to provide these results in tabular form.

IIb) Characterization of the Methods and Specifications of the Nuclear Data Basis Used at Various Laboratories

The following Table III characterizes some of the important features of the contributions from various laboratories. It is succeeded by a listing of the references for the different nuclear data bases used.

The results from Germany have been determined at Karlsruhe with the KFKINR-Set of group constants. As Karlsruhe was mainly responsible for the specifications of the proposed benchmark, we followed our own suggestions concerning the fission spectrum, the data for the fission products and the temperatures for fuel- and non-fuel isotopes. The basic results are listed in Table A1 of the Appendix. As an example, corresponding results for the specific steam density coefficients are added as Table A1a.

The Japanese results are reproduced in Table A2 of the Appendix as taken from the original table of data and as stored in the computer and reproduced as listing for the present purpose.

The results obtained from Switzerland have been partially determined at EIR Würenlingen and the remaining cases under contract at Winfrith. The UK code MURALB has been used in the P1 approximation. The corresponding results and the specifications and comments according to them are reproduced from the original contribution in Table A3 of the Appendix.

The French results have been published in an internal technical note of the Centre d'études nucléaires de Cadarache. The essential part of the results has been reproduced as Table A4 in the Appendix.

The results from the US are reproduced in Table A5 of the Appendix from an ANL publication. Minor corrections and additions to the original table should help to facilitate the understanding of the table-content. We felt it extremely useful to include (besides the

Table III

Important Features of the Calculational Methods used at Various Laboratories

Country	Organi-zation	Group Constant Set	Number of energy groups	Fission spectrum	Fission products
Germany	KfK	KFKINR	26	MAXW. Θ = 1.41 MeV	1 Pseudo-FPP[3]
Switzer-land	EIR	FGL4 [1]	2240	MAXW. Θ = 1.41 MeV	1 single fission product nuclide
		FGL5 [2]			
UK	UKAEA	FGL5 [2]	2240	MAXW. Θ = 1.41 MeV	
France	CEA	CARNAVAL-III	25		
Japan	JAERI	JAERI-2 Rev.	25		
USA	ANL	3 methods	11 broad groups		

1) Cases B4, B5, B6 only; FLG4 has been used previously for the analysis of PROTEUS experiments.

2) Cases B4, B5, B6 calculated at EIR Würenlingen, the other cases corresponding to T = 1500 K were calculated for EIR under contract at Winfrith.

3) It was recommended and usually accepted to use data for FPP which correspond to fission of ^{239}Pu.

data table) also the comments contained in the ANL publication because that part gives explanations concerning the calculational methods.

References for Group Constant Sets:

KFKINR :

E. Kiefhaber et al.: The KFKINR-Set of Group Constants; Nuclear Data Basis and First Results of its Application to the Recalculation of Fast Zero-Power Reactors. KFK-Report 1572 (1972).

CARNAVAL-III :

J. P. Chaudat et al.: "Formulaire CARNAVAL III", International Symposium on Fast Reactors Physics. Rapport A 34 - Tokyo (1973).

JAERI - Fast Reactor Group Constants Version 2 Revised Set :

S. Katsuragi et al.: JAERI Fast Reactor Group Constants Systems Part I; JAERI 1195(1970), and Part II-1; JAERI 1199(1970).

Group Sets FGL5 and FGL4
(used for results obtained from Switzerland)

See comments following the page in the Appendix which reproduces the original EIR data table.

Nuclear Data for ANL-results

See comments following the page in the Appendix which reproduces the original ANL data table; nuclear data basis not specified explicitly.

III) Results and Discussions

The numerical results for the criticality values obtained from the participating laboratories can be found in Tables A1 - A5 of Appendix A. To facilitate intercomparison, they are also given in graphical form in Figs. 1 - 8 for the Steam Ingress Reactivity (SIR), $k_{eff}(\rho)$. The corresponding Specific Steam Density Reactivity Coefficients (SSDRCs) are presented in Figs. 9 - 16. For the results obtained at Karlsruhe these coefficients are given as tabulated results in Table A1a. Concerning the drawings for the cases B3 and B5 we decided to present two types of figures, namely figures showing all available results and figures labelled ...a, showing the same results except that the ANL results obtained without the application of the narrow resonance approximation have been omitted because of their extraordinary shape upon variation of the steam density which is absolutely unique compared to that of all other contributions. Please note the different ordinate scales used in the figures for a clear presentation of various cases. To compare the dependence of SIR and SSDRC, respectively, on steam density for all cases simultaneously in one figure, the Karlsruhe results are shown together in Fig. 17 (for $k_{eff}(\rho)$) and in Fig. 18 (for $dk_{eff}(\rho)/d\rho$), which correspond to Tables A1 and A1a, respectively.

IIIa) Influence of Specified Parameter Variations on $k_{eff}(\rho = 0)$

Before commenting on the intercomparison of the results of various laboratories it may be worthwhile to mention on the basis of Figs. 17 and 18 some important tendencies observed upon changing the specifications of the different cases. Since the effect on criticality for steam density equal to zero seems to be rather plausible we will not repeat obvious explanations but restrict ourselves to the discussion of SSDRC (at zero steam density). The difference between a fresh core with absorber poison and a burnt core with fission products (and reduced ^{238}U concentration) is fairly small, less than $\sim$ 20 % for (B3 $\rightarrow$ B0). The influence of

the temperature change 1500 K → 300 K is about twice as large, ∿ 50 % for (B0 → B4), but still small compared to the influence of other parameter variations.

The effect of the plutonium isotopic composition is quite large. When following the transition B2 → B1 → B0 it becomes evident that - contrary to some previous publications - it might not always be sufficient to classify a specific plutonium composition as "more dirty" than another and deduce from this oversimplified basis an expected influence on the steam ingress reactivity. To the contrary it is always important to specify properly the isotopic composition of plutonium because ^{240}Pu and ^{241}Pu usually have an opposite influence on the steam reactivity coefficient. As could be expected, the addition of any poison material like ^{10}B or FPP leads to a decrease of the SSDRC. For the cases considered here, the reduction is roughly equivalent to that observed for the increase of the fuel temperature from 300 K to 1500 K (compare e.g. in Fig. 18 the transition form B5 to B0 and B3 or from B6 to B1 and take into account the temperature effect included in the above transitions by reducing the related SSDRC differences by the corresponding difference for the transition B4 to B0). This means that fresh cores without any additional poison, especially if they are operated at a low temperature, generally have a considerably larger steam ingress reactivity compared to similar cores with poison added to compensate the burn-up reactivity swing and possibly operating at typical power reactor fuel temperatures. As is well known from the literature (see e.g. /6/), there is a tremendous effect of the reactor size (simulated here by the buckling) on the steam reactivity coefficient: there is a remarkable reduction (caused by the reduction of the positive leakage component of the reactivity effect) if the buckling is halved (B0 → B7) and the fuel enrichment is changed correspondingly to maintain (roughly) the criticality condition. The last three effects (size, presence of poison, plutonium isotopic composition) are quite important if one wants to extrapolate or correlate with some confidence results measured in critical assemblies to the real power reactor behaviour in the case of an assumed steam ingress.

IIIb) Relevance of ANL-Results

The most remarkable result of the present intercomparison consists in the fact that, according to the ANL-investigations, the Narrow Resonance Approximation leads to severe discrepancies for the steam entry reactivity compared to the RABANL method of group cross section generation using Integral Transport Theory and avoiding the Narrow Resonance Approximation. As one could expect these discrepancies increase with increasing steam density because due to the spectrum softening the resonance energy range becomes more important. For the evaluation of experiments in critical assemblies and for the design and safety analysis of planned power reactors it seems important to note that a different group cross section treatment in the resonance range could cause a change of sign of the reactivity disturbance associated with a hypothetical ingress of hydrogeneous material into a reactor core. In addition, the ANL comments indicate the possible importance of numerical effects, e.g. the round-off problem encountered in single precision fine group calculations or the algorithm used in the solution of the neutron attenuation in an ultra-fine group scheme.

We have decided not to include the US-results which one could derive for the SSDRC for Benchmark B3 because in this case US-criticality values are available only for two steam densities referring to abscissa values which are fairly distant from each other (see Fig. 4). Therefore the accuracy and reliability of a SSDRC determined under these circumstances would have been questionable. Furthermore, disregarding the results obtained without narrow resonance approximation, the US SSDRC-value would probably not be too different from results of other participating laboratories.

For Benchmark B5 we have omitted in Fig. 14a the US-results without narrow resonance approximation in order to obtain a more detailed presentation than that possible in Fig. 14. In Fig. 14b all US-results have been omitted so that this presentation is in better accordance with the presentation for the SSDRCs of all other Benchmark cases.

IIIc) General Comments to the Presentation of Results

For the presentation of the results as a function of steam density, we have chosen two different types of graphs: The first kind shows the criticality (for the various cases B0 - B7 or the values obtained from various laboratories), the second kind the Specific Steam Density Reactivity Coefficient (SSDRC). Note that the steam density (in g/cm^3) as used here corresponds to the average density of H_2O per cm^3 of core volume. The corresponding real average steam density can be derived from the above quantity by dividing it by the average coolant volume fraction in the core. In a similar manner we defined the SSDRC: If S_i characterizes the different steam density cases considered in the calculations (i = 0,1,...19) and $\rho(S_i)$ and $k_{eff}(S_i)$ the correlated values of steam density per cm^3 of core volume and criticality, respectively, SSDRC characterizes the mean criticality change caused by an assumed increase of the steam density by 1 $g(H_2O)$ per cm^3 (of core volume), i.e. of 1 g of water - hypothetically - added to 1 cm^3 of the average core composition. In the figures the SSDRC-values are attributed to the corresponding median steam densities, i.e.

$$SSDRC_{i+1/2} = SSDRC(0.5*(\rho(S_i) + \rho(S_{i+1})) =$$

$$= (k_{eff}(S_{i+1}) - k_{eff}(S_i)) \; / \; (\rho(S_{i+1}) - \rho(S_i))$$

IIId) General Tendencies Observed in the Intercomparison

In general it can be observed from Figs. 1 - 8 that at least for low steam densities the following relations hold (with unimportant exceptions):

Group 1 (higher k_{eff}-values):
k_{eff}(JAERI) $\gtrsim$ k_{eff}(KFKINR) $\gtrsim$ k_{eff}(SWISS-FGL4)

Group 2 (lower k_{eff}-values):
k_{eff}(FRANCE) $\gtrsim$ k_{eff}(SWISS-FGL5)

The ANL broad group results obtained without using the narrow resonance approximation (ANL W/O NRA) show an opposite slope of the curve $k_{eff}(\rho)$. The remaining scarce ANL results lie in between the two groups of k_{eff}-values just mentioned above. Because of the few ANL results available, we will not consider them for the following detailed discussions, although their availability was quite significant for an appropriate overall judgement of the state of the art and the uncertainty which should be attributed to the reliability of calculated steam ingress reactivities.

For the SSDRC we find also some kind of grouping of the results. In general the slope of $k_{eff}(\rho)$, i.e. $dk/d\rho$, is low for group constant sets leading to high k_{eff}-values. We observe from Figs. 9 - 16:

Group 1 (lower SSDRC):
SSDRC(JAERI) $\lesssim$ k_{eff}(KFKINR)

Group 2 (higher SSDRC):
SSDRC(FRANCE) $\gtrsim$ SSDRC(SWISS-FGL5) $\gtrsim$ SSDRC(SWISS-FGL4)

These relations which hold at least for low steam densities (with minor exceptions) should be kept in mind during the following discussions.

IIIe) Influence of Specified Parameter Variations on Steam Ingress Reactivity (SIR) and Specific Steam Density Reactivity Coefficient (SSDRC)

When discussing the influence of parameter variations (cases B0 - B7) on $k_{eff}(\rho)$ one should be aware that the variations were performed so as to keep the number of heavy atoms constant. No provisions were taken to obtain the same criticality value for the different cases at zero steam density (This would have been possible e.g. by an adjustment of the geometric buckling or of the fuel enrichment).

Comparing the sequence B2 → B1 → B0, i.e. going from pure ^{239}Pu to a fairly dirty plutonium isotopic composition one concludes that the presence of ^{240}Pu leads to a reduction of the steam ingress reactivity whereas ^{241}Pu tends to increase this reactivity because this isotope is a more efficient fissionable isotope than ^{239}Pu due to its higher fission cross section and lower α-value ($\alpha \triangleq \sigma_c/\sigma_f$). The transition B6 → B5 confirms the validity of the above statement. The influence of different neutron poisons (fission products or ^{10}B) on $k_{eff}(\rho)$ is fairly similar as can be seen when comparing Figs. 1 and 4. The influence of the fuel temperature is quite pronounced: case B4, with the lower temperature compared to B0, showing the larger steam ingress reactivity. Reducing the amount of poisoning material by exchanging ^{238}U against FPP (i.e. B4 → B5) leads to an additional increase of the steam ingress reactivity. Finally, Fig. 8 for B7 demonstrates the remarkable influence of the geometric buckling or the reactor size on the steam ingress reactivity. Except for the French results, all other calculations produced a reactivity reduction if small amounts of steam enter the voided coolant channels of a typical 300 MW_e GCFR. The differences between cases B0 and B7 indicate that it is essential to determine the important contributions to the steam ingress reactivity - namely the leakage term and the spectrum or degradation term - separately with sufficient accuracy if one wants to extrapolate the results obtained in small critical assemblies to designed power reactors of sizes corresponding to 300 MW_e or even larger.

When discussing the results for the SSDRC, the analogous comments apply as already mentioned in the context of the curves showing the criticality as a function of steam density: compared to the deviation of the ANL-results obtained with RABANL (no NRA)-group cross sections all other results could be considered to be fairly similar. But the figures for SSDRC indicate that even the remaining curves from four laboratories show significant disparity. (In the SSDRC-drawings the US-results for case B3 have been omitted and the US-results for case B5 might be uncertain or somewhat unreliable because only 4 out of 10 different steam densities have been dealt with as can be seen from Fig. 6 and Table A5 so that the derivates required to determine the SSDRC-values might be subject to numerical inaccuracies.) Except for case B6 - simulating a cold clean core (i.e. without poison or fission product absorber) with a fairly clean plutonium isotopic composition - where the differences in SSDRC are as low as 10 - 20 %, the deviations in all other cases are of the order of a factor of 1.5 for large values of SSDRC. This factor rises extremely if fairly low values (or even negative ones) of SSDRC are considered.

As could already be seen from the results of the criticality values, the influence of the geometry buckling, which represents the reactor size in this fundamental mode intercomparison, becomes also evident when comparing the SSRDC values of B0 with those of B7. It may be worthwhile to mention that for case B7 - simulating a large gas cooled fast power reactor - the French results predicts for the SSDRC at low steam densities a sign which is opposite to that obtained by all other participants. The results for cases B0 and B3 are fairly similar, thus demonstrating that the kind of poisoning is not too important for the SSDRC, i.e. it is influenced by the presence of absorbers in the same way, no matter whether the absorbing material is ^{10}B or fission products provided the reactivity taken by the two absorbers is nearly equal. For the power reactor this would mean that the uncertainty in SSDRC (caused by burn-up effects is not very pronounced). A comparison of B5 and B4 shows the influence of the addition of an absorber poison (in this case fission products) to a clean core composition: the SSDRC reduces. Bearing in mind, as discussed

before, that the kind of poison has no pronounced influence on SSDRC, we conclude that it is essential to include a reasonable amount of absorber material in the core composition if one wants to derive results for the steam density reactivity from a critical assembly which are representative for equivalent properties of a power reactor.

Comparing B0 and B4 one realizes that a reduction of the fuel temperature increases the SSDRC by about 50 %. Therefore, the steam ingress (in our case into a small reactor core) produces a larger reactivity insertion if the reactor is cold than if the reactor is at operating condition (if all other parameters, e.g. the amount of poison present for control purposes, are essentially unchanged). This considerable influence of the fuel temperature has also to be taken into account if the results of a "cold" mockup experiment in a critical assembly are going to be used during the design period as a reliable basis for corresponding calculated results attributed to an operating power reactor.

The influence of the plutonium isotopic composition on the SSDRC is quite remarkable and generally similar for the various nuclear data sets used in the intercomparison. Introducing ^{240}Pu into a fuel composition consisting originally of ^{239}Pu and ^{238}U, i.e. the transition B2 → B1, leads to a consistent reduction of SSDRC by roughly 25 % (except for low SSDRC-values at low steam densities). Using fairly "dirty" plutonium (probably available from thermal or fast reactors with appreciable fuel burn-up - in excess of roughly 30 000 MWd/t -) instead of fairly "clean" plutonium (which might be produced in thermal reactors at low fuel burn-up rates), leads usually to an increase of SSDRC by an amount of about 25 % for the transition B1 to B0 and by about 40 % for B6 → B5 (but for both transitions the more severe changes occur at low steam densities). A comparison of B2 and B0 shows that the SSDRC increases if pure ^{239}Pu is replaced by an equivalent amount of "dirty" plutonium. The decreasing slope of SSDRC as a function of steam density observed for the cases B0, B3, B4 illustrates that the absorption effect of ^{240}Pu becomes more dominant as the steam density increases.

IIIf) Discussion of Perturbation Theory Results

Figs. 19 - 24 present specific results of exact perturbation calculations for the energy dependence of the SSDRC. We have chosen cases B0, B6 and B7 because they may represent typical examples of practical interest. These figures and the numerical values added to them clearly demonstrate that in general

(a) the degradation contribution is of dominant importance
(b) the positive and negative degradation contributions have about equal magnitude, thus leading to an extensive mutual cancellation in determining the net degradation contribution. Therefore, this net value is significantly (most times more than one order of magnitude) smaller than the absolute values of both the positive and negative contributions. Especially at low steam densities the net degradation effect is usually even much smaller than the absolute value of the largest contribution from one single energy group.
(c) the leakage contribution is significant only for energies above about 10 keV
(d) the capture contribution and all other remaining contributions (i.e. the fission and source term which have been omitted in Figs. 19 - 24) are always fairly small
(e) below about 100 eV the contribution from the degradation term is the only noticeable one
(f) for increasing steam densities the low energy range of the neutron spectrum becomes more and more important (e.g. for $\rho_{H_2O} \gtrsim 5 \cdot 10^{-4}$ g/(cm^3 core volume) there is a relatively small, but for the total effect still important contribution from the range below 100 eV, whereas for $\rho_{H_2O} \gtrsim 0.01$ g/(cm^3 core volume) even the range below 10 eV may be of relevance for the total steam entry reactivity effect.

The last finding agrees with a corresponding result presented in the work of McCombie et al. /6/. It underlines the necessity for an accurate treatment of the energy range of resolved resonances. It can be imagined from Figs. 22 and 24, that for fairly high

steam densities the 1 eV resonance of ^{240}Pu or even the 0.3 eV resonance of ^{239}Pu may become important. Thus, in these extreme cases - as already mentioned by Ingram et al. /13/ - even the lowest resonances of fuel isotopes have to be treated appropriately upon deriving group constants and performing diffusion calculations.

In all cases of Figs. 19 - 24 the leakage term amounts to about 6 % of the positive degradation term. This relation is approximately valid for the effect of both steam concentrations studied here by exact perturbation theory, i.e. for the ingress of steam leading to average densities of $5 \cdot 10^{-4}$ (Figs. 19, 21, 23) and of $2.5 \cdot 10^{-2}$ (Figs. 20, 22, 24) g H_2O per 1 cm^3 of average core composition, respectively. The ratio of the two terms mentioned above increases slightly as the steam density increases. For low steam densities the partial cancellation of the positive and negative degradation components is extremely effective as can be seen from the numerical values included in Figs. 19, 21, 23. For case B7 the net degradation component is negative for the entry of low density steam (Fig. 23), so that it can be counterbalanced to a large extent by the positive leakage component. Consequently, the absolute value of the total effect is more than 2 orders of magnitude smaller than the most important individual contribution. In addition one has to bear in mind that this largest degradation component (usually that with positive sign) is again due to differences of group cross sections. Therefore it is evident, that under certain circumstances the pronounced influence of numerical effects may render the reliable prediction of the steam entry reactivity effect more difficult. For the same reason, namely mutual cancellation of already small contributions, fairly small differences or changes in the nuclear data basis may cause fairly remarkable changes in the calculated steam entry reactivity. These data deviations lead e.g. to differences in the energy distribution of the neutron importance and thus influence the degradation term which depends on the differences of the neutron importance (adjoint flux) between different energy ranges.

The above remarks concerning calculations for the steam entry reactivity and the related hydrogen material worth underline findings already known from earlier publications: For a reliable prediction of the desired values the following recommendations should be taken into account:

(A) To use a sufficient number of energy groups; as e.g. mentioned in /11/ p. 24 and /12/ p. 32, 10-group analyses might not be adequate.

(B) To choose an appropriate energy group structure taking into account the variation of the importance of different energy regions upon an increase in steam density.

(C) The above two conditions are especially important if one considers group collapsing. For that purpose bilinear averaging is preferable to usual flux averaging schemes, as already observed by Greenspan /14/ and discussed in two paragraphs of chapter I of the present paper.

(D) Bearing in mind the items mentioned before, it is obvious that the methods and the weighting spectrum adopted upon establishing a group constant set which is subsequently used as a basic library for nuclear calculations may have a considerable influence on the predicted SSDRC-values. According to this influence, the use of a single weighting spectrum may not be sufficient for all purposes; i.e. if the number of energy groups is not large enough, it may be appropriate or necessary to modify the weighting spectrum in accordance with major changes of the steam density.

(E) The applicability of first order perturbation theory may be fairly restricted, especially if combined with a rather coarse group structure; corresponding comments could be found e.g. on page 23 of /11/. The reason seems quite plausible if one is aware (I) that the degradation term is caused by differences $(\phi_i^+ - \phi_j^+)$ in the adjoint neutron flux between different

energy regions and (II) that a neutron of certain energy scattered on hydrogen may be slowed down to all lower energies so that the addition of hydrogen affects the down-scattering probabilities from each group to all lower energy groups and, therefore, leads to appreciable changes of the values for the group averaged adjoint neutron flux ϕ_i^+ and the corresponding differences $(\phi_i^+ - \phi_j^+)$. Due to uncertainties about the range of applicability of first order perturbation theory, it may be preferable or mandatory in many cases to use exact perturbation theory.

(F) Recommendation (A) suggests using as many energy groups as reasonable or possible. Although this proposal seems to be quite natural and straightforward, one has to be aware that at the same time one has to ascertain whether the numerical procedures implemented in fine groups or ultra-fine group algorithms are suitable to avoid possible undesirable numerical effects such as e.g. round-off errors mentioned in section IIIb) of the present paper. This kind of deficiences may sometimes occur when codes are applied which use only single precision for the internal data representation. Due to the large number of summations which are usually necessary (if no special provisions have been taken) when hydrogeneous material is a mixture constituent, this numerical problem may sometimes aggravate the difficulties in calculating the steam ingress reactivity.

IV) Conclusions

The present GCFR Steam Entry Benchmark intercomparison has been a useful exercise in several respects:

(I) It provided a common uniform data reference for the specifications of simple calculational models which could be used by all participants. These specifications included several compositions so that the influence of some parameters could be identified which are known to influence significantly the steam ingress reactivity.

(II) Due to the simplicity of the models the results primarily reveal the influence of the differing nuclear data bases used within this international intercomparison on the calculated steam ingress reactivity effect.

(III) The observed discrepancies between the results of fundamental mode neutronic calculations provided by various laboratories indicate that an intercomparison effort for more complicated or more realistic configurations may not be very meaningful at present and should probably be postponed until the still existing discrepancies have been reduced to acceptable limits or until at least the reasons for these discrepancies are well known so that they could be taken into account in more advanced intercomparisons.

(IV) If - in spite of the preceding considerations - a more complex benchmark configuration should be analyzed in an intercomparison study in the near future, one should take precautions so that differences in the nuclear data bases would not preclude an easy and clear interpretation of the results. For that purpose it might be necessary to specify a uniform nuclear data basis although this could lead to difficulties because the methods used to arrive at macroscopic group constants for reactor compositions or reactor regions usually differ between various laboratories.

The following conclusions can be drawn from the results which became available during this intercomparison:

(I) There still exist considerable differences in the calculated steam ingress reactivity even for these simple fundamental mode benchmarks. These differences are essentially attributable to differences in the nuclear data bases applied at various laboratories to derive the results of this study.

(II) Due to these discrepancies one has to be very careful if one tries to compare results obtained at different laboratories for the steam ingress reactivity of reactors with different configurations, e.g. differing mainly in the plutonium isotopic composition. One should be cautious when tracing back the reasons for observed differences for the steam ingress reactivity to specific differences in special parameters or design features.

(III) According to the present experience it seems quite probable that a similar intercomparison for the reactivity effect of the entry of lubricating oil into an LMFBR core would show up comparable differences as those observed here for the ingress of low density steam into a GCFR core. Evidently the amount of hydrogeneous material which may enter a LMFBR core is determined by the amount of lubricating oil (from the sodium coolant circulating pumps) which could accidentally be introduced into the coolant circuit. Although probably unrealistic, it might be appropriate to consider the worst case of an inhomogeneous distribution of that material which then in the calculations should replace the sodium coolant within those spatial regions which yield the highest hydrogen worth. By this means the problem of oil stripes which possibly could exist in the coolant flow could be covered by an estimation of the upper limit of the reactivity increase caused by such an assumed inhomogeneous distribution of the added hydrogeneous material.

(IV) Therefore, it might be adequate to measure the reactivity worth of hydrogen in several critical assemblies differing appreciably in their material composition and/or their geometric arrangement. Examples of this kind of experiments and of the corresponding analyses are given in /7/ and, for the ZEBRA cores 13 and 16 (BZB/3), in /13/. The latter study stresses the importance of the spatial distribution of the hydrogen material worth, thereby indicating that a single measurement of the central hydrogen worth might not be sufficient but should favorably be supplemented by measurements at other spatial positions to be able to distinguish between the separate influence of the leakage term and the moderation term and the corresponding uncertainties which one should attribute to both terms which are essential for the predicted steam entry reactivity. At the same time one would obtain an indication whether or not the analysis is able to predict the position of maximum reactivity and the magnitude of the hydrogen worth at that position.

(V) As could be expected and as has been demonstrated here by the results of perturbation calculations, the reactivity effect of an addition of hydrogenous material to a reactor composition is mainly caused by the moderation - or degradation term. This term is composed of positive and negative contributions (from the high and low energy range, respectively) of about equal magnitude. Thus, there is to a large extent a mutual cancellation of both components, which may cast some doubts on the numerical accuracy and reliability of the calculated net degradation term (This underlines the importance of the number of energy groups, the energy group structure, the weighting spectrum used on establishing a set of group constants and the kind of group collapsing (e.g. bilinear weighting) applied when deriving few group constants in a coarse group scheme). Due to this partial compensation, the leakage term also plays a significant role for the total reactivity effect (This indicates that

for a real reactor environment additional aspects ask for careful attention, e.g. geometric modelling, heterogeneity-, streaming- and transport-effects).

(VI) In some special cases it might be appropriate to check the accuracy and reliability of advanced calculational methods and algorithms. Numerical effects such as round-off errors in codes with single precision internal data representation might become important in fine group or ultra-fine group schemes especially for compositions with an appreciable concentration of hydrogen.

(VII) In determining accurately the steam ingress reactivity, it is essential to treat properly the energy range of resolved resonances, i.e. - contrary to the situation usually encountered in GCFR calculations for normal operation conditions - the energy range below 1 keV becomes important. For fairly high steam densities even the lowest resonances of plutonium isotopes may have a non-negligible influence.

(VIII) The supplementary, restricted sensitivity study has shown, within its intentionally limited scope, the influence of some fairly simple nuclear data changes on the calculated steam ingress reactivity. However, this study was too crude to deduce explanations concerning reasons for the discrepancies observed between the results of various laboratories. Such an extensive analysis would require a closer examination of the nuclear data sets involved in the intercomparison to find out which data in which energy range are mainly responsible for the observed differences. This type of detailed study would eventually be quite useful but it exceeds by far the effort which we were able to devote to this international intercomparison.

(IX) Dependent on the general interest in GCFRs and the corresponding development efforts, one should consider whether or not it seems desirable to repeat or extend this type of intercomparison on the basis of more modern nuclear data libraries.

Acknowledgments

The authors appreciate the fruitful cooperation with all those interested in and contributing to the benchmark, especially to those submitting their results fairly early. They are pleased to acknowledge continuous support received for this work in their own laboratory by Dr. M. Dalle Donne and Prof. K. Wirtz. The authors would also like to express their gratitude to the directors of their institute (Prof. K. Wirtz succeeded by Dr. G. Kessler) and to the management of the "Projekt Schneller Brüter" (represented by the project manager Dr. G. Kessler succeeded by Dr. W. Marth) for the patience during the accomplishment of the present work and for the opportunity to finish it after many delays. The continuing interest of members of the NEACRP in the present activity is also gratefully acknowledged, encouraging us to continue and to complete this work. Finally they want to thank Mrs. G. Bunz for preparing a clear manuscript.

References

/1/ P. Fortescue, R. Shanstrom, J. Broido, J. M. Stein, A. Baxter, and H. Fenech: Safety Characteristics of Large Gas-Cooled Fast Power Reactors. Proceedings of the Conference on Safety, Fuels, and Core Design in Large Fast Power Reactors, October 11 - 14, 1965. ANL 7120, pp. 230 - 260, Argonne National Laboratory (1965).

/2/ E. Eisemann: Considerations on the Accident: Water Ingress in the Primary Loop of a Helium Cooled Fast Breeder Reactor with Secondary Steam Cycle. KFK 1487, Kernforschungszentrum Karlsruhe (1971).

/3/ E. Eisemann: Neutron Streaming in GCFR-Lattices: Theory and Results. Proc. Int. Conf. Advanced Reactors: Physics, Design and Economics. Atlanta, Georgia, Sept. 8 - 11, 1974, CONF-740902, p. 206. Edited by J. M. Kallfelz and R. A. Karam, Pergamon Press (1975).

/4/ A. Torri, and J. Discroll: Reactivity Insertion Mechanisms in the GCFR. General Atomic Report GA-A12934, April 10 (1974).

/4a/ A. L. Hess and C. J. Hamilton: Steam Ingress Reactivity Effects in the GCFR. GCFR Program: Technical Review Proceedings. Presented by Helium Breeder Associates, Department of Energy; May 30, 31 & June 1, 1979. San Diego, California.

/5/ S. Iijima, T. Osugi and H. Yoshida: Heterogeneity Effect on Safety-Related Reactivity in a 1000 MWe Gas-Cooled Breeder Reactor. Int. Sympos. Fast Reactor Physics, Aix-en-Provence, France, 24 - 28 Sept. 1979, Paper IAEA-SM-244/1 (1979).

/6/ C. McCombie, G. Brunson, W. Heer, M. Jerman, R. Richmond, S. Seth: Effect of Steam Entry in a GCFR Core. Proc. Int. Meeting Fast Reactor Safety and Related Physics. Chicago, Illinois, Oct. 5 - 8, 1976. CONF-761001, p. 541 (1976).

/7/ S. K. Bhattacharyya: An Experimental Study of the Neutronics of the First Gas Cooled Fast Reactor Benchmark Assembly (GCFR Phase-I Assembly). ERDA Report ANL-76-36, Argonne National Laboratory (1976).

/8/ R. B. Pond, ed.: Reactor Physics Studies in the GCFR Phase-II Critical Assembly. ERDA Report ANL-76-108, Argonne National Laboratory (1976).

/9/ S. K. Bhattacharyya, E. M. Bohn, L. G. LeSage, and R. B. Pond: Experimental Studies of GCFR Safety Physics Parameters in the ZPR-9 Critical Assemblies. Proc. Int. Meeting Fast Reactor Safety and Related Physics. Chicago, Illinois, Oct. 5 - 8, 1976. CONF-761001, p. 521 (1976).

/10/ E. M. Bohn, S. K. Bhattacharyya, L. G. LeSage, R. B. Pond, R. A. Moore, A. L. Hess and R. J. Cerbone: The Gas-Cooled Fast Breeder Reactor Critical Experiments Program. Nucl. Engng. Design 40, 27 (1977).

/11/ A. L. Hess, R. A. Rucker, and R. A. Moore: Analysis of Steam-Entry Experiments in the Phase-I GCFR Critical Assembly. GA-A14798, General Atomic Company (1978).

/12/ A. L. Hess and R. A. Rucker: Analysis of Full Core Steam Flooding Experiments for the Phase-II GCFR Critical Assembly. GA-A14834, General Atomic Company (1978).

/13/ G. Ingram, D. W. Sweet: Studies of the reactivity effects of hydrogenous material in a sodium cooled fast reactor. Int. Sympos. Fast Reactor Physics, Aix-en-Provence, France, 24 - 28 September 1979, Paper IAEA-SM-244/41 (1979).

/14/ E. Greenspan: Consistent vs Conventional Few Group Reactivity Calculations. Trans. Am. Nucl. Soc. 10, 583 (1967).

/15a/ E. Kiefhaber: Comment on the Calculation of Neutron Lifetime and Material Worth. KFK 882, EUR 4161e, Kernforschungszentrum Karlsruhe (1968).

/15b/ E. Kiefhaber: Comment on the Calculation of Neutron Lifetime. Nucl. Sci. Eng. 38, 178 (1969).

/16/ T. A. Pitterle: Bilinear Averaging for Diffusion Theory Parameters. Dissertation, University of Wisconsin, University Microfilms, Inc. (1965).

/17/ E. Greenspan: Developments in Perturbation Theory. Adv. Nucl. Sci. Technol. 9, 181 (1976).

/18/ D. C. Wade and R. G. Bucher: Conservation of the Adjoint Neutron Spectrum by Use of Bilinear-Weighted Cross Sections and Its Effect on Fast Reactor Calculations. Nucl. Sci. Eng. 64, 517 (1977).

/19/ E. M. Gelbard, D. C. Wade, R. W. Schaefer, and R. E. Phillips: Calculations of Void Streaming in the Argonne Gas-Cooled Fast Reactor Critical Experiments. Nucl. Sci. Eng. 64, 624 (1977).

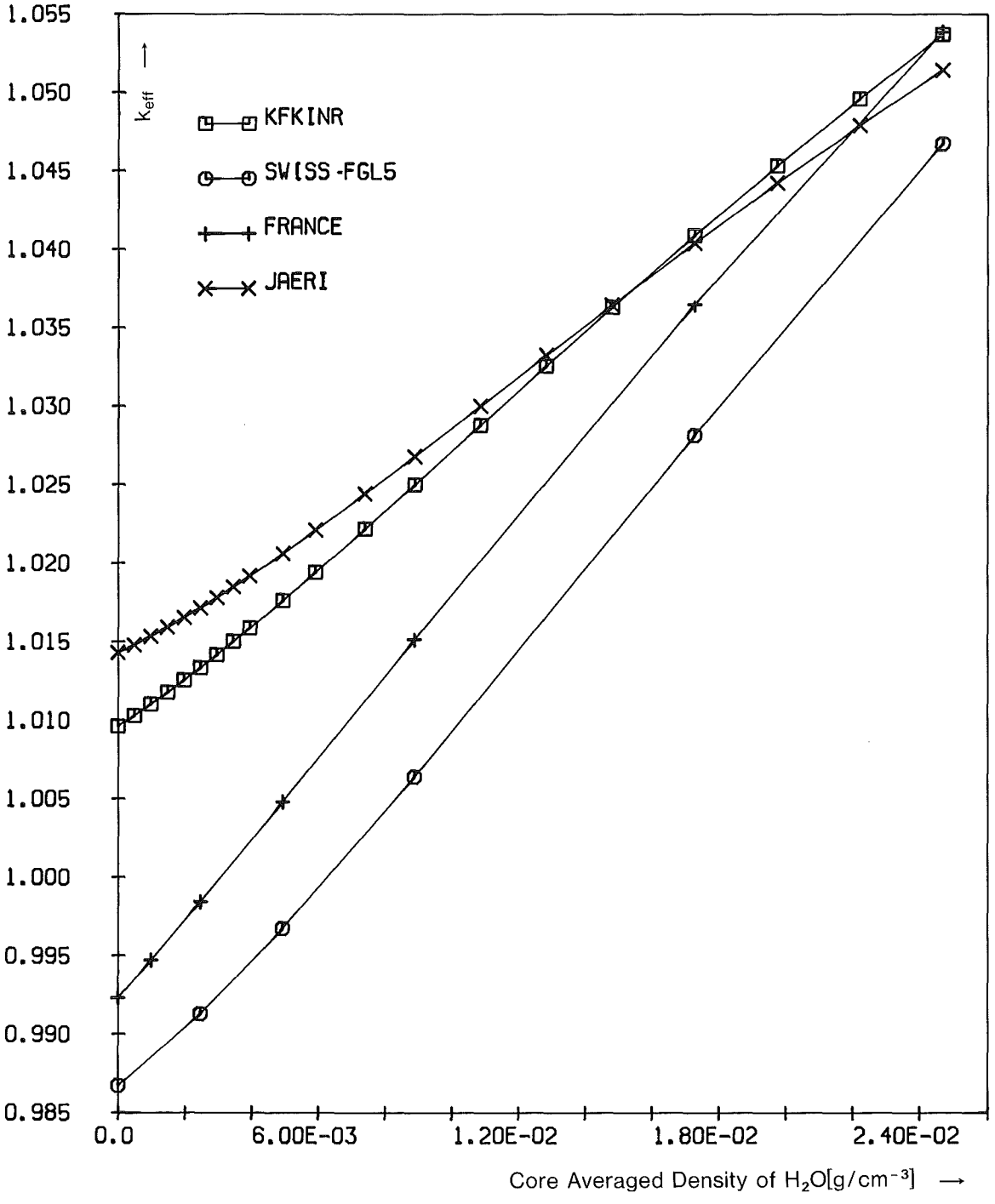

Fig 1.: k_{eff} versus ρ_{H_2O} [g/cm^{-3} core vol.] for GCFR Benchmark Bo:
Size: ≙ 300 MWe; Fiss. Prod.: yes; B^{10}: no; T_{fuel}: 1500 K; Pu: dirty

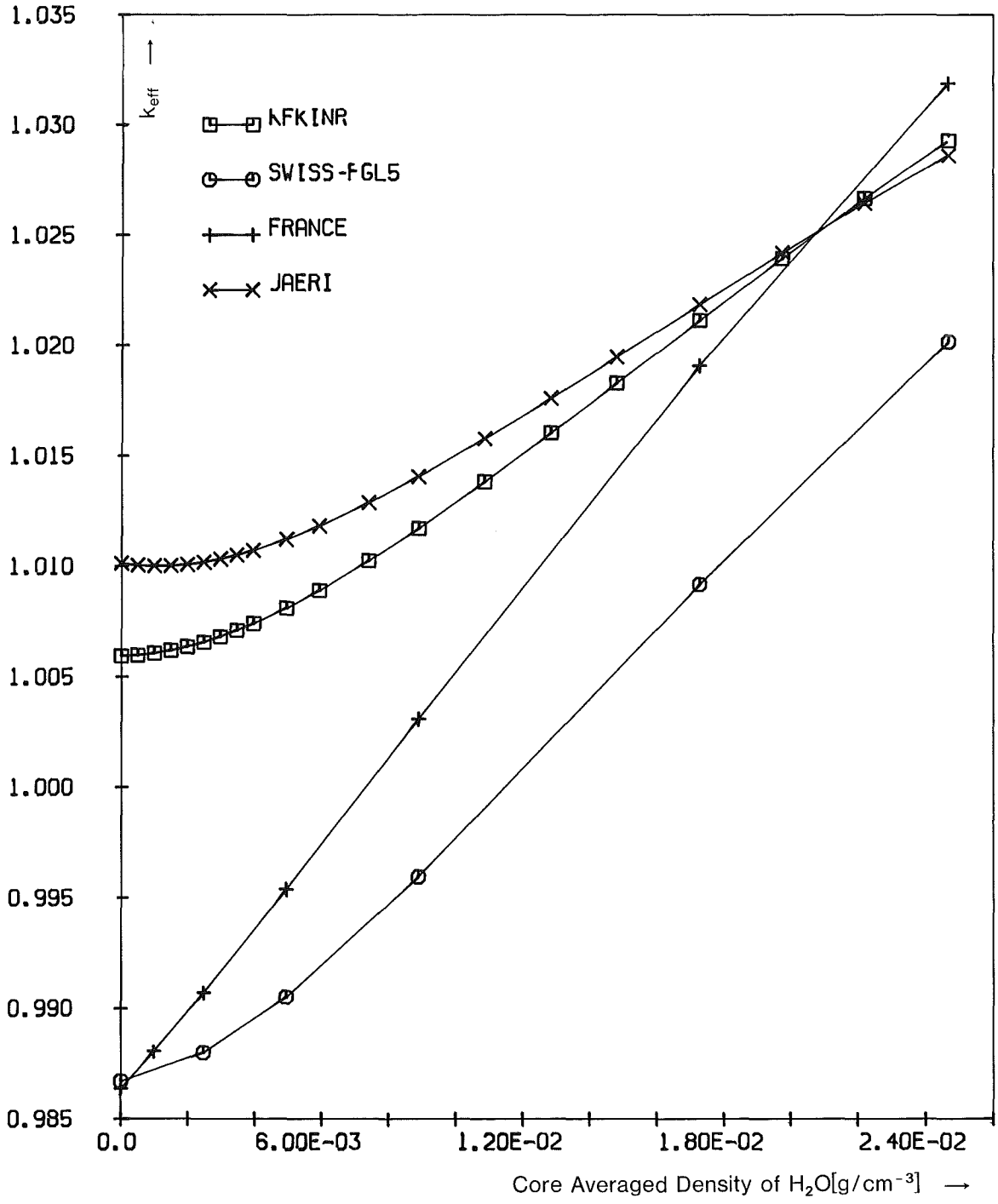

Fig. 2.: k_{eff} versus ρ_{H_2O} [g/cm^{-3} core vol.] for GCFR Benchmark B1:
Size: ≙ 300 MWe; Fiss. Prod.: yes; B^{10}: no; T_{fuel}: 1500 K; Pu: less dirty

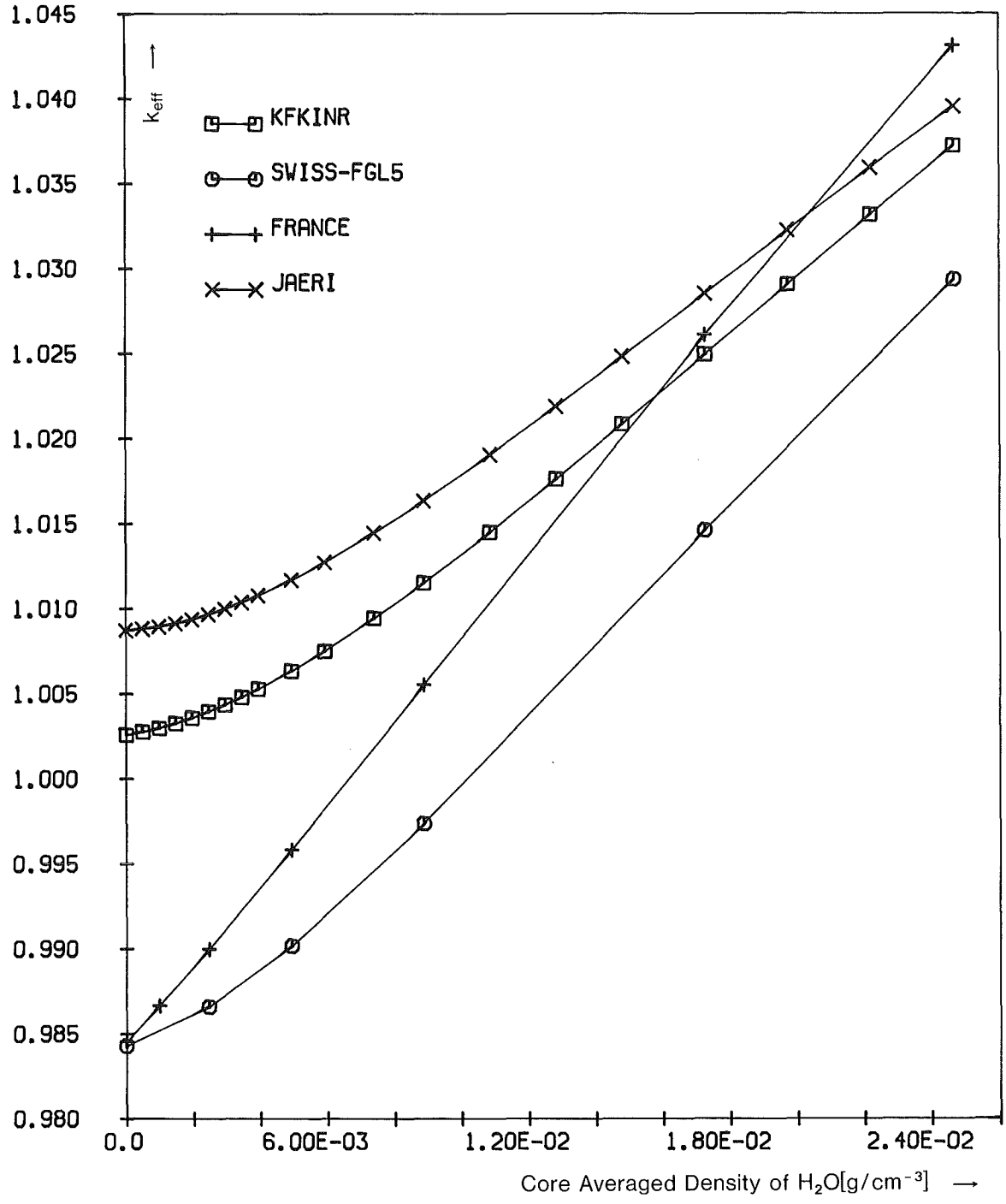

Fig 3.: k_{eff} versus ρ_{H_2O} [g/cm^{-3} core vol.] for GCFR Benchmark B2:
Size: ≙ 300 MWe; Fiss. Prod.: yes; B^{10}: no; T_{fuel}: 1500 K; Pu: clean Pu239

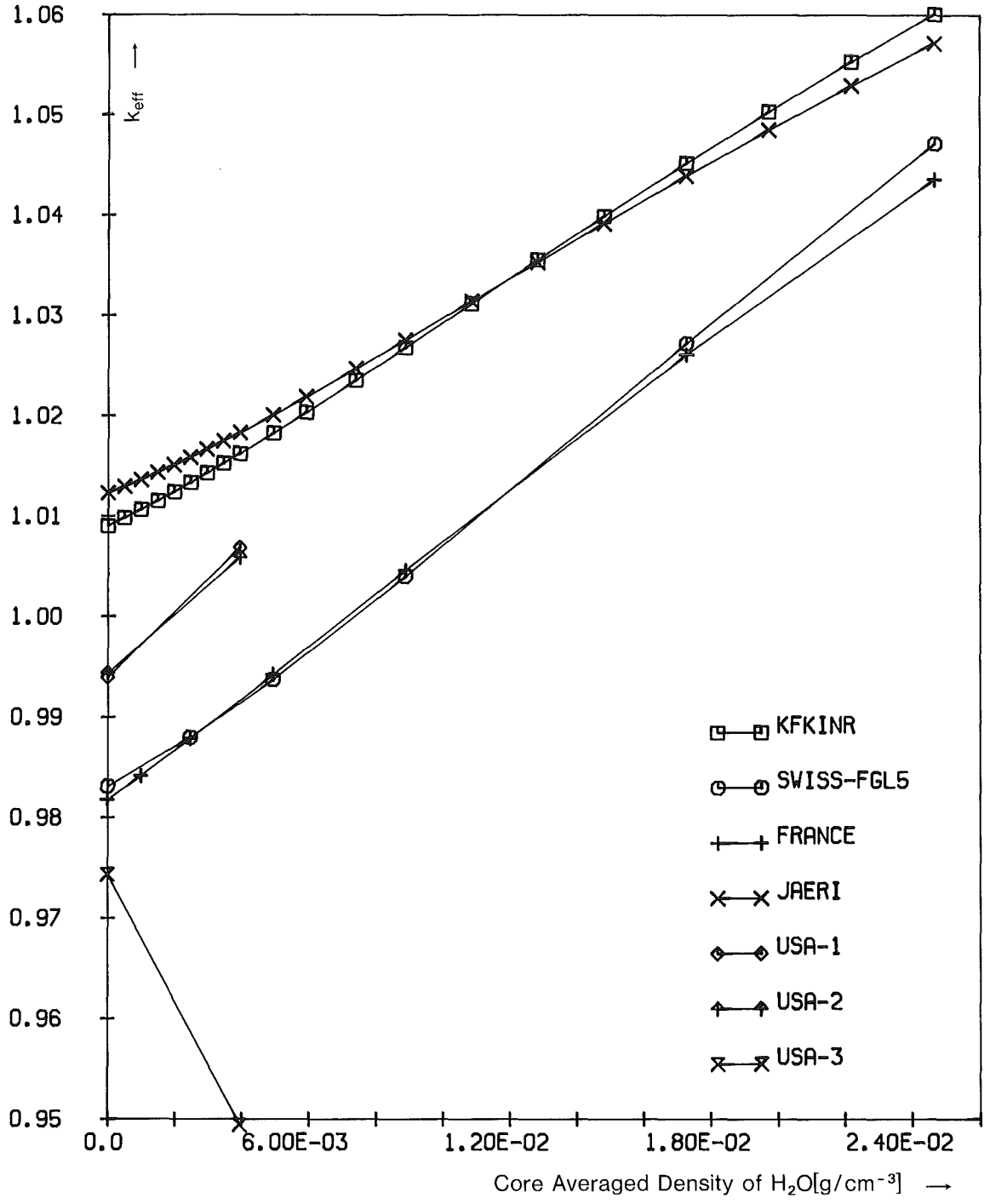

Fig 4.: k_{eff} versus ρ_{H_2O} [g/cm^{-3} core vol.] for GCFR Benchmark B3:
Size: ≙ 300 MWe; Fiss. Prod.: no; B^{10}: yes; T_{fuel}: 1500 K; Pu: dirty

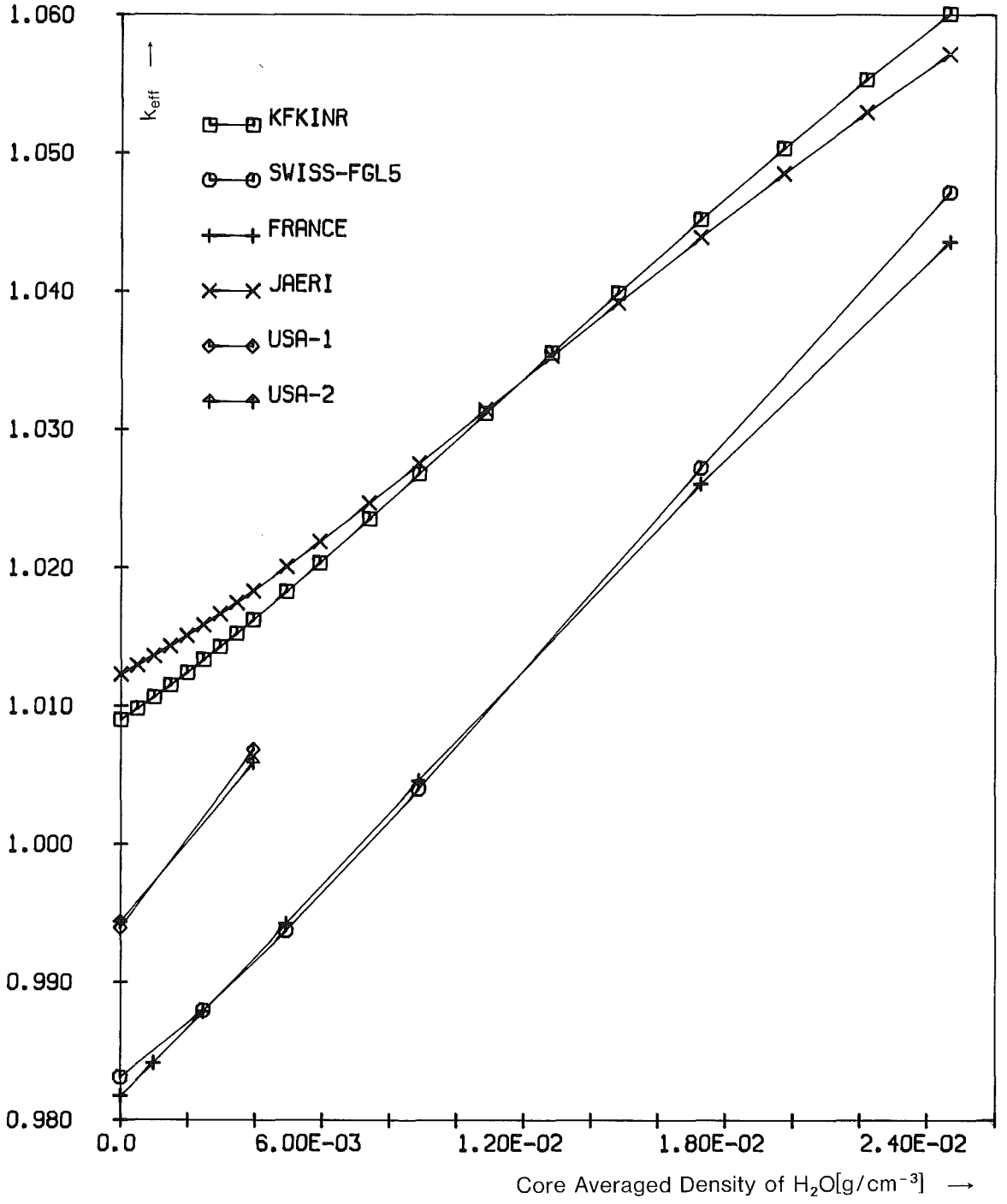

Fig 4a.: k_{eff} versus ρ_{H_2O} [g/cm^{-3} core vol.] for GCFR Benchmark B3:
Size: ≙ 300 MWe; Fiss. Prod.: no; B^{10}: yes; T_{fuel}: 1500 K; Pu: dirty
US-results W/O NRA omitted

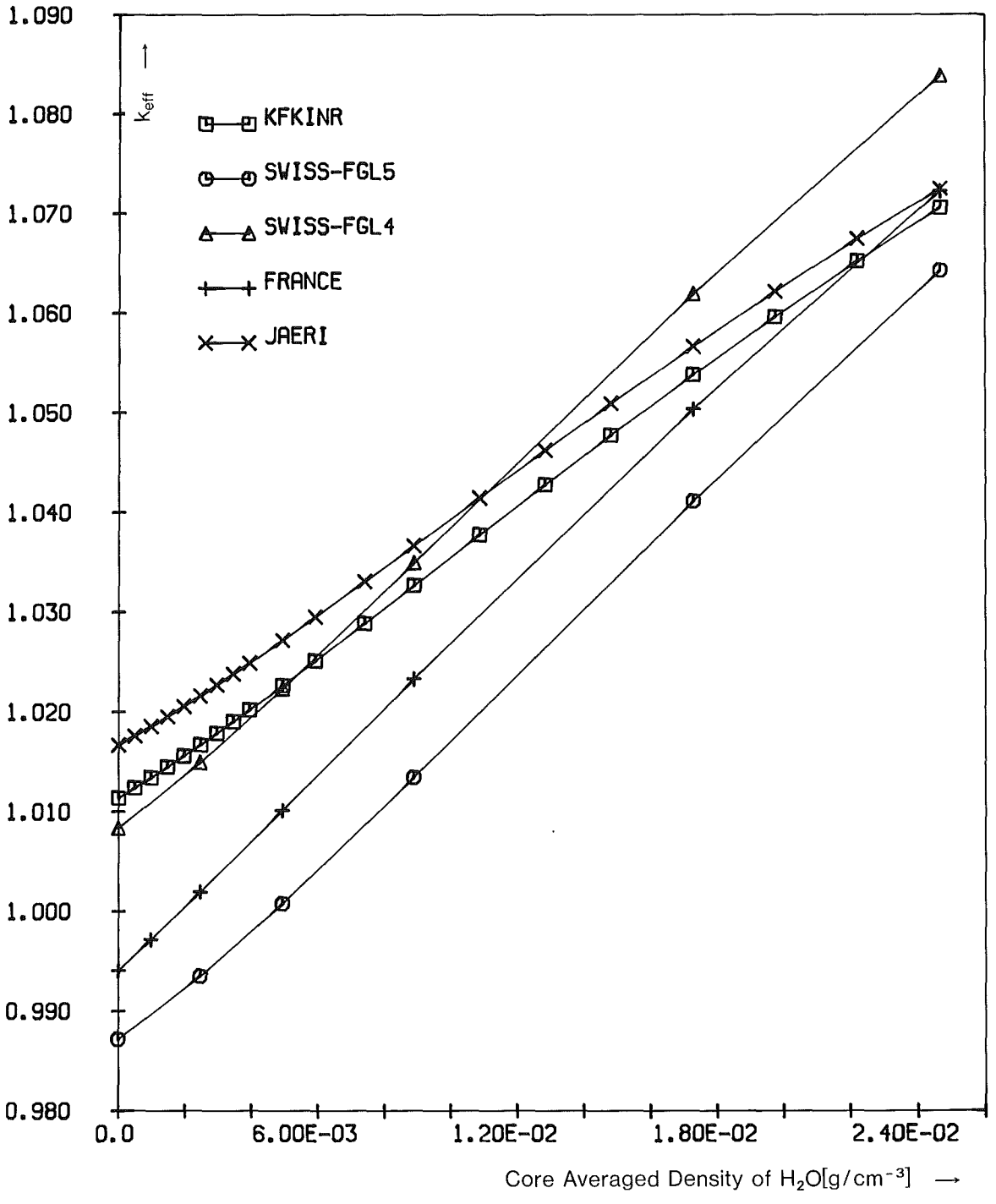

Fig 5.: k_{eff} versus ρ_{H_2O} [g/cm^{-3} core vol.] for GCFR Benchmark B4:
Size: ≙ 300 MWe; Fiss. Prod.: yes; B^{10}: no; T_{fuel}: 300 K; Pu: dirty

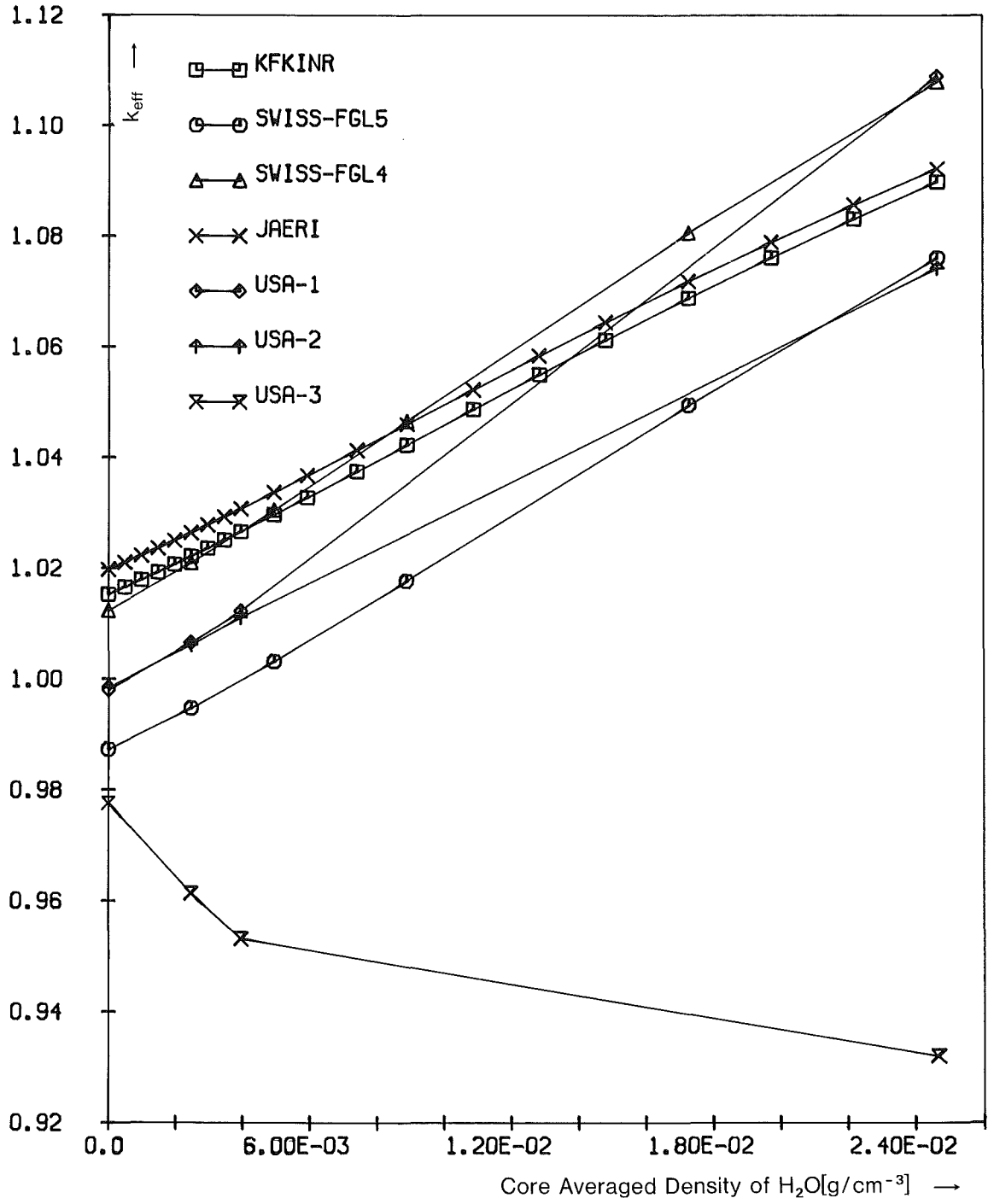

Fig 6.: k_{eff} versus ρ_{H_2O} $[g/cm^{-3}$ core vol.] for GCFR Benchmark B5:
Size: ≙ 300 MWe; Fiss. Prod.: no; B^{10}: no; T_{fuel}: 300 K; Pu: dirty

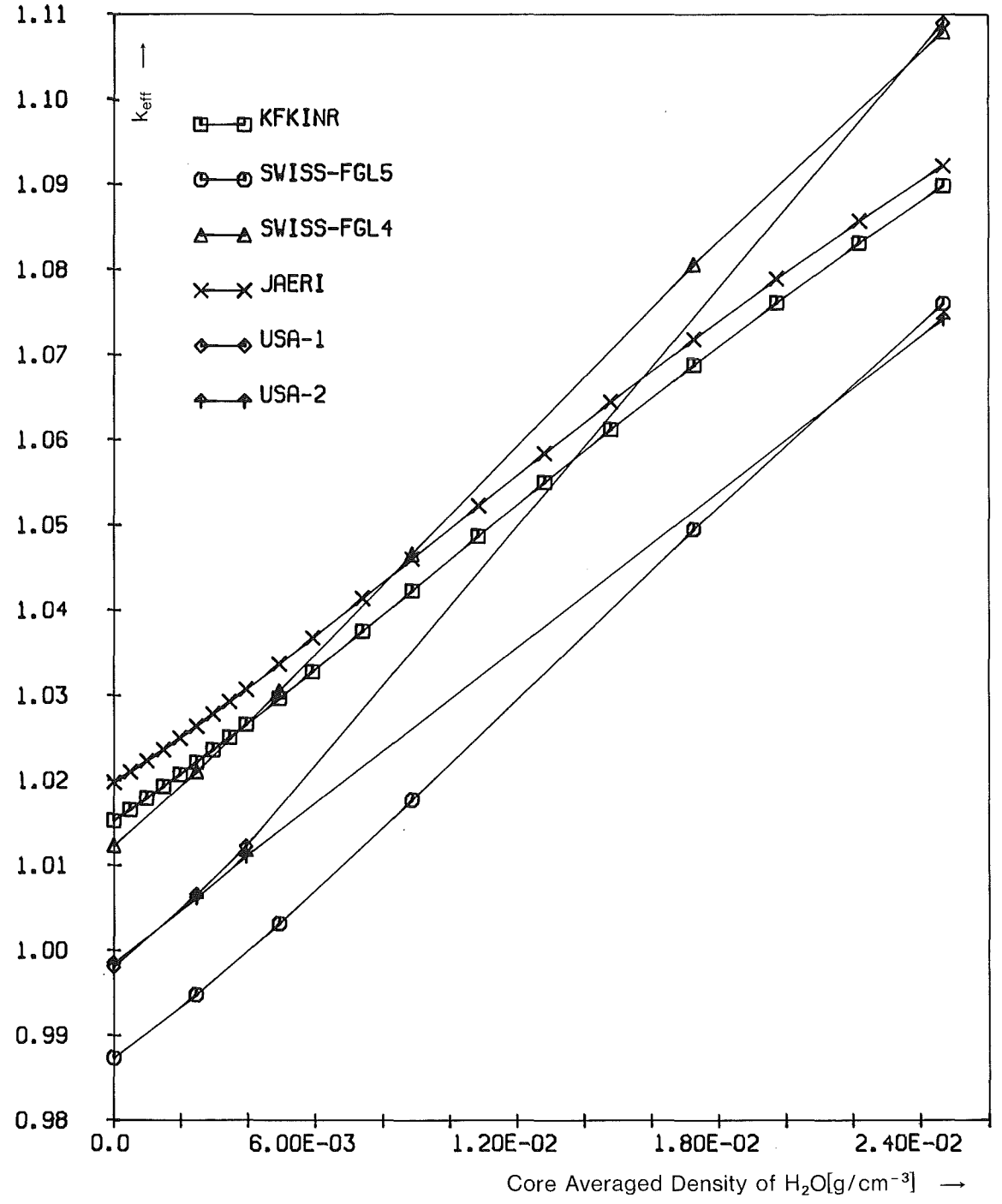

Fig 6a.: k_{eff} versus ρ_{H_2O} [g/cm^{-3} core vol.] for GCFR Benchmark B5:
Size: ≙ 300 MWe; Fiss. Prod.: no; B^{10}: no; T_{fuel}: 300 K; Pu: dirty
US-results W/O NRA omitted

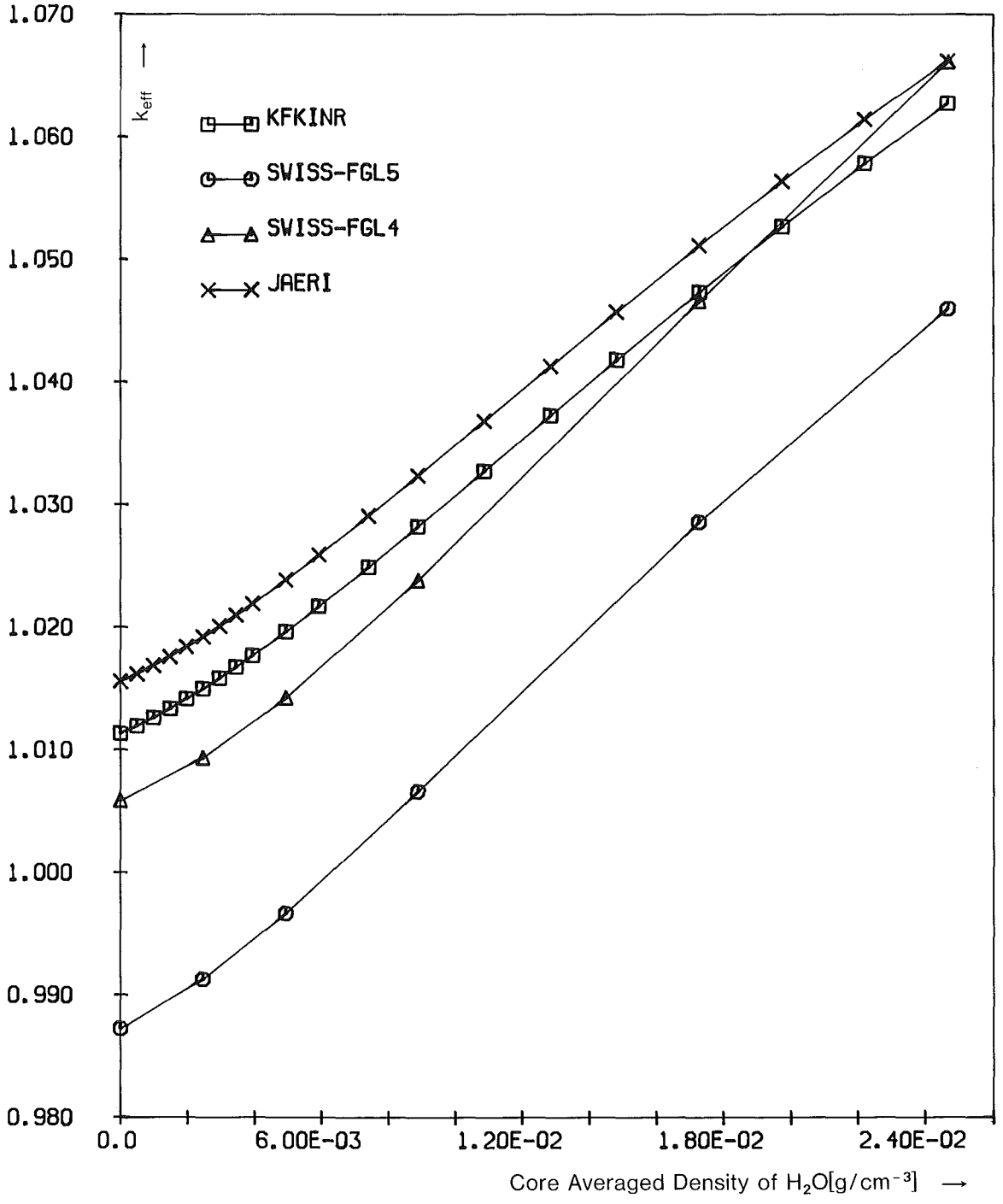

Fig 7.: k_{eff} versus ρ_{H_2O} [g/cm^{-3} core vol.] for GCFR Benchmark B6:
Size: ≙ 300 MWe; Fiss. Prod.: no; B^{10}: no; T_{fuel}: 300 K; Pu: less dirty

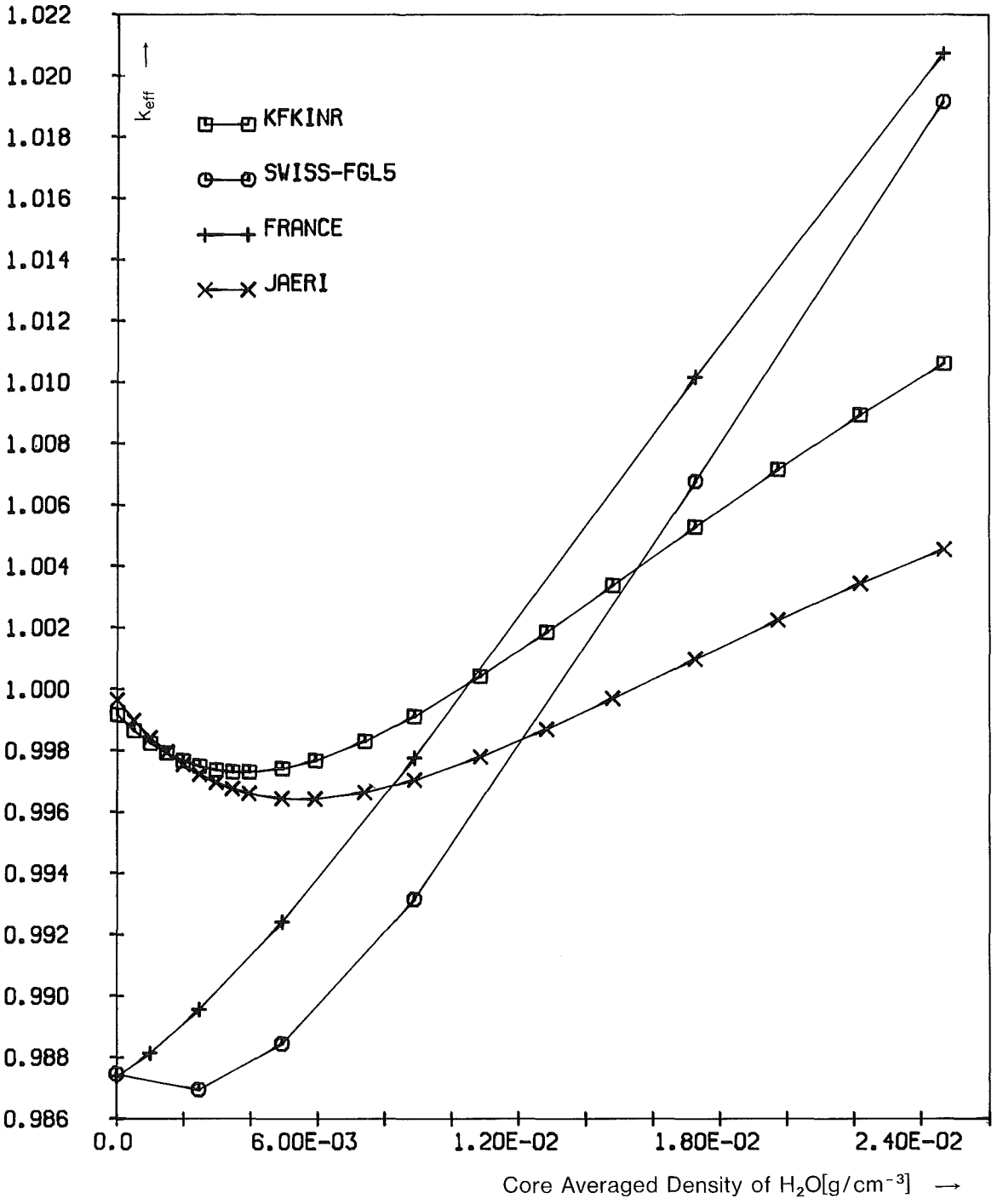

Fig 8.: k_{eff} versus ρ_{H_2O} [g/cm^{-3} core vol.] for GCFR Benchmark B7:
Size: ≙ 1000 MWe; Fiss. Prod.: yes; B^{10}: no; T_{fuel}: 1500 K; Pu: dirty

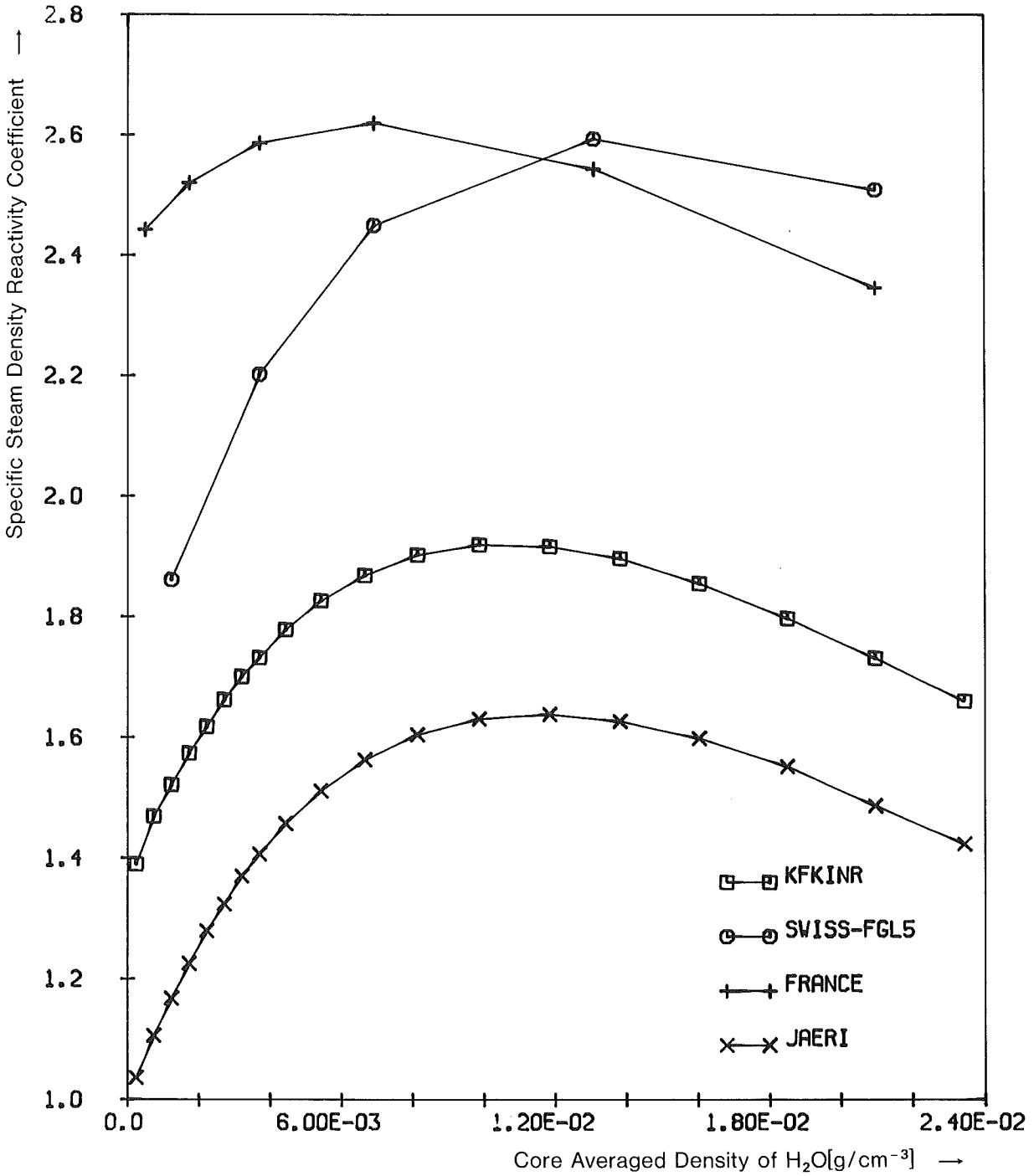

Fig 9.: SSDRC versus ρ_{H_2O} [g/cm^{-3} core vol.] for GCFR Benchmark Bo:
Size: ≙ 300 MWe; Fiss. Prod.: yes; B^{10}: no; T_{fuel}: 1500 K; Pu: dirty

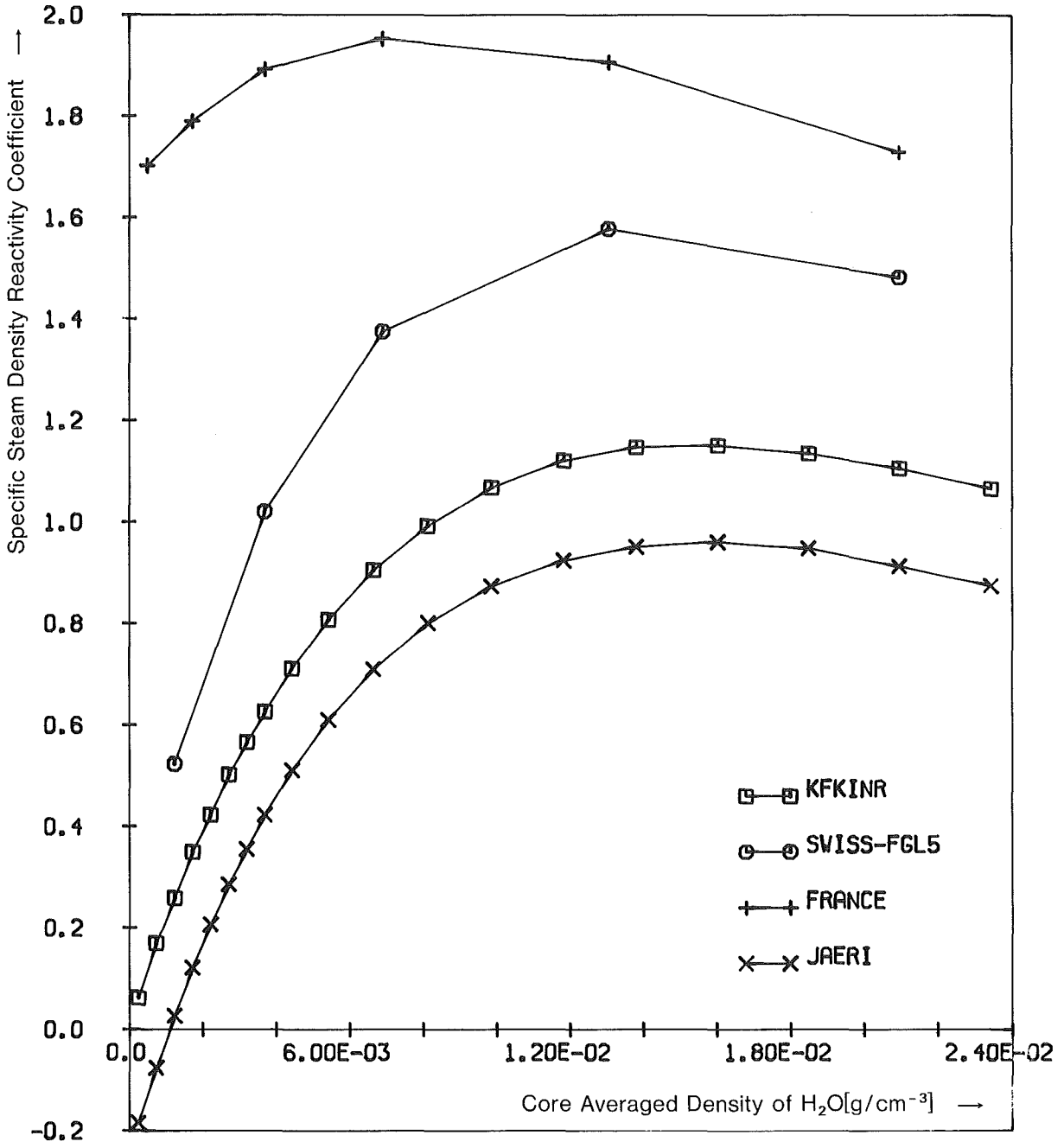

Fig 10.: SSDRC versus ρ_{H_2O} [g/cm^{-3} core vol.] for GCFR Benchmark B1:
Size: ≙ 300 MWe; Fiss. Prod.: yes; B^{10}: no; T_{fuel}: 1500 K; Pu: less dirty

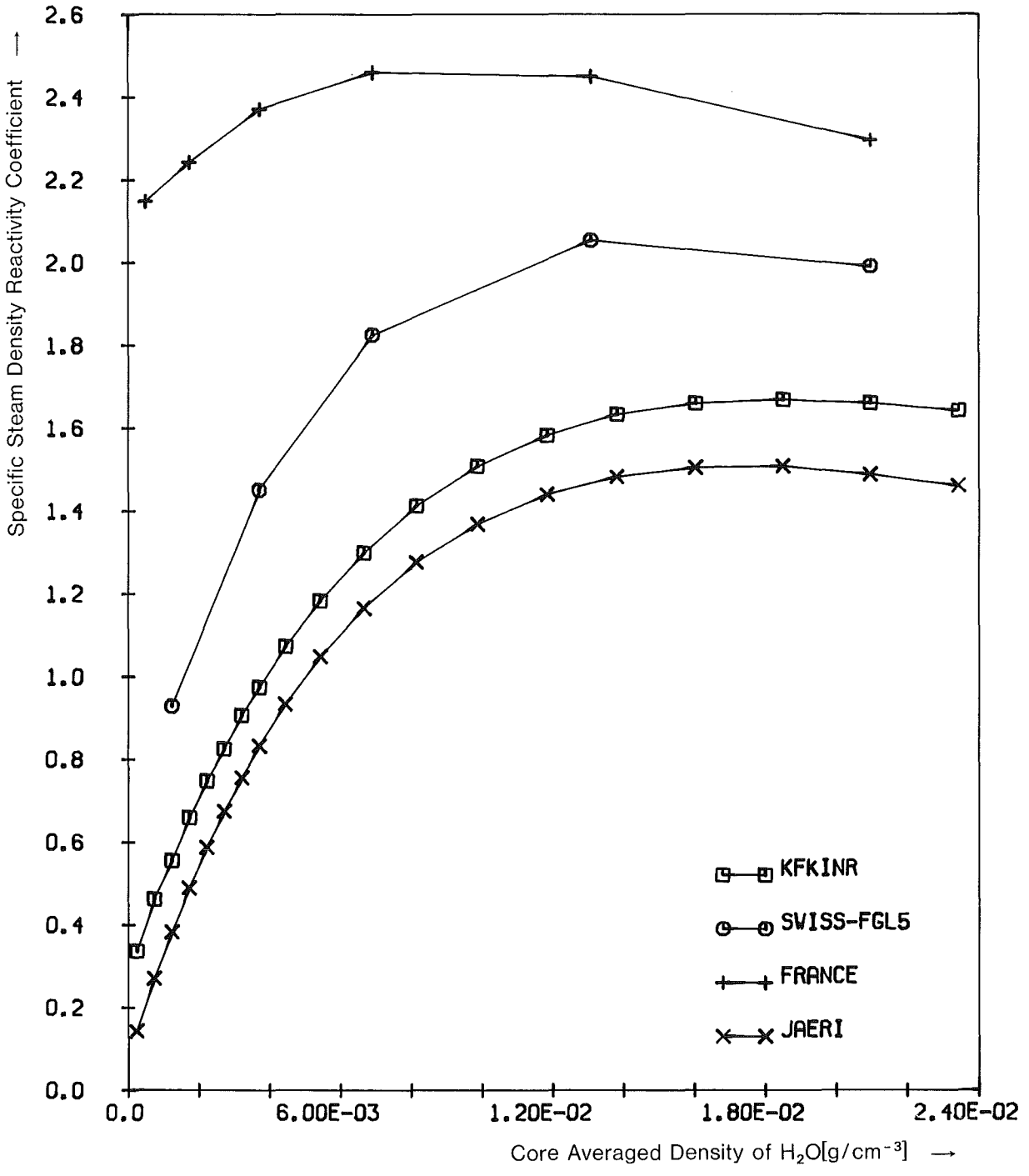

Fig 11.: SSDRC versus ρ_{H_2O} [g/cm^{-3} core vol.] for GCFR Benchmark B2:
Size: ≙ 300 MWe; Fiss. Prod.: yes; B^{10}: no; T_{fuel}: 1500 K; Pu: clean Pu239

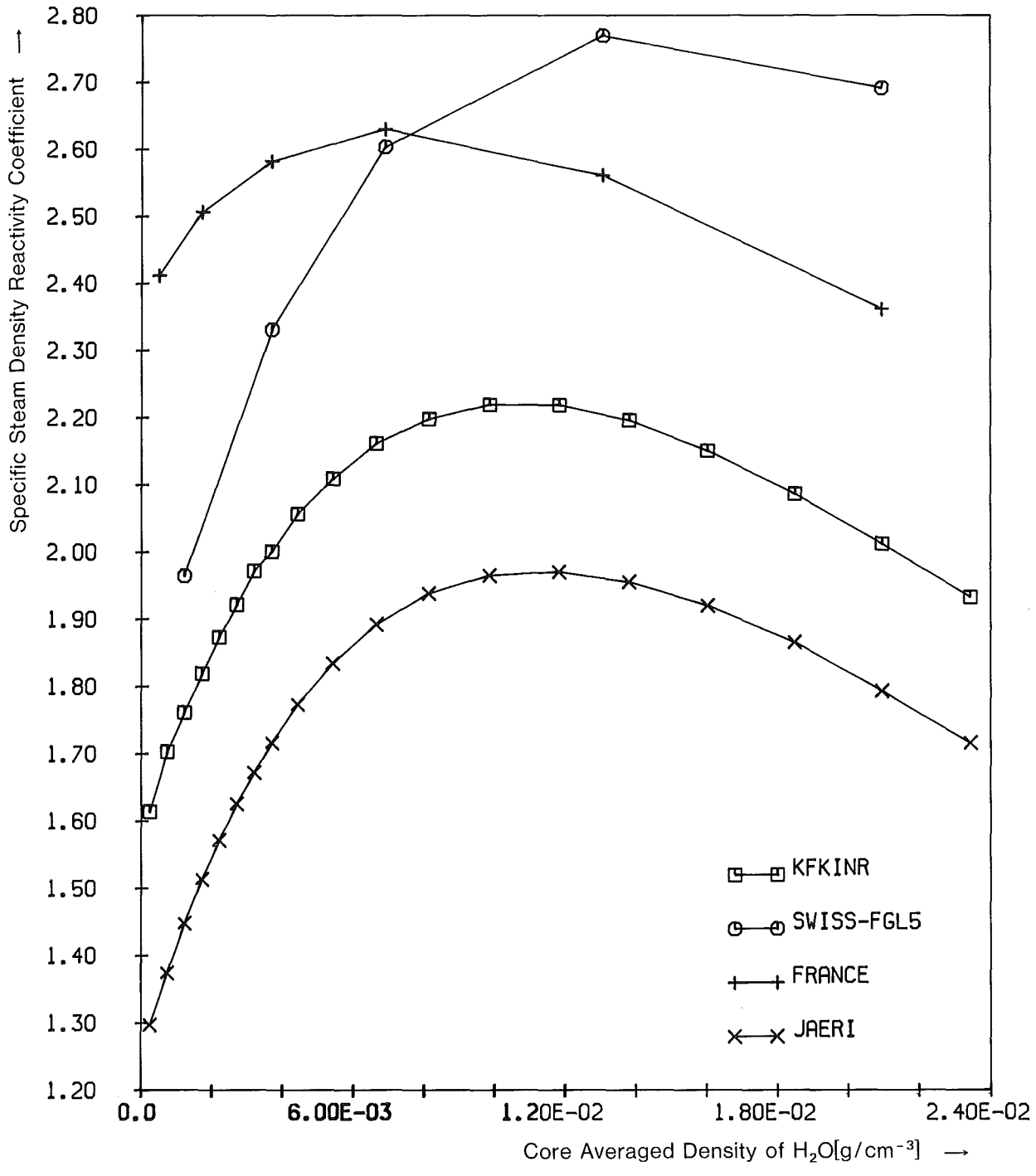

Fig 12.: SSDRC versus ρ_{H_2O} [g/cm^{-3} core vol.] for GCFR Benchmark B3:
Size: ≙ 300 MWe; Fiss. Prod.: no; B^{10}: yes; T_{fuel}: 1500 K; Pu: dirty

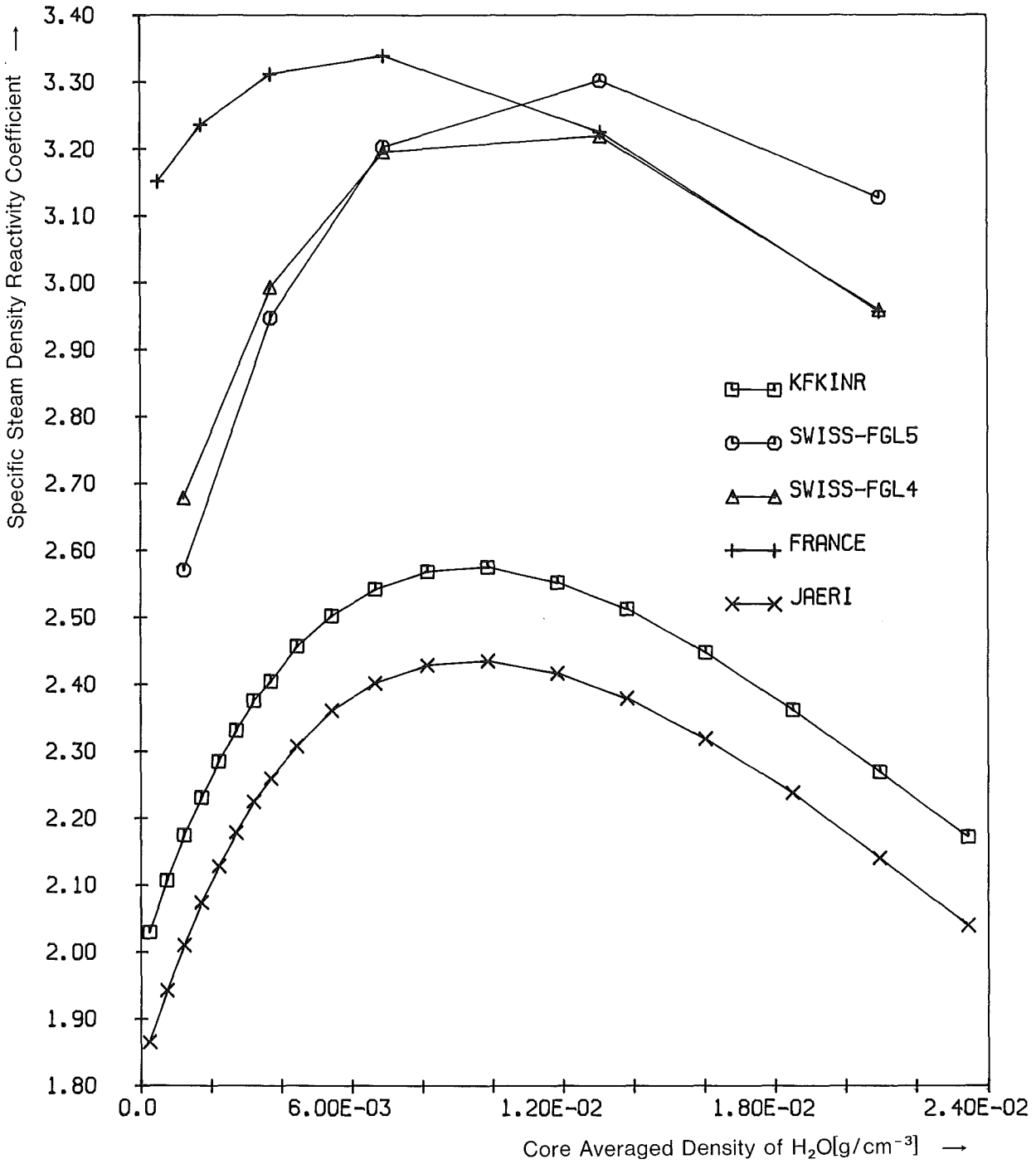

Fig 13.: SSDRC versus ρ_{H_2O} [g/cm^{-3} core vol.] for GCFR Benchmark B4:
Size: ≙ 300 MWe; Fiss. Prod.: yes; B^{10}: no; T_{fuel}: 300 K; Pu: dirty

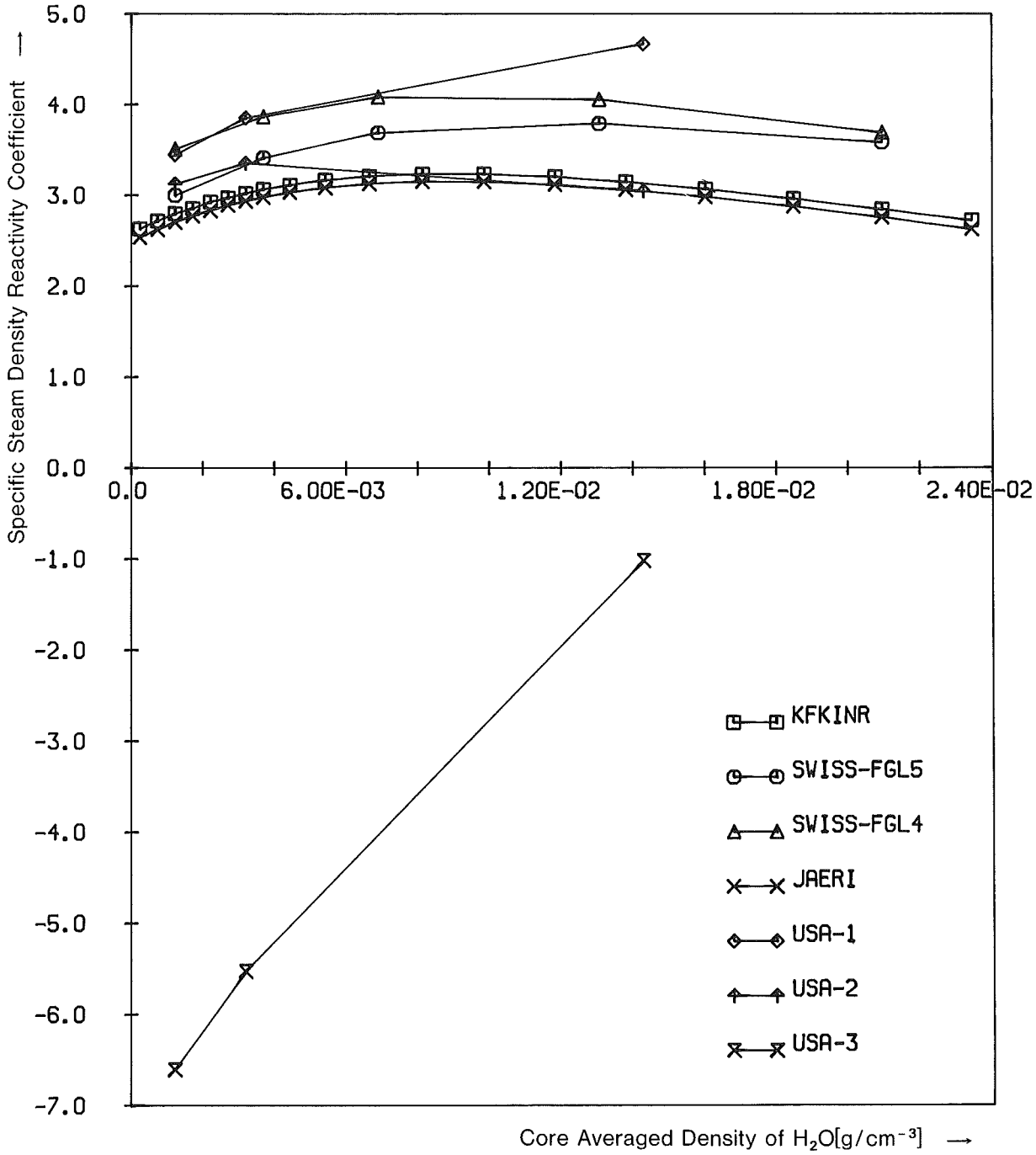

Fig 14.: SSDRC versus ρ_{H_2O} [g/cm^{-3} core vol.] for GCFR Benchmark B5:
Size: ≙ 300 MWe; Fiss. Prod.: no; B^{10}: no; T_{fuel}: 300 K; Pu: dirty

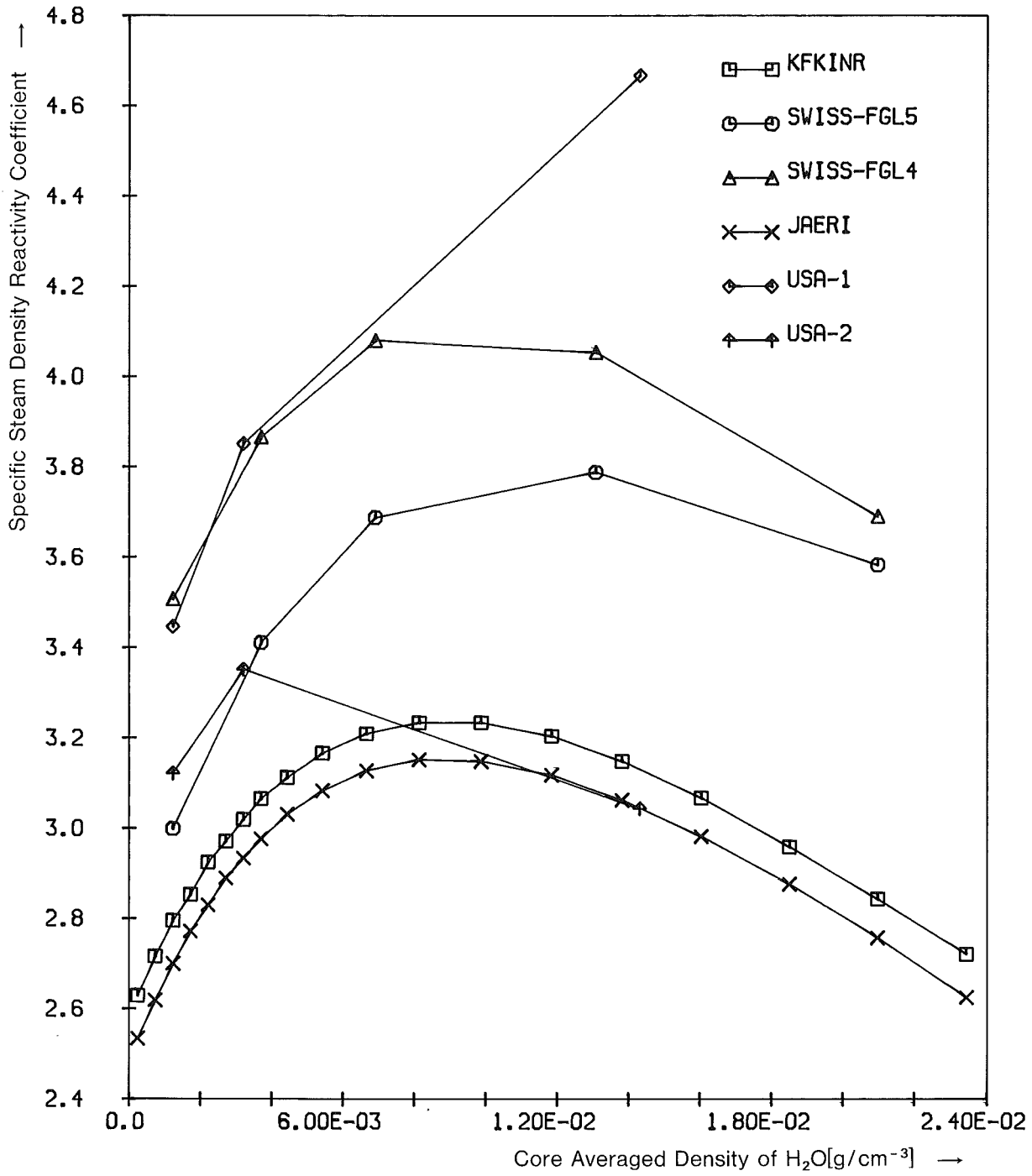

Fig 14a.: SSDRC versus ρ_{H_2O} [g/cm^{-3} core vol.] for GCFR Benchmark B5:
Size: ≙ 300 MWe; Fiss. Prod.: no; B^{10}: no; T_{fuel}: 300 K; Pu: dirty
US-results W/O NRA omitted

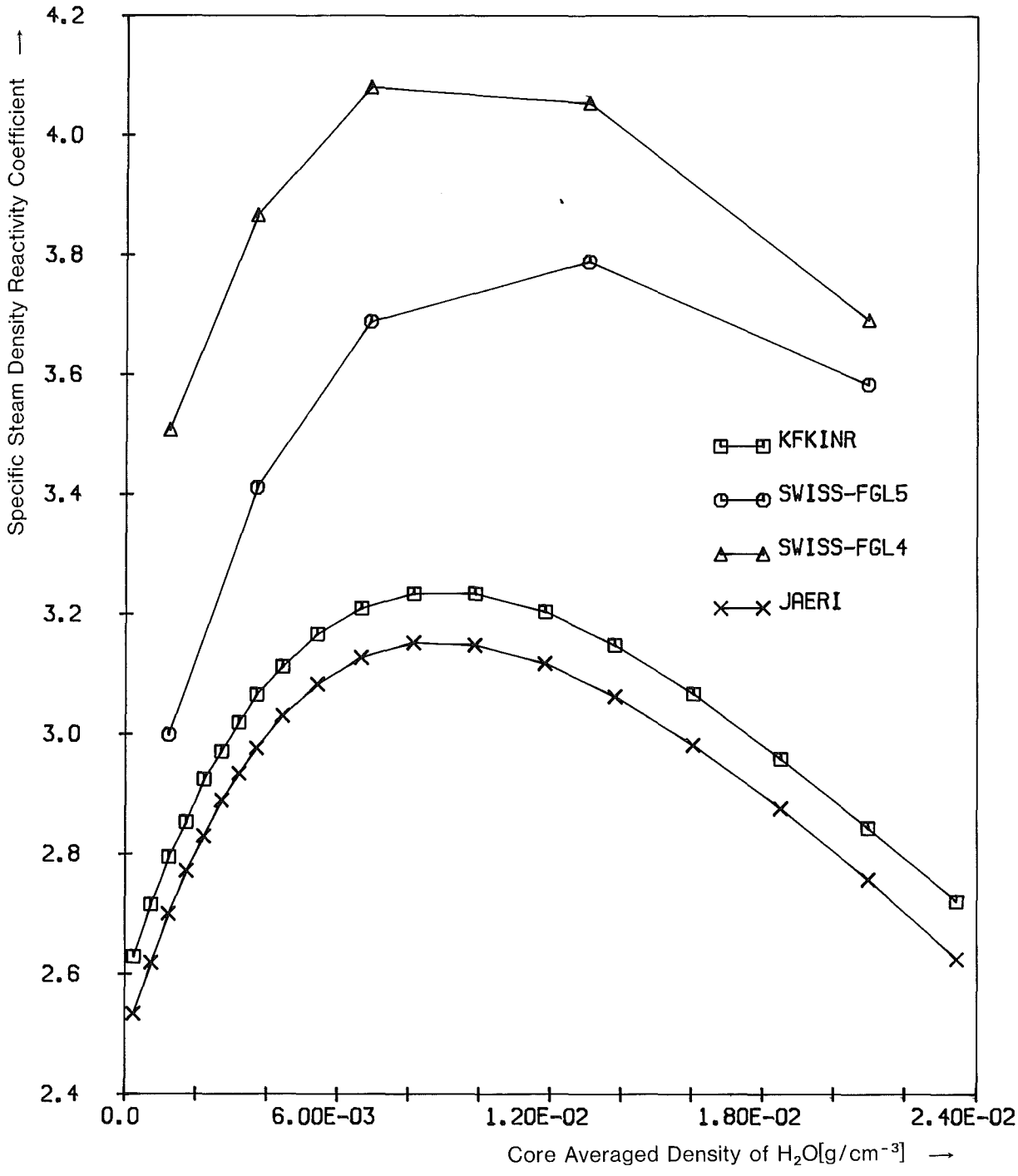

Fig 14b.: SSDRC versus ρ_{H_2O} [g/cm^{-3} core vol.] for GCFR Benchmark B5:
Size: ≙ 300 MWe; Fiss. Prod.: no; B^{10}: no; T_{fuel}: 300 K; Pu: dirty
US-results completely omitted

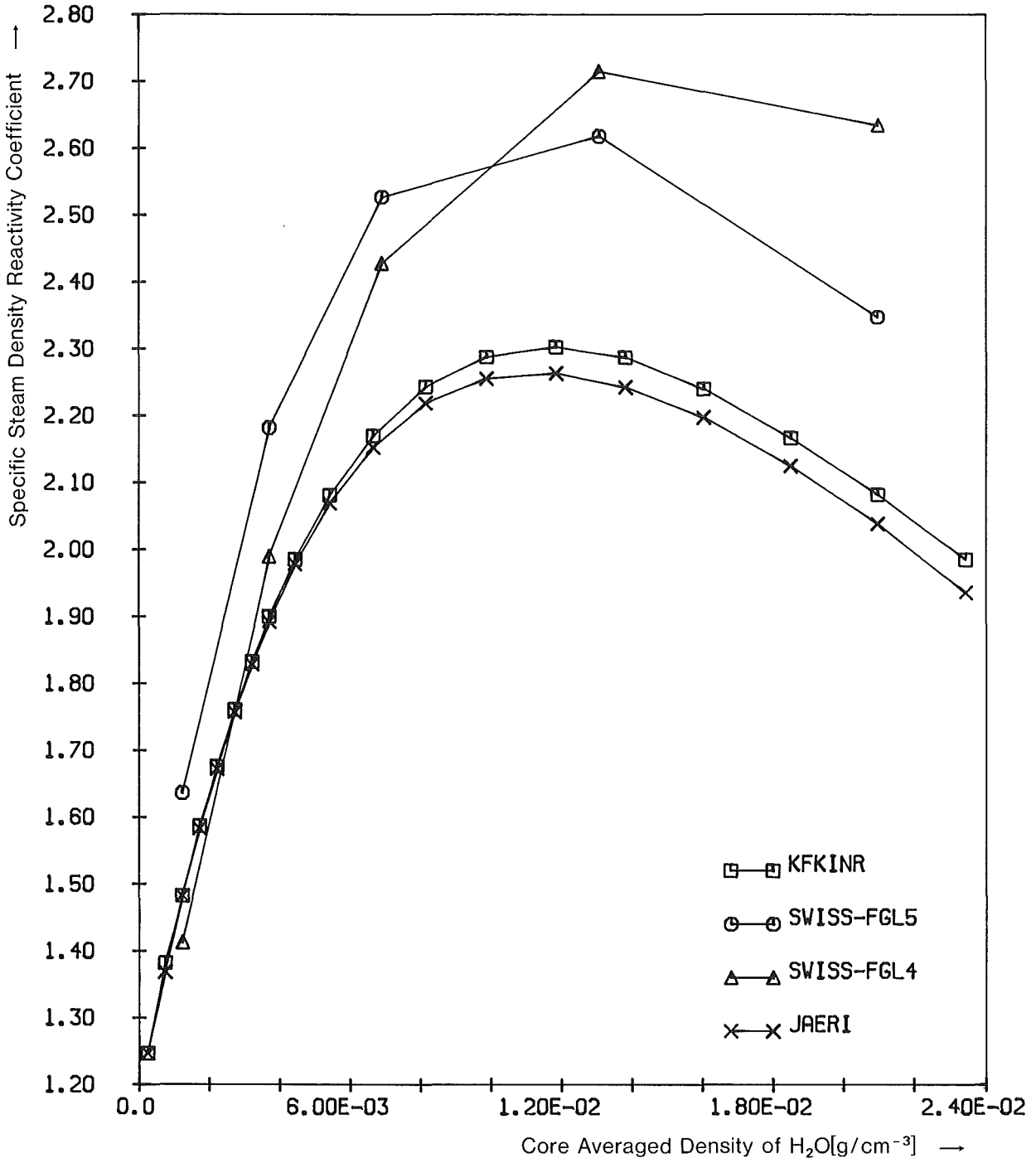

Fig 15.: SSDRC versus ρ_{H_2O} [g/cm^{-3} core vol.] for GCFR Benchmark B6:
Size: ≙ 300 MWe; Fiss. Prod.: no; B^{10}: no; T_{fuel}: 300 K; Pu: less dirty

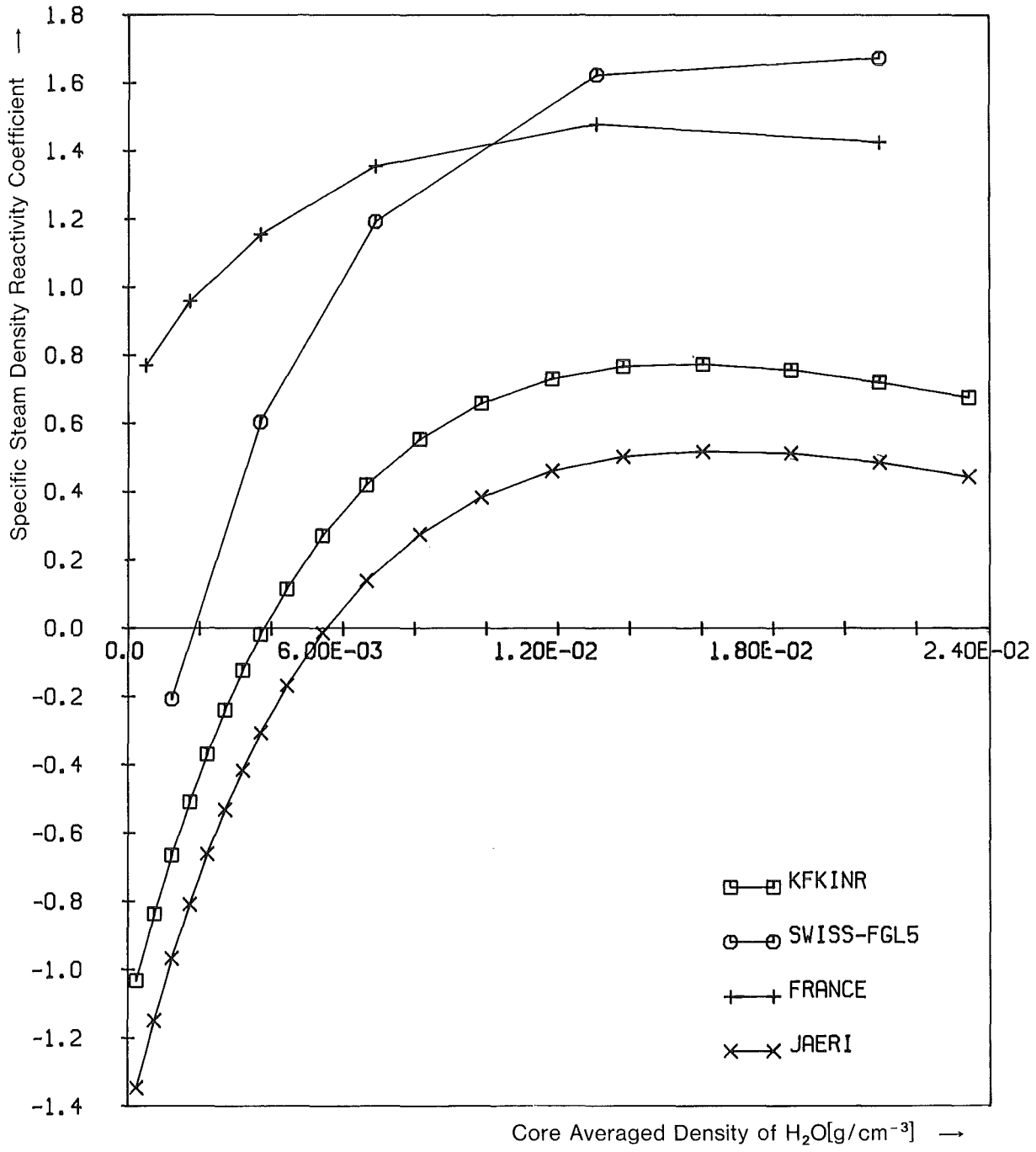

Fig 16.: SSDRC versus ρ_{H_2O} [g/cm^{-3} core vol.] for GCFR Benchmark B7:
Size: ≙ 1000 MWe; Fiss. Prod.: yes; B^{10}: no; T_{fuel}: 1500 K; Pu: dirty

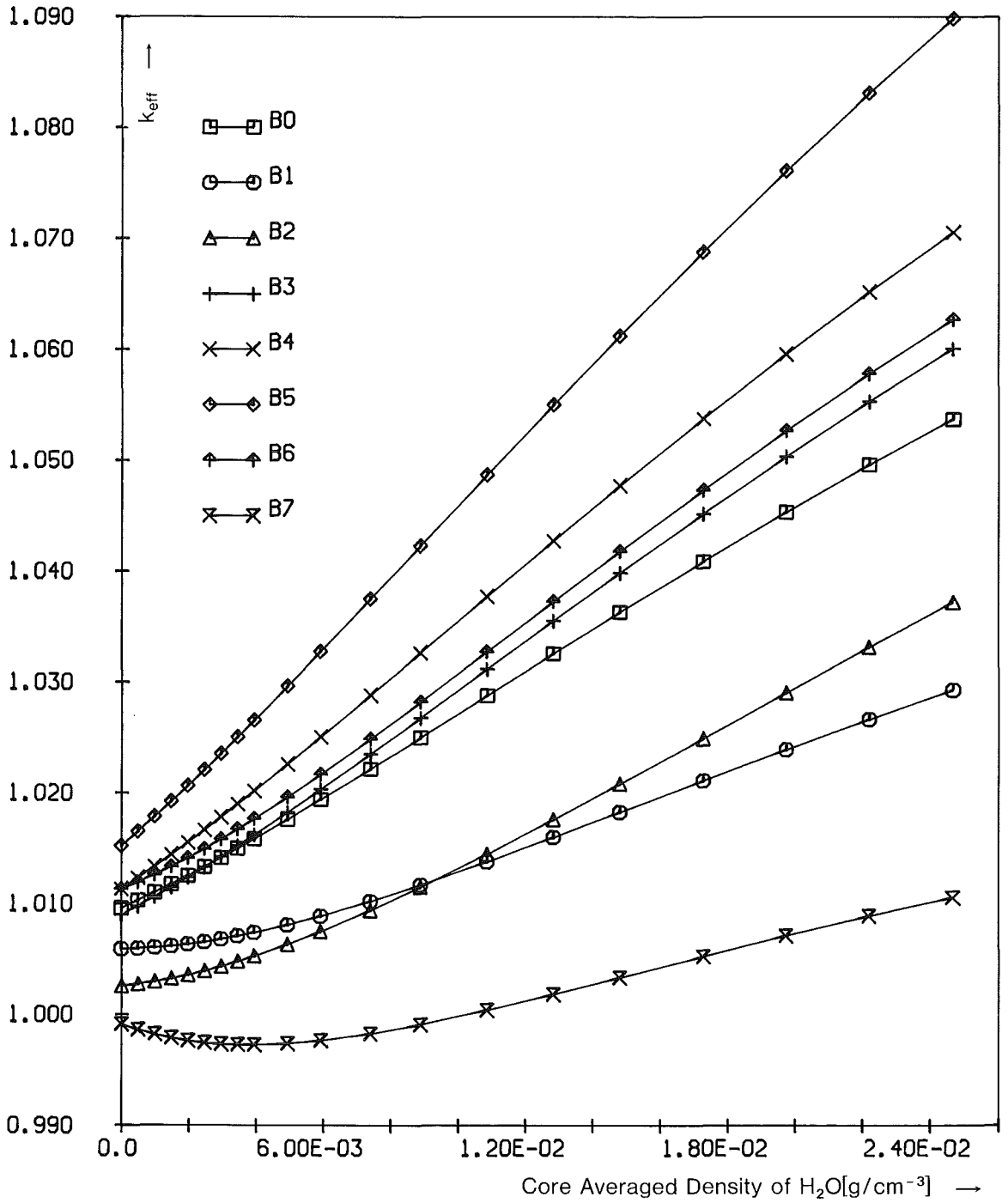

Fig 17.: Criticality values as function of the average core steam density for steam ingress into a GCFR core
German results for all Benchmark cases Bo ... B7

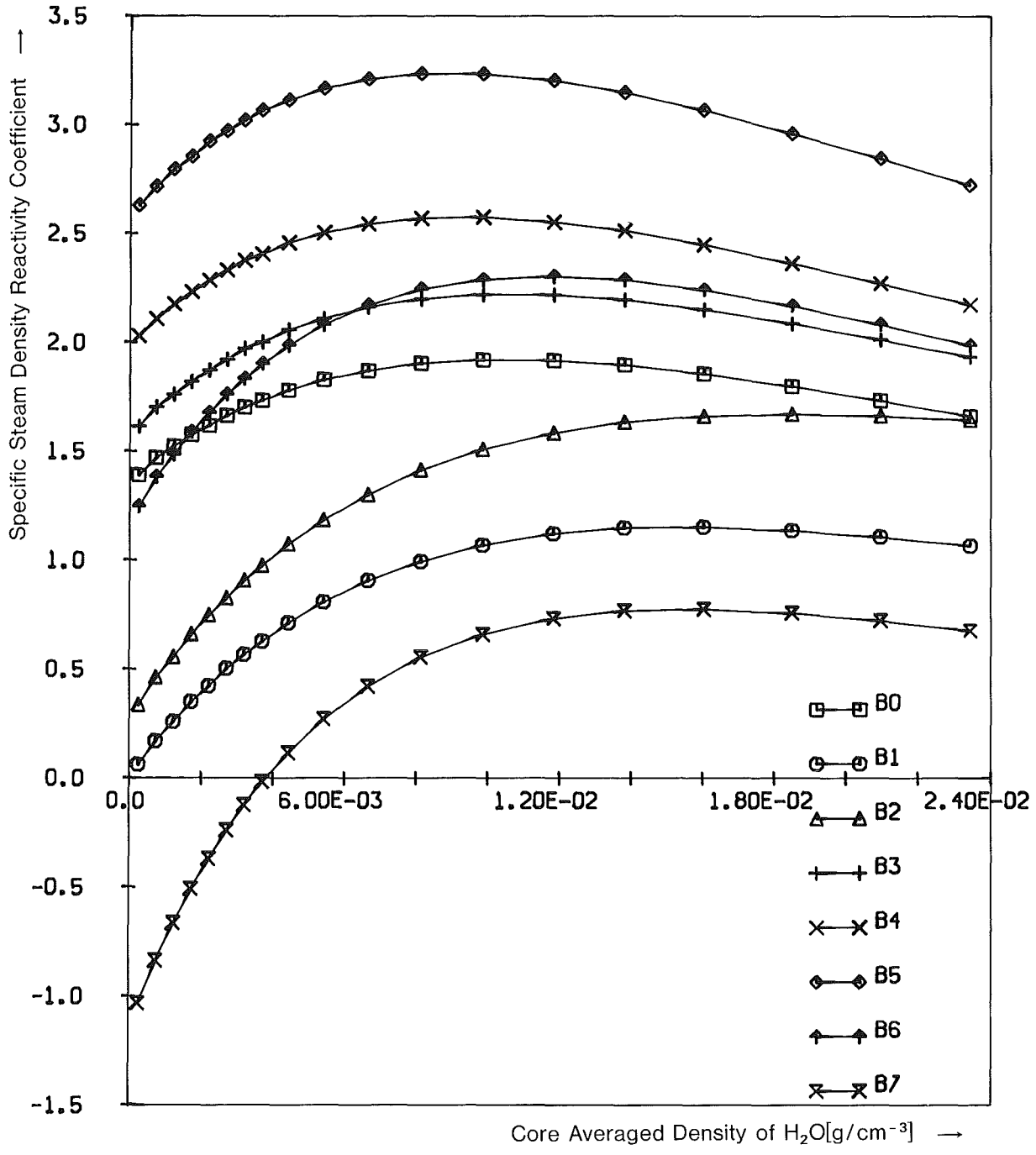

Fig 18.: Specific steam density reactivity coefficients as function of the average core steam density for steam ingress into a GCFR core German results for all Benchmark cases Bo ... B7

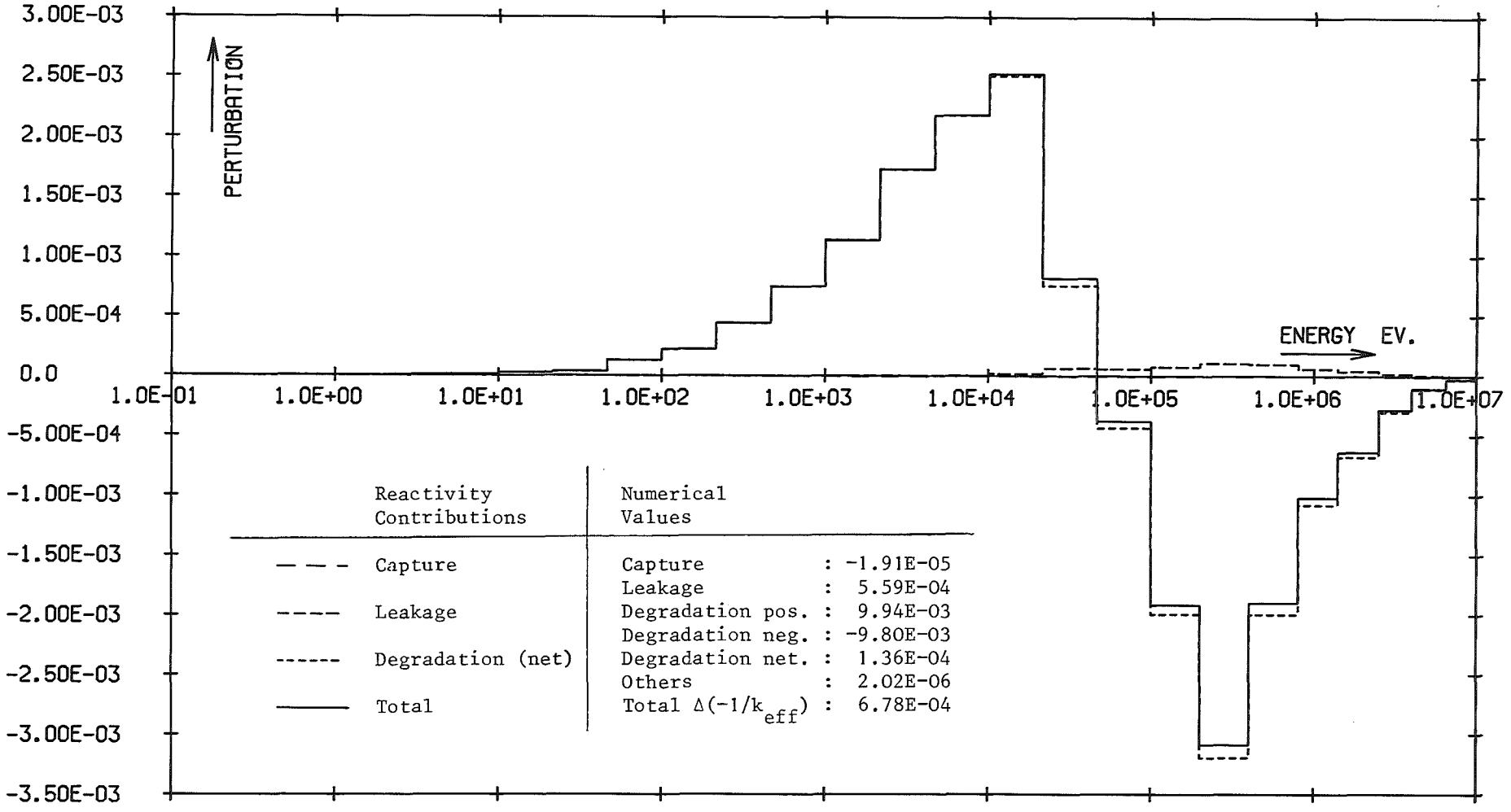

Fig. 19
Reactivity change caused by the addition of about $5 \cdot 10^{-4}$ g of water per 1 cm^3 of average core composition of a GCFR.
Group-wise representation of individual components and total values $[\Delta(-1/k_{eff})]$ from fundamental mode calculations for case B_o

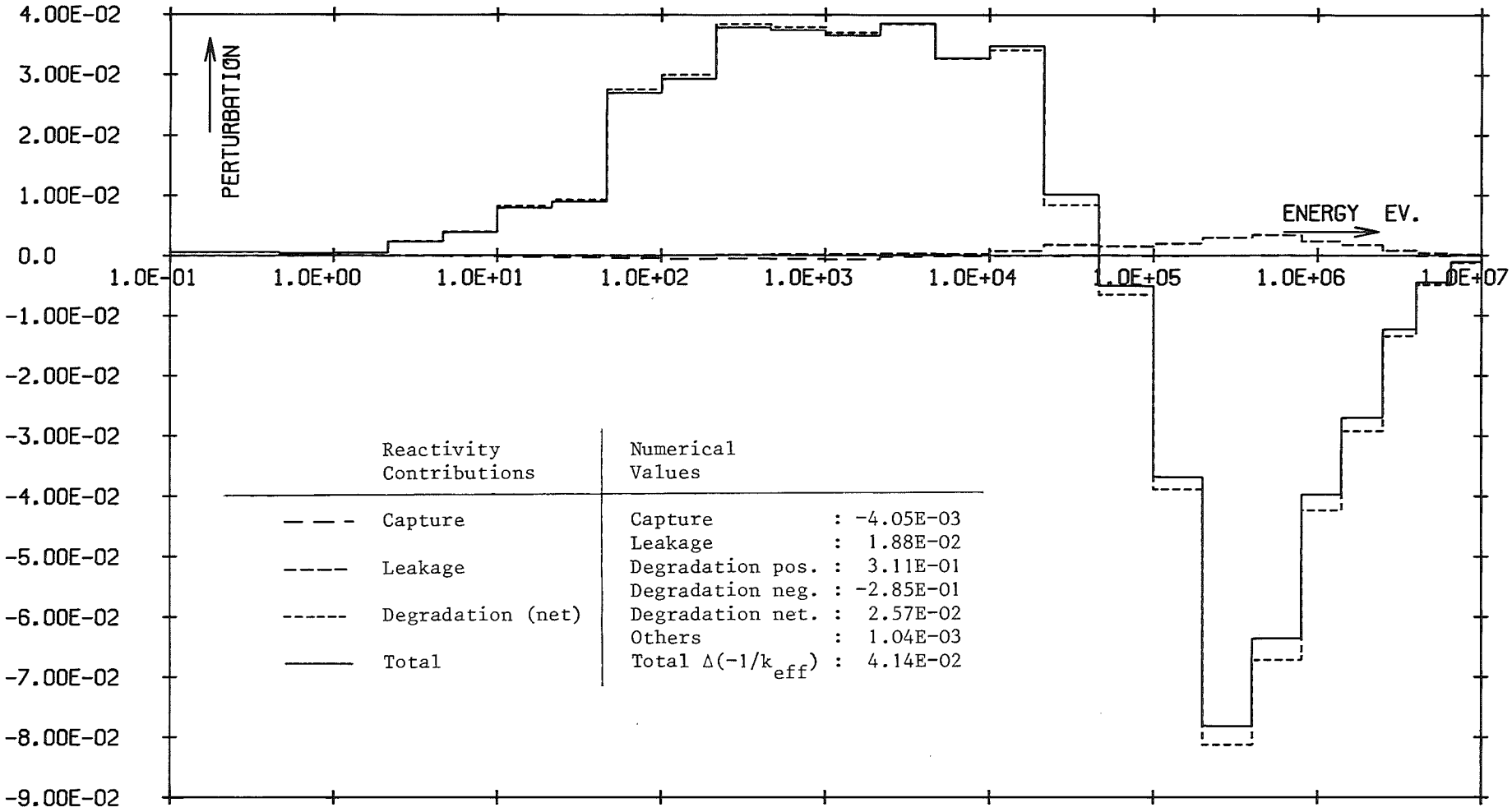

Fig. 20

Reactivity change caused by the addition of about $2.5 \cdot 10^{-2}$ g of water per 1 cm^3 of average core composition of a GCFR.

Group-wise representation of individual components and total values $[\Delta(-1/k_{eff})]$ from fundamental mode calculations for case B_o

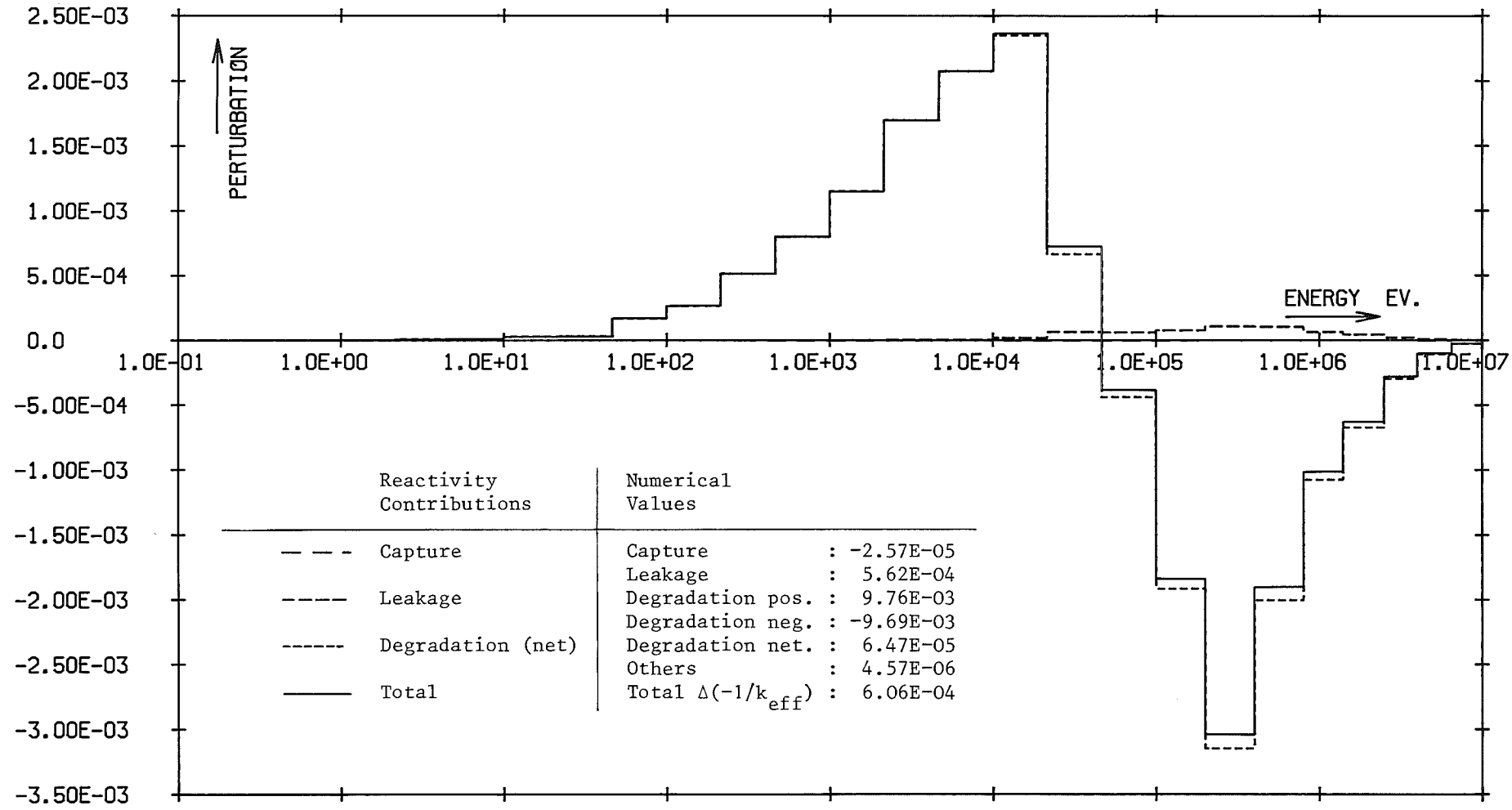

Fig. 21

Reactivity change caused by the addition of about $5 \cdot 10^{-4}$ g of water per $1 cm^3$ of average core composition of a GCFR.

Group-wise representation of individual components and total values $[\Delta(-1/k_{eff})]$ from fundamental mode calculations for case B6

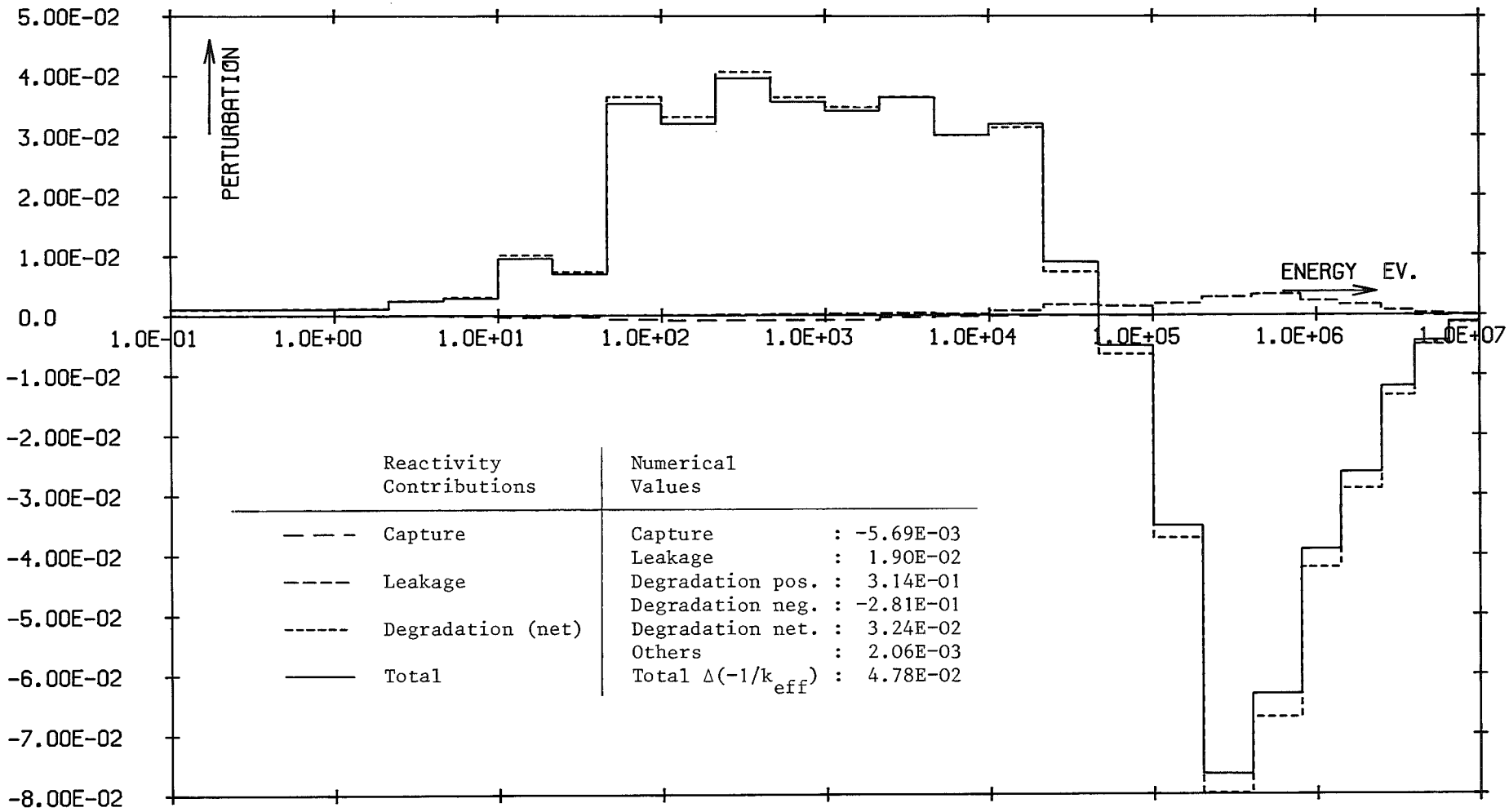

Fig. 22

Reactivity change caused by the addition of about $2.5 \cdot 10^{-2}$ g of water per 1 cm^3 of average core composition of a GCFR.

Group-wise representation of individual components and total values $[\Delta(-1/k_{eff})]$ from fundamental mode calculations for case B6

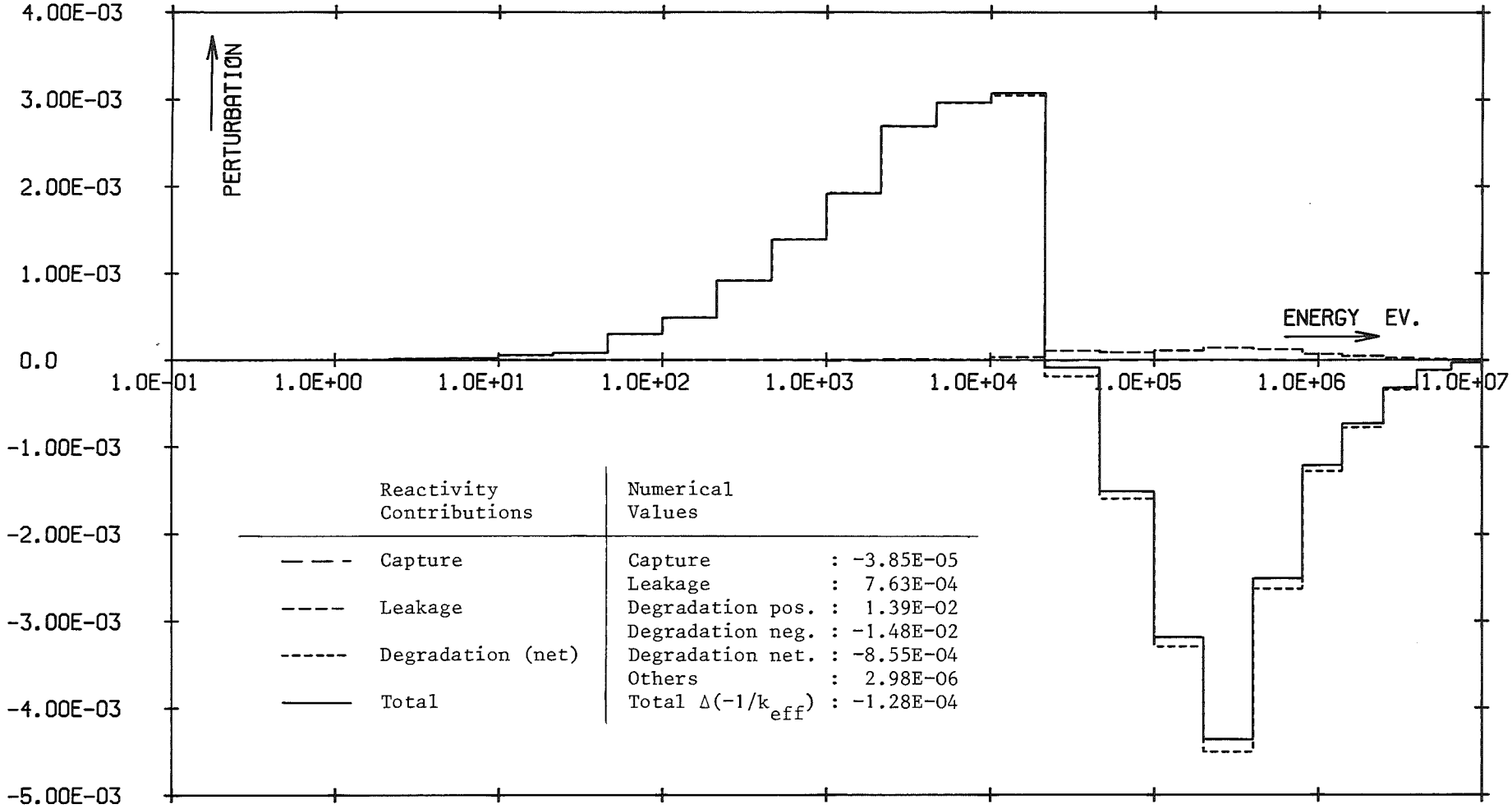

Fig. 23

Reactivity change caused by the addition of about $5 \cdot 10^{-4}$ g of water per 1 cm^3 of average core composition of a GCFR.

Group-wise representation of individual components and total values $[\Delta(-1/k_{eff})]$ from fundamental mode calculations for case B7

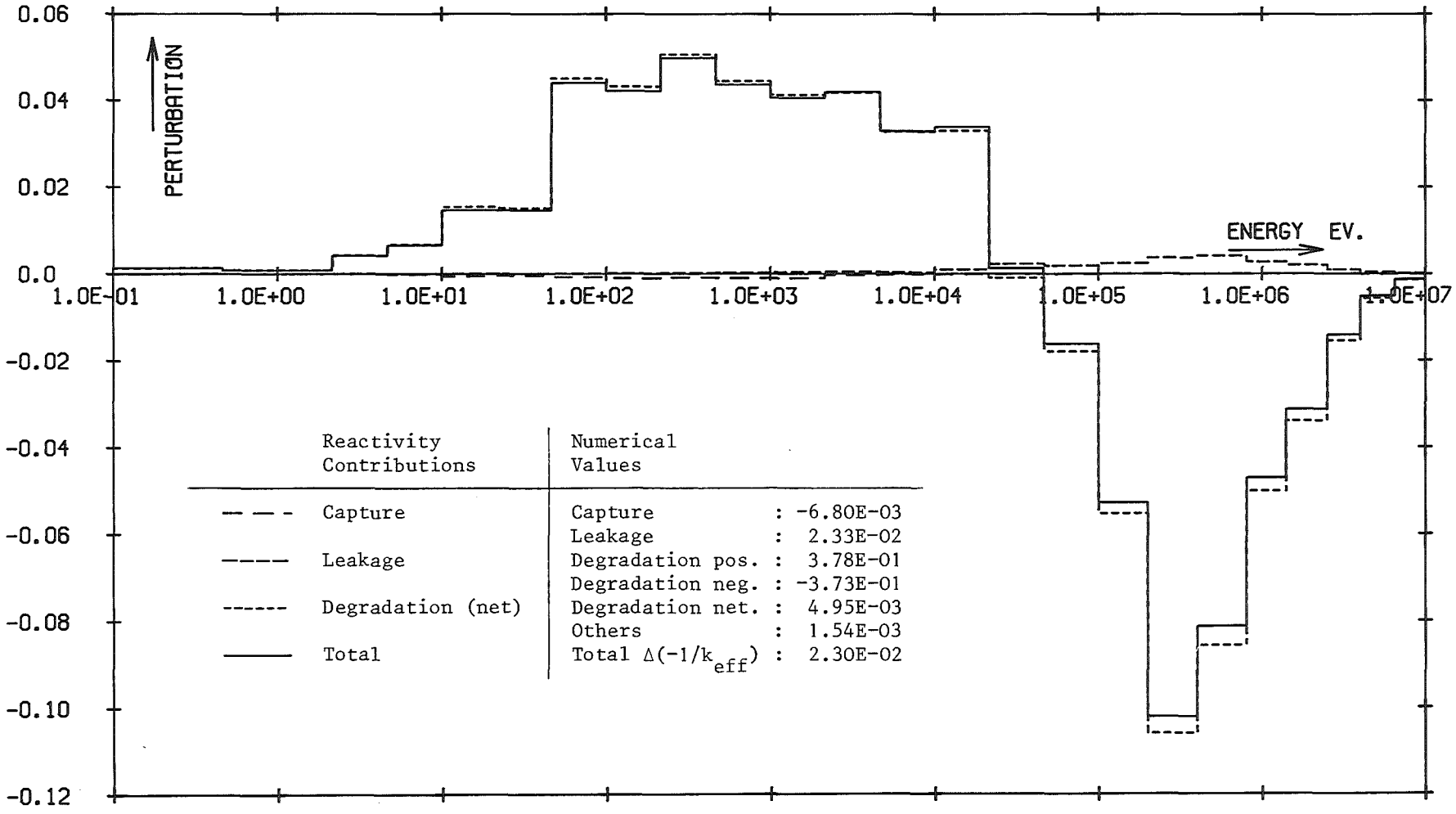

Fig. 24

Reactivity change caused by the addition of about $2.5 \cdot 10^{-2}$ g of water per 1 cm^3 of average core composition of a GCFR.
Group-wise representation of individual components and total values $[\Delta(-1/k_{eff})]$ from fundamental mode calculations for case B7

APPENDIX A

Documentation of Contributed Results

The Tables given in the following serve as a documentation of the results contributed by the various laboratories participating in this intercomparison effort.

	B0	B1	B2	B3	B4	B5	B6	B7
S0	1.009621	1.005941	1.002582	1.009008	1.011353	1.015247	1.011333	0.999161
S1	1.010396	1.005972	1.002748	1.009805	1.012354	1.016544	1.011949	0.998652
S2	1.011031	1.006056	1.002975	1.010645	1.013393	1.017884	1.012630	0.998239
S3	1.011782	1.006184	1.003249	1.011514	1.014466	1.019263	1.013362	0.997911
S4	1.012558	1.006356	1.003574	1.012411	1.015567	1.020671	1.014145	0.997660
S5	1.013356	1.006565	1.003943	1.013335	1.016694	1.022114	1.014972	0.997478
S6	1.014176	1.006813	1.004351	1.014283	1.017844	1.023580	1.015841	0.997360
S7	1.015016	1.007092	1.004798	1.015256	1.019016	1.025069	1.016745	0.997299
S8	1.015870	1.007401	1.005279	1.016243	1.020203	1.026582	1.017682	0.997290
S9	1.017625	1.008103	1.006337	1.018272	1.022627	1.029653	1.019641	0.997403
S10	1.019427	1.008900	1.007504	1.020353	1.025096	1.032777	1.021694	0.997670
S11	1.022193	1.010240	1.009427	1.023553	1.028858	1.037527	1.024906	0.998292
S12	1.025009	1.011708	1.011518	1.026806	1.032660	1.042314	1.028227	0.999112
S13	1.028797	1.013816	1.014494	1.031185	1.037741	1.048696	1.032742	1.000413
S14	1.032579	1.016028	1.017618	1.035563	1.042777	1.055018	1.037286	1.001856
S15	1.036323	1.018293	1.020843	1.039897	1.047736	1.061232	1.041800	1.003370
S16	1.040899	1.021132	1.024938	1.045201	1.053774	1.068798	1.047325	1.005280
S17	1.045333	1.023932	1.029056	1.050347	1.059600	1.076097	1.052670	1.007147
S18	1.049603	1.026660	1.033152	1.055311	1.065198	1.083111	1.057805	1.008925
S19	1.053695	1.029287	1.037203	1.060078	1.070556	1.089823	1.062702	1.010593

Table A1: German criticality values for steam densities So ... S19 and composition variations Bo ... B7

ρ_{H_2O} [g/cm^{-3} Core Vol.]	B0	B1	B2	B3	B4	B5	B6	B7
2.47E-04	1.389782	0.061854	0.336331	1.614003	2.029585	2.628796	1.246744	-1.031705
7.40E-04	1.469032	0.170099	0.461972	1.702918	2.106902	2.715777	1.382051	-0.837083
1.23E-03	1.521222	0.259814	0.554753	1.760906	2.174555	2.795028	1.482563	-0.664810
1.73E-03	1.573411	0.349862	0.659132	1.818894	2.230610	2.853016	1.586942	-0.508725
2.22E-03	1.617868	0.423313	0.748047	1.873016	2.284732	2.924535	1.675857	-0.368829
2.71E-03	1.662326	0.502564	0.825364	1.921340	2.331122	2.970925	1.760906	-0.239201
3.21E-03	1.700985	0.566351	0.906548	1.971597	2.375581	3.019249	1.832425	-0.123587
3.70E-03	1.731912	0.626272	0.974201	2.000590	2.404574	3.065639	1.900078	-0.018242
4.44E-03	1.778308	0.711323	1.072783	2.056651	2.456771	3.112039	1.985132	0.114527
5.43E-03	1.826624	0.807001	1.182957	2.108833	2.502186	3.166149	2.080806	0.270551
6.66E-03	1.868505	0.905258	1.298933	2.161667	2.541811	3.209318	2.170043	0.420253
8.14E-03	1.902658	0.992243	1.412335	2.197754	2.568233	3.233809	2.243500	0.553989
9.87E-03	1.919405	1.067946	1.508173	2.219010	2.574671	3.233802	2.287629	0.659192
1.18E-02	1.916510	1.121104	1.583077	2.218532	2.551963	3.203847	2.302614	0.731134
1.38E-02	1.896693	1.147680	1.633814	2.195815	2.512816	3.148270	2.287147	0.767376
1.60E-02	1.855234	1.150871	1.660007	2.150201	2.447487	3.067187	2.239889	0.773549
1.85E-02	1.797243	1.135019	1.669283	2.086024	2.361661	2.958551	2.166434	0.756938
2.10E-02	1.731140	1.105640	1.660395	2.012189	2.269270	2.843353	2.081775	0.720986
2.34E-02	1.660007	1.065049	1.642224	1.932165	2.171850	2.720804	1.985128	0.676142

Table A1a: German results for the specific steam reactivity density coefficients (SSDRCs); (for definition see Chapter IIIc) in the text

	B0	B1	B2	B3	B4	B5	B6	B7
S0	1.014292	1.010138	1.008729	1.012294	1.016654	1.019740	1.015578	0.999647
S1	1.014803	1.010647	1.008800	1.012934	1.017574	1.020990	1.016193	0.998983
S2	1.015348	1.010810	1.008933	1.013612	1.018533	1.022283	1.016869	0.998416
S3	1.015924	1.010823	1.009122	1.014326	1.019525	1.023615	1.017600	0.997939
S4	1.016529	1.010883	1.009363	1.015073	1.020548	1.024982	1.018381	0.997540
S5	1.017160	1.010985	1.009653	1.015848	1.021598	1.026379	1.019206	0.997214
S6	1.017814	1.011326	1.009986	1.016650	1.022673	1.027804	1.020073	0.996952
S7	1.018490	1.011502	1.010359	1.017475	1.023770	1.029252	1.020975	0.996747
S8	1.019184	1.011711	1.010770	1.018322	1.024885	1.030721	1.021909	0.996596
S9	1.019892	1.011215	1.011691	1.019072	1.027163	1.033711	1.023861	0.996430
S10	1.022114	1.011818	1.012726	1.021882	1.029492	1.036754	1.025903	0.996417
S11	1.024427	1.012869	1.014452	1.024683	1.033048	1.041383	1.029089	0.996624
S12	1.026803	1.014054	1.016341	1.027552	1.036642	1.046048	1.032373	0.997031
S13	1.030322	1.015779	1.019042	1.031429	1.041448	1.052261	1.036824	0.997789
S14	1.033256	1.017694	1.021884	1.035317	1.046217	1.058414	1.041291	0.998699
S15	1.036467	1.019482	1.024810	1.039176	1.050913	1.064459	1.045717	0.999692
S16	1.040410	1.021852	1.028522	1.043912	1.056633	1.071815	1.051138	1.000970
S17	1.044238	1.024191	1.032242	1.048513	1.062154	1.078910	1.056379	1.002234
S18	1.047906	1.026443	1.035912	1.052937	1.067434	1.085712	1.061408	1.003433
S19	1.051417	1.028600	1.039515	1.057169	1.072466	1.092188	1.066183	1.004529

Table A2: Japanese criticality values for steam densities So ... S19 and composition variations Bo ... B7

(B) CALCULATION RESULTS

Criticality values k_{eff} calculated with the British Nuclear Data Basis FGL5

Steam ingress	B0	B1	B2	B3	B4	B5	B6	B7
S_0	.986720	.986704	.984295	.983117	.987158	.987340	.987225	.987456
S_5	.991310	.987995	.986585	.987963	.993498	.994737	.991261	.986944
S_9	.996741	.990512	.990163	.993714	1.000769	1.003151	.996643	.988435
S_{12}	1.006409	.995940	.997369	1.003990	1.013411	1.017707	1.006617	.993143
S_{16}	1.028157	1.009172	1.014592	1.027217	1.041105	1.049478	1.028573	1.006761
S_{19}	1.046722	1.020142	1.029325	1.047135	1.064247	1.075996	1.045943	1.019143

Criticality values k_{eff} calculated with the British Nuclear Data Basis FGL4

Steam ingress	B4	B5	B6
S_0	1.008318	1.012307	1.005849
S_5	1.014924	1.020959	1.009334
S_9	1.022307	1.030496	1.014242
S_{12}	1.034921	1.046598	1.023824
S_{16}	1.061917	1.080597	1.046591
S_{19}	1.083814	1.107911	1.066087

Table A3: Results from EIR Würenlingen, Switzerland

Table A3 continued

(A) Details of FGL5 steam entry benchmark calculations

(1) The calculations were carried out using the UK code MURALB (ref 1) which solved the homogeneous problems in the P1 approximation.

(2) The dataset used was FGL5 which covers the energy range from 15 MeV to thermal using 2240 groups of lethargy width 1/128.

(3) The temperature for U235, U238, Pu239 and Pu240 was 1500 ^{o}K, for other nuclides the temperature was 300 ^{o}K.

(4) A Maxwellian fission spectrum with Θ = 1.41 MeV was chosen.

(5) Fission products are represented in FGL5 by a single nuclide so that in all cases twice the concentration specified in the benchmark for fission product pairs was input to the calculations. The data were originally obtained by combining a selection of the fission product data in reference 2 with Pu239 thermal yield data from reference 3.

References

1 Macdougall J. et al UKAEA AEEW M-843 (1969)
2 Bertram W.K. et al AAEC E214 (1971)
3 Slynn K.F. and Glendenin L.E. ANL 7749

Table A4: Results from France (Cadarache)
Keff, ΔKeff in pcm (note: 1 pcm $\hat{=}$ 10^{-5} ΔKeff)

	B0	B1	B2	B3	B4	B5*)
S0 0 = 0 H = 0	Keff 0,99231	0,98638	0,98454	0,98177	0,99406	0,98738
S2 0 =0,33 H =0,66	Keff 0,99472 ΔKeff 241	0,98806 168	0,98666 212	0,98415 238	0,99717 311	0,98814 76
S5 0=0,825 H=1,65	Keff 0,99845 ΔKeff 614	0,99071 433	0,98998 544	0,98786 609	1,00196 790	0,98956 218
S9 0=1,65 H=3,30	Keff 1,00483 ΔKeff 1252	0,99538 900	0,99583 1129	0,99423 1246	1,01013 1607	0,99241 503
S12 0=2,97 H=5,94	Keff 1,01517 ΔKeff 2286	1,00309 1671	1,00554 2100	1,00461 2284	1,02331 2925	0,99776 1038
S16 0=5,775 H=11,55	Keff 1,03650 ΔKeff 4419	1,01908 3270	1;02609 4155	1,02609 4432	1,05036 5630	1,01016 2278
S19 0=8,25 H=16,5	Keff 1,05386 ΔKeff 6155	1,03188 4550	1,04308 5854	1,04357 6180	1,07224 7818	1,02072 3334
$\frac{\Delta Keff}{\Delta N_{(H)}}$ pcm.10^{20}	373	275,5	354	374	473	202

*) Internal French labelling; corresponds to B7 of usual labelling, i.e. $B^2 = 6 \cdot 10^{-4}$ cm^{-2}

Table A5: Results from US (ANL)

TABLE XXVII. Results of Steam-Entry International Benchmark Calculations

Description	With narrow resonance Approximations (Eigenvalue)		W/O NRA k	Worth of steam entry Δk/k	
	MC^2-2 (Fine Group)	DIFID (Broad Group)	DIFID (Broad Group)	With NRA	W/O NRA
A. Clean (unpoisoned) cases					
1. No steam reference (B_5S_0)	0.99804	0.99846	0.97761	-	-
2. Steam-filled case (B_5-S_5) (H = 0.165, $\phi = 0.0825 \times 10^{21}$ atom/cm^3)	1.00654	1.00616	0.96131	+0.00771	-0.01665
3. Steam-filled case (B_5-S_8) (H = 0.264, $\phi = 0.132 \times 10^{21}$ atom^3)	1.01224	1.01112	0.95313	+0.01268	-0.02505
4. Steam-filled case (B_5-S_{19}) (H = 1.650, $\phi = 0.825 \times 10^{21}$ atom^3)	1.10895	1.07419	0.93200	+0.07585	-0.044665
B. Poisoned case					
1. No steam reference (B_3S_0) ($^{10}B = 0.020 \times 10^{21}$ atom/cm^3)	0.99393	0.99434	0.97431	-	-
2. Steam filled case B_3S_8)	1.00686	1.00590	0.94942	+0.01160	-0.02549

Table A5 continued

E. The International Steam Entry Benchmark Problem

The problem of steam entry has aroused sufficient interest to lead to an international benchmark problem proposed by Edgar Kiefhaber of Karlsruhe. A small subset of the proposed benchmark calculations were performed to provide for a comparison of the calculations performed in the various laboratories. The results of the calculations performed are of interest since they shed some light on the effect of the narrow resonance approximation.

Table XXVI shows the atom concentrations of the isotope in the benchmark problem. The composition of the reference configuration matches approximately the GCFR demonstration plant composition. Note that there are large differences from the GCFR Phase II critical assembly atom concentration (See Table XXVII. The "fine group" eigenvalue obtained from MC^2-2 and the "broad group" eigenvalue obtained from a DIF1D model using the 11 group cross-section. This procedure was necessary because the present version of MC^2-2 does not recompute a broad-group eigenvalue with the RABANL cross-sections. The RABANL cross-sections were generated using Integral Transport Theory and the Narrow Resonance Approximation was avoided. From the results of Table XXVII several interesting conclusions can be drawn. First of all the MC^2-2 fine group eigenvalue does not agree with the broad group eigenvalue (and the disagreement gets worse with more steam in the configuration). For the dry case, this difference is caused by a round-off problem in the single precision MC^2-2 fine group calculation. For the steam-filled case the discrepancy has been attributed to the inadequacy of the ultra-fine group attenuation algorithm[18] in the resolved resonance range. The consequences of this is to cause a growing error in the ultra fine group spectrum as the calculation proceeds down through the resolved energy range and this affects the eigenvalue.* Secondly, the eigenvalues obtained with the RABANL (no NRA) cross-sections were consistently lower than the eigenvalues with the MC^2-2 (with NRA) cross-sections. The disparity between the two values increased with increasing amounts of steam. As seen from the last two columns of the Table XXVII, the two sets of calculations actually predicted opposite behaviors on steam entry. The "with NRA" cross-sections calculations predicted a positive worth of steam entry monotonically increasing with steam density while the "non NRA" cross-sections predicted a negative worth of steam entry monotonically decreasing with increasing steam density. For a ^{10}B containing initial configuration the worth of steam entry was reduced (by 8.5% according to the with-NRA calculations and by 1.8% according to the non-NRA calculations).

In the interpretation of these results, one has to keep in mind the simplified nature of the benchmark problem. The problem was designed to compare basic data and methods used in various laboratories and not to compare with experiment. There are two features of the calculation that make it difficult to relate these results to the steam entry experiment viz, a) the homogeneous nature of the calculation and, b) the inadequate treatment of leakage (through a fixed buckling) in the problem. Schaefer[19] has shown that the effects of heterogeneity can be very large and, in fact, can change the sign of the steam entry worth. The buckling term would, in case of actual steam entry, be altered to reflect a change in leakage. Thus, the sole purpose of presenting these results here is to emphasize the large effect of the narrow resonance approximation. Future comparisons of the results with those of other laboratories might yield important insight into the impact of data bases and methods on the steam worth.

*Note that this would impact on parameters like the ^{10}B worth and ^{238}U Doppler effect.

APPENDIX B

Restricted Sensitivity Study for Specific Nuclear Data Changes

a) Purpose and Specifications of the Sensitivity Study

The purpose of the present restricted sensitivity study is to get some rough information about the influence of nuclear data changes on the steam ingress reactivity, i.e. on $k_{eff}(\rho)$ and SSDRC(ρ). As a reference we have used the KFKINR-set of group constants. We have modified specific nuclear data by amounts which are comparable to existing nuclear data uncertainties.

1) σ_c(Fe): It seems conceivable or at least not completely unreasonable that the capture cross section is overestimated in KFKINR by about 30 %.

2) $\sigma_c(^{239}Pu)$: A reduction of the capture cross section of ^{239}Pu by about 10 % brings it in closer agreement with older evaluations of $\alpha(^{239}Pu)$.

3) $\sigma_c(^{238}U)$: An increase of the capture cross section of ^{238}U by about 10 % brings it in closer correspondence to the ENDF/B-IV evaluation.

4) $\sigma_{inel.}(^{238}U)$: Presently an uncertainty of about 20 % in the inelastic scattering cross section of ^{238}U cannot be excluded according to the differences still existing between various measurements and different evaluations of this quantity. An increase by that amount would lead to a closer agreement of the modified values with those derived from ENDF/B-IV.

All modifications have been applied uniformly in the energy range 10 eV - 10.5 MeV. Below 10 eV the data are usually of minor importance for the present problem (except for very large steam densities) and moreover, in that energy range the data, in general, are

assumed to be reasonably well known and are considered to be fairly reliable because, for a long time, they have been evaluated for and applied to the design of thermal reactors. For the sake of completeness it should be mentioned that we have always modified accordingly the elastic scattering cross section - keeping the usually well known total cross section constant - in order to compensate for the arbitrary changes of the specific reaction cross sections indicated in cases 1 - 4 above.

It is expected that the influence of this consistency-readjustment of $\sigma_{el}(Fe, {}^{239}Pu, {}^{238}U)$ on k_{eff} and SSDRC is fairly small or practically negligible because: (a) it consists of only a minor relative change of σ_{el} in the energy range which is most important for a GCFR; this is due to the relation $\sigma_c << \sigma_{el}$ which holds in those energy groups (especially above 1 keV) which have a remarkable influence on reaction rates for a normal GCFR neutron spectrum, (b) the contribution of these materials to the scattering matrix is not very pronounced (compared e.g. to the contribution of the oxygen of the oxide fuel), (c) the changes are confined in diffusion theory (disregarding unimportant changes of the diffusion constant or the transport cross section) using the well known Russian 26-group structure to the lower sub-diagonal term $\Sigma_{i \to i+1}$ of the scattering matrix, whereas e.g. the presence of hydrogen brings about that the complete lower triangular matrix ($\Sigma_{i \to j}$ for $j > i$) is filled up, (d) the adjustment changes remain essentially constant upon variation of the steam density; thus, they will have only an indirect influence on the steam ingress reactivity via the neutron importance distribution, (e) due to the above mentioned property of the scattering probabilities of these materials, a change of $\sigma_{el,i}$, the elastic scattering cross section in group i, will have a direct influence - if at all - only on the real flux and adjoint flux ratio between adjacent energy groups, i.e. on ϕ_{i+1}/ϕ_i and ϕ_{i+1}^+/ϕ_i^+, respectively. Especially if the mixture contains hydrogenous material this influence will be relatively small because - contrary to the usual conditions in a voided GCFR where these ratios are determined mainly by the scattering matrix element for adjacent groups - the complete down-scattering capabil-

ity of hydrogen leads to the fact that all higher energy groups contribute to ϕ_i and all lower energy groups contribute to ϕ_i^+ so that the importance of the directly adjacent group is considerably diminished and the real and adjoint flux distributions remain nearly unaffected by the consistency adjustment of $\sigma_{el}(Fe, {}^{239}Pu, {}^{238}U)$.

Intentionally, from the very beginning the size and goal of the present sensitivity study were rather limited. It should only provide some insight into the effects of a restricted number of fairly simple data changes. A more extensive sensitivity study should take into account that the range of uncertainty for the neutron cross sections or group constants usually depends on the neutron energy (or - equivalently - on the group index). With respect to the influence on the adjoint neutron flux and the correlated importance differences appearing in the expressions for the degradation term of the perturbation calculations it may even be necessary to consider - in a more advanced sensitivity study - cross section modifications which have different signs in different energy regions.

In addition to the variations 1 - 4 described above, the influences of a modification of the capture cross section of (a) ^{240}Pu and (b) fission products (FPP) have also been investigated. We have found, that as long as the deviations remain below about 10 %, the curves for k_{eff} and SSDRC remain fairly close to the corresponding original KFKINR-values. Therefore, these results have not been included in the drawings shown as Figs. B1 - B16 and the corresponding Tables B1 - B8. This fact indicates that an increase of about 10 % in $\sigma_c(^{240}Pu)$ - which would correspond to using more recent evaluations - and a reduction by about 10 % of $\sigma_c(FPP)$ - which would result in a closer agreement with recent ECN-data will have only a negligible significance for the stream entry reactivity compared to the influence of other existing nuclear data uncertainties.

b) Results of the Sensitivity Study

A first glance at Figs. B1 - B8 shows that the influence of the data changes on the criticality at normal conditions (i.e. corresponding here to $\rho = 0.$) and on $k_{eff}(\rho)$ is fairly similar for cases B0 - B6; case B7, with the lower enrichment and the lower buckling, shows a behavior quite different from that observed for the other cases. In each of the Figs. B1 - B8 the curves seem to be roughly parallel to each other. Therefore, the impression of fairly similar slopes of the various $k_{eff}(\rho)$ curves for each of the benchmark cases might lead one to the supposition that the corresponding SSDRC-values would be nearly equal for all data changes. However, the existing slight systematic differences in the slopes, which are not so obvious from Figs. B1 - B8, bring about the remarkable deviations for the SSDRC(ρ) curves shown in Figs. B9 - B16. For each case these curves are fairly parallel, thus indicating the same global dependence of the SSDRC on steam density for all nuclear data changes considered here. The absolute difference of the maximum and minimum SSDRC-values (about 0.6) at low steam densities is about the same for all cases B0 - B7 as could be seen from Figs. B9 - B16 (please note the varying the different ordinate scales in Figs. B1 - B16). The relative change of the SSDRC is, of course, considerably different for the different cases, as can be seen from Fig. B10 where a change of sign can be observed at low steam densities.

The influence of the data changes on k_{eff} and SSDRC are as expected. They can be characterized in the following way (minor exceptions occurring at high steam densities):

		k_{eff}	SSDRC
FE	SCAPT * 0.7	considerably increased	increased
PU239	SCAPT * 0.9	considerably increased	considerably increased
U 238	SCAPT * 1.1	considerably reduced	considerably reduced
U 238	SCAPT * 1.2	slightly reduced	slightly increased

In general, the differences obtained in the present sensitivity study as influence of nuclear data changes are by far less pronounced than those observed between the results of the various participating laboratories.

c) Conclusions from the Present Sensitivity Study

Comparing the differences between the results of various laboratories participating in the intercomparison study with the deviations observed upon the nuclear data variations discussed in the preceding sections one may deduce the following conclusions:

1. The present sensitivity study is probably too crude; a uniform variation in all energy groups may not be adequate to give sufficiently detailed information on the influence of nuclear data uncertainties. In reality the cross section differences usually have different amounts and even different signs in different energy regions. From Figs. 19 - 24 and the corresponding discussion it is obvious that realistic cross section differences may lead to fairly complicated variations of the adjoint neutron group flux ϕ_i^+ and, consequently, to even more complex variations of the differences $(\phi_i^+ - \phi_j^+)$ ultimately needed to determine the degradation term.

2. The data modifications presently studied are not sufficient to explain the existing discrepancies observed in Figs. 1 - 16. Thus, the real differences between the different nuclear data bases used within the present intercomparison must be more complicated than the crude modifications assumed for the present sensitivity study. This means, that - as mentioned before - the amount and sign of the differences have to be considered in detail including their energy dependence. In addition to the four types of nuclear data considered here, other types of data (e.g. $\sigma_f(^{239}Pu)$) and other kinds of influences (e.g. the effect of the weighting spectra used to establish the various sets of group constants) have to be taken into account too. Such a

further detailed and extensive intercomparison analysis - although quite useful - would require a considerable effort which exceeds the scope of the present study.

	B0	B1	B2	B3	B4	B5	B6	B7
S0	1.014441	1.010635	1.007324	1.013774	1.016251	1.020189	1.016146	1.006547
S1	1.015189	1.010718	1.007548	1.014635	1.017323	1.021564	1.016837	1.006095
S2	1.015971	1.010853	1.007830	1.015534	1.018430	1.022981	1.017587	1.005733
S3	1.016777	1.011032	1.008157	1.016463	1.019570	1.024434	1.018388	1.005457
S4	1.017606	1.011252	1.008531	1.017418	1.020734	1.025917	1.019237	1.005254
S5	1.018459	1.011509	1.008948	1.018397	1.021925	1.027424	1.020128	1.005116
S6	1.019330	1.011799	1.009404	1.019399	1.023133	1.028961	1.021060	1.005038
S7	1.020217	1.012121	1.009897	1.020422	1.024362	1.030516	1.022022	1.005013
S8	1.021121	1.012473	1.010423	1.021460	1.025606	1.032091	1.023017	1.005038
S9	1.022963	1.013255	1.011567	1.023583	1.028132	1.035281	1.025087	1.005217
S10	1.024847	1.014124	1.012816	1.025752	1.030702	1.038516	1.027245	1.005535
S11	1.027724	1.015563	1.014852	1.029071	1.034599	1.043421	1.030598	1.006223
S12	1.030637	1.017123	1.017039	1.032432	1.038517	1.048345	1.034044	1.007090
S13	1.034539	1.019332	1.020131	1.036936	1.043737	1.054888	1.038710	1.008434
S14	1.038418	1.021630	1.023357	1.041419	1.048893	1.061347	1.043383	1.009902
S15	1.042239	1.023966	1.026666	1.045842	1.053951	1.067684	1.048004	1.011423
S16	1.046895	1.026876	1.030850	1.051238	1.060091	1.075371	1.053641	1.013320
S17	1.051394	1.029732	1.035038	1.056458	1.065997	1.082770	1.059072	1.015158
S18	1.055712	1.032499	1.039193	1.061481	1.071662	1.089865	1.064276	1.016897
S19	1.059842	1.035155	1.043287	1.066290	1.077066	1.096641	1.069228	1.018515

Table B1: k_{eff}-values for GCFR-Benchmarks (KFKINR-Set; σ_c(Fe) * 0.7)

ρ_{H_2O} [g/cm^{-3} Core Vol.]	B0	B1	B2	B3	B4	B5	B6	B7
2.47E-04	1.517356	0.168166	0.454240	1.745442	2.172622	2.785363	1.401380	-0.916213
7.40E-04	1.585009	0.272544	0.570217	1.822760	2.244141	2.872345	1.519289	-0.734516
1.23E-03	1.633332	0.363392	0.662998	1.882681	2.311793	2.945797	1.623668	-0.558619
1.73E-03	1.679723	0.446509	0.757712	1.934871	2.358184	3.005718	1.720314	-0.411716
2.22E-03	1.729979	0.519960	0.846627	1.985126	2.414239	3.054042	1.807297	-0.278343
2.71E-03	1.764771	0.587613	0.923944	2.029585	2.449032	3.115895	1.888480	-0.158501
3.21E-03	1.797632	0.653333	0.999329	2.074042	2.489624	3.150688	1.950334	-0.050256
3.70E-03	1.832425	0.713254	1.065048	2.103036	2.522484	3.193213	2.016054	0.050256
4.44E-03	1.866257	0.792507	1.159765	2.152332	2.560184	3.232847	2.098209	0.180730
5.43E-03	1.909740	0.880452	1.266072	2.197748	2.603664	3.278259	2.186151	0.322800
6.66E-03	1.943889	0.972267	1.374962	2.242206	2.633303	3.313697	2.265401	0.464549
8.14E-03	1.967733	1.054097	1.478055	2.270561	2.646840	3.326591	2.328549	0.585681
9.87E-03	1.977393	1.119169	1.566645	2.282314	2.645223	3.315468	2.363980	0.681360
1.18E-02	1.965316	1.164596	1.634784	2.271688	2.612368	3.272950	2.367851	0.743699
1.38E-02	1.936318	1.183439	1.676338	2.241239	2.563073	3.211090	2.341752	0.770758
1.60E-02	1.887321	1.179866	1.696347	2.187313	2.488852	3.115897	2.285120	0.768923
1.85E-02	1.823918	1.157442	1.697504	2.116179	2.394135	2.999530	2.201227	0.744954
2.10E-02	1.750083	1.121878	1.684362	2.036158	2.296331	2.875826	2.109610	0.705136
2.34E-02	1.674312	1.076647	1.659621	1.949175	2.190793	2.746706	2.007550	0.655653

Table B1a: SSDRC-values for GCFR-Benchmarks (KFKINR-Set; σ_c(Fe) * 0.7)

	B0	B1	B2	B3	B4	B5	B6	B7
S0	1.012777	1.010131	1.006966	1.012126	1.014582	1.018538	1.015703	1.002779
S1	1.013608	1.010347	1.007332	1.013071	1.015738	1.020003	1.016543	1.002434
S2	1.014475	1.010615	1.007758	1.014058	1.016934	1.021514	1.017442	1.002182
S3	1.015368	1.010929	1.008229	1.015074	1.018157	1.023059	1.018396	1.002015
S4	1.016286	1.011284	1.008751	1.016119	1.019409	1.024639	1.019399	1.001921
S5	1.017224	1.011676	1.009316	1.017191	1.020689	1.026247	1.020443	1.001893
S6	1.018186	1.012100	1.009919	1.018284	1.021988	1.027878	1.021525	1.001927
S7	1.019162	1.012560	1.010559	1.019398	1.023305	1.029533	1.022644	1.002013
S8	1.020154	1.013049	1.011233	1.020527	1.024640	1.031204	1.023789	1.002150
S9	1.022178	1.014097	1.012671	1.022839	1.027353	1.034596	1.026165	1.002547
S10	1.024242	1.015237	1.014211	1.025197	1.030103	1.038034	1.028626	1.003084
S11	1.027392	1.017070	1.016681	1.028797	1.034274	1.043242	1.032428	1.004092
S12	1.030577	1.019016	1.019292	1.032441	1.038468	1.048469	1.036312	1.005273
S13	1.034837	1.021725	1.022936	1.037315	1.044044	1.055408	1.041538	1.007021
S14	1.039063	1.024505	1.026698	1.042165	1.049550	1.062256	1.046748	1.008873
S15	1.043224	1.027300	1.030519	1.046941	1.054948	1.068967	1.051881	1.010762
S16	1.048289	1.030756	1.035317	1.052768	1.061495	1.077107	1.058122	1.013092
S17	1.053180	1.034124	1.040085	1.058396	1.067795	1.084939	1.064117	1.015333
S18	1.057872	1.037372	1.044785	1.063808	1.073827	1.092443	1.069843	1.017447
S19	1.062358	1.040478	1.049393	1.068991	1.079584	1.099607	1.075282	1.019414

Table B2: k_{eff}-values for GCFR-Benchmarks (KFKINR-Set; $\sigma_c(^{239}Pu * 0.9)$

ρ_{H_2O} [g/cm^{-3} Core Vol.]	B0	B1	B2	B3	B4	B5	B6	B7
2.47E-04	1.683589	0.438777	0.742248	1.915541	2.342720	2.968992	1.702918	-0.699724
7.40E-04	1.757040	0.543156	0.864023	2.000590	2.425837	3.061773	1.820827	-0.510296
1.23E-03	1.811162	0.635937	0.954871	2.058578	2.478026	3.131359	1.934871	-0.338264
1.73E-03	1.859486	0.719053	1.057317	2.118500	2.537947	3.202878	2.031517	-0.191361
2.22E-03	1.902011	0.794437	1.146232	2.172622	2.594003	3.258933	2.116567	-0.056055
2.71E-03	1.943401	0.860157	1.221617	2.215146	2.632661	3.305324	2.193884	0.069586
3.21E-03	1.979328	0.931676	1.297001	2.257671	2.669387	3.355580	2.267336	0.173964
3.70E-03	2.010255	0.991597	1.366587	2.288598	2.706113	3.386507	2.321458	0.276410
4.44E-03	2.050853	1.062152	1.457438	2.342727	2.749612	3.437739	2.407480	0.403019
5.43E-03	2.092402	1.154929	1.559879	2.390075	2.786327	3.484117	2.494453	0.544122
6.66E-03	2.128162	1.238367	1.668768	2.432278	2.818220	3.518588	2.568228	0.681038
8.14E-03	2.151363	1.315043	1.764131	2.461922	2.833691	3.530839	2.624290	0.797660
9.87E-03	2.158606	1.372384	1.846437	2.469809	2.824986	3.516010	2.648122	0.885768
1.18E-02	2.141697	1.408629	1.906362	2.457250	2.790198	3.470110	2.639912	0.938442
1.38E-02	2.108350	1.416359	1.935835	2.420035	2.735105	3.400517	2.600765	0.957287
1.60E-02	2.053167	1.400993	1.945310	2.362051	2.653925	3.299913	2.529830	0.944434
1.85E-02	1.982419	1.365426	1.932549	2.281637	2.553795	3.174654	2.430473	0.908480
2.10E-02	1.902012	1.316331	1.905105	2.193886	2.445168	3.042059	2.321073	0.857065
2.34E-02	1.818508	1.259116	1.867991	2.100718	2.333830	2.904047	2.204710	0.797144

Table B2a: SSDRC-values for GCFR-Benchmarks (KFKINR-Set; σ_c(^{239}Pu * 0.9)

	B0	B1	B2	B3	B4	B5	B6	B7
S0	1.000458	0.996824	0.993006	0.999444	1.002238	1.005540	1.001677	0.982769
S1	1.001019	0.996742	0.993051	1.000101	1.003118	1.006695	1.002161	0.982114
S2	1.001616	0.996711	0.993152	1.000803	1.004041	1.007894	1.002712	0.981558
S3	1.002244	0.996728	0.993306	1.001536	1.004998	1.009134	1.003317	0.981091
S4	1.002903	0.996788	0.993509	1.002305	1.005985	1.010409	1.003974	0.980705
S5	1.003583	0.996889	0.993758	1.003099	1.007001	1.011720	1.004677	0.980392
S6	1.004288	0.997029	0.994049	1.003921	1.008042	1.013059	1.005423	0.980146
S7	1.005014	0.997203	0.994380	1.004766	1.009108	1.014423	1.006207	0.979961
S8	1.005760	0.997410	0.994747	1.005632	1.010193	1.015809	1.007025	0.979832
S9	1.007298	0.997910	0.995582	1.007423	1.012416	1.018643	1.008755	0.979717
S10	1.008894	0.998512	0.996534	1.009278	1.014693	1.021537	1.010589	0.979770
S11	1.011368	0.999572	0.998147	1.012146	1.018188	1.025960	1.013485	0.980095
S12	1.013906	1.000780	0.999941	1.015095	1.021735	1.030441	1.016511	0.980648
S13	1.017352	1.002560	1.002542	1.019092	1.026500	1.036445	1.020661	0.981633
S14	1.020822	1.004471	1.005322	1.023115	1.031253	1.042418	1.024873	0.982804
S15	1.024273	1.006459	1.008224	1.027125	1.035951	1.048314	1.029079	0.984083
S16	1.028520	1.008985	1.011950	1.032058	1.041690	1.055519	1.034262	0.985742
S17	1.032655	1.011504	1.015727	1.036870	1.047253	1.062494	1.039300	0.987403
S18	1.036656	1.013978	1.019514	1.041531	1.052613	1.069215	1.044159	0.989016
S19	1.040507	1.016376	1.023279	1.046021	1.057757	1.075665	1.048813	0.990548

Table B3: k_{eff}-values for GCFR-Benchmarks (KFKINR-Set; $\sigma_c(^{238}U * 1.1)$

ρ_{H2O} [g/cm^{-3} Core Vol.]	B0	B1	B2	B3	B4	B5	B6	B7
2.47E-04	1.136567	-0.166233	0.091210	1.331794	1.782168	2.340788	0.981932	-1.327565
7.40E-04	1.210019	-0.062820	0.204771	1.422642	1.871083	2.429703	1.117238	-1.126903
1.23E-03	1.273806	0.034430	0.312049	1.486429	1.940669	2.514751	1.225482	-0.946536
1.73E-03	1.335660	0.121654	0.411474	1.557947	2.000590	2.584337	1.331794	-0.782357
2.22E-03	1.378184	0.204650	0.504738	1.610137	2.058578	2.655856	1.424575	-0.634487
2.71E-03	1.428441	0.283779	0.589788	1.664259	2.110767	2.713844	1.511557	-0.498577
3.21E-03	1.472898	0.352640	0.670850	1.714516	2.159091	2.766034	1.590808	-0.374990
3.70E-03	1.511557	0.419568	0.743819	1.755107	2.199683	2.808558	1.656528	-0.261430
4.44E-03	1.558918	0.506733	0.846206	1.815034	2.252845	2.872354	1.753180	-0.116520
5.43E-03	1.616900	0.610083	0.964777	1.879780	2.307925	2.932263	1.858518	0.053699
6.66E-03	1.671345	0.716113	1.089773	1.937446	2.361403	2.988318	1.956776	0.219590
8.14E-03	1.714519	0.816225	1.212034	1.992217	2.396202	3.027630	2.044407	0.373581
9.87E-03	1.746408	0.901715	1.317719	2.025233	2.414237	3.041958	2.103034	0.499120
1.18E-02	1.758008	0.968403	1.409113	2.038768	2.408442	3.026500	2.133965	0.593352
1.38E-02	1.748823	1.007543	1.469997	2.031999	2.380410	2.987836	2.131545	0.648077
1.60E-02	1.721475	1.023685	1.510398	1.999432	2.326485	2.920671	2.100718	0.672494
1.85E-02	1.676242	1.021363	1.531272	1.950719	2.254963	2.827498	2.042340	0.673314
2.10E-02	1.622122	1.002809	1.535140	1.889255	2.173010	2.724284	1.969665	0.653865
2.34E-02	1.561041	0.971882	1.526248	1.820441	2.085255	2.614880	1.886548	0.621029

Table B3a: SSDRC-values for GCFR-Benchmarks (KFKINR-Set; $\sigma_c(^{238}U * 1.1)$

	B0	B1	B2	B3	B4	B5	B6	B7
S0	1.008711	1.004807	1.001945	1.007948	1.010500	1.014358	1.010196	0.994305
S1	1.009415	1.004848	1.002121	1.008766	1.011522	1.015681	1.010838	0.993843
S2	1.010153	1.004940	1.002357	1.009624	1.012584	1.017050	1.011539	0.993474
S3	1.010920	1.005079	1.002641	1.010513	1.013679	1.018459	1.012296	0.993190
S4	1.011710	1.005261	1.002976	1.011429	1.014803	1.019900	1.013102	0.992982
S5	1.012525	1.005483	1.003355	1.012375	1.015948	1.021368	1.013951	0.992844
S6	1.013360	1.005737	1.003774	1.013341	1.017121	1.022862	1.014845	0.992766
S7	1.014215	1.006029	1.004229	1.014332	1.018311	1.024382	1.015770	0.992745
S8	1.015085	1.006350	1.004722	1.015339	1.019518	1.025920	1.016731	0.992775
S9	1.016869	1.007074	1.005802	1.017406	1.021984	1.029044	1.018734	0.992966
S10	1.018699	1.007891	1.006994	1.019524	1.024492	1.032223	1.020833	0.993306
S11	1.021506	1.009260	1.008950	1.022774	1.028312	1.037046	1.024108	0.994032
S12	1.024359	1.010765	1.011074	1.026077	1.032164	1.041904	1.027488	0.994951
S13	1.028195	1.012911	1.014091	1.030519	1.037306	1.048371	1.032080	0.996372
S14	1.032023	1.015162	1.017258	1.034953	1.042404	1.054773	1.036695	0.997929
S15	1.035807	1.017460	1.020518	1.039340	1.047415	1.061061	1.041268	0.999548
S16	1.040427	1.020340	1.024659	1.044703	1.053514	1.068707	1.046864	1.001576
S17	1.044902	1.023175	1.028815	1.049903	1.059393	1.076077	1.052273	1.003550
S18	1.049211	1.025933	1.032949	1.054917	1.065039	1.083154	1.057457	1.005430
S19	1.053338	1.028589	1.037033	1.059724	1.070437	1.089920	1.062403	1.007190

Table B4: k_{eff}-values for GCFR-Benchmarks (KFKINR-Set; $\sigma_{inel.}(^{238}U * 1.2)$

ρ_{H_2O} [g/cm^{-3} Core Vol.]	B0	B1	B2	B3	B4	B5	B6	B7
2.47E-04	1.426508	0.081183	0.357593	1.658461	2.072109	2.682918	1.300867	-0.936388
7.40E-04	1.496094	0.187495	0.477436	1.737711	2.151360	2.773766	1.422642	-0.747926
1.23E-03	1.554082	0.282209	0.576015	1.803431	2.219012	2.856882	1.532820	-0.575653
1.73E-03	1.602406	0.369191	0.680394	1.855620	2.278934	2.920669	1.633332	-0.421622
2.22E-03	1.650728	0.448442	0.767376	1.917474	2.321458	2.974792	1.722247	-0.279672
2.71E-03	1.693254	0.516094	0.848560	1.958066	2.377513	3.028913	1.811162	-0.158018
3.21E-03	1.733845	0.591479	0.922011	2.008322	2.410373	3.079170	1.874949	-0.042645
3.70E-03	1.762839	0.649467	0.999329	2.041183	2.447099	3.117828	1.948401	0.060888
4.44E-03	1.807302	0.734518	1.095012	2.095310	2.499295	3.166161	2.029591	0.193536
5.43E-03	1.854651	0.827297	1.208085	2.145558	2.541811	3.221237	2.127195	0.344546
6.66E-03	1.896854	0.925232	1.321484	2.195815	2.580469	3.258930	2.212567	0.490523
8.14E-03	1.927142	1.016726	1.434886	2.231902	2.602383	3.282133	2.283447	0.620877
9.87E-03	1.944050	1.087276	1.528469	2.250421	2.605597	3.276810	2.326772	0.720019
1.18E-02	1.939705	1.140917	1.604823	2.247042	2.583374	3.243956	2.338373	0.788941
1.38E-02	1.916989	1.164110	1.652177	2.222877	2.538911	3.185962	2.317590	0.820380
1.60E-02	1.873017	1.167495	1.678564	2.173783	2.472229	3.099661	2.268110	0.822248
1.85E-02	1.813867	1.149323	1.684747	2.108060	2.383309	2.987546	2.192722	0.799849
2.10E-02	1.746603	1.118011	1.675858	2.032679	2.288599	2.868481	2.101491	0.762351
2.34E-02	1.673152	1.076647	1.655369	1.948402	2.188473	2.742840	2.004844	0.713255

Table B4a: SSDRC-values for GCFR-Benchmarks (KFKINR-Set; $\sigma_{inel.}$ ($^{238}U * 1.2$)

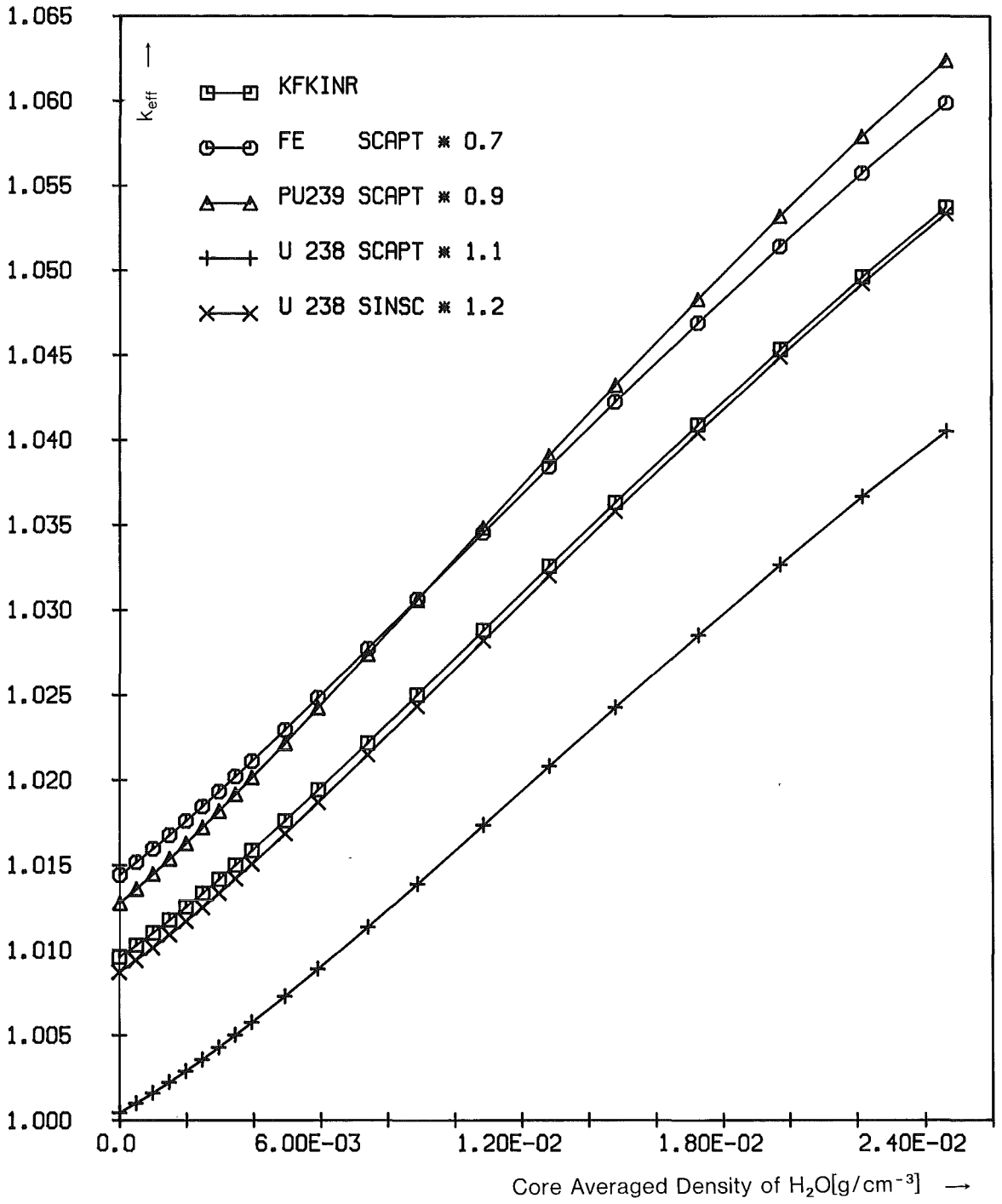

Fig. B1: Influence of cross-section changes on k_{eff} (ρ_{H_2O}) for GCFR Benchmark Bo: Size: ≙ 300 MWe; Fiss. Prod.: yes; B^{10}: no; T_{fuel}: 1500 K; Pu: dirty

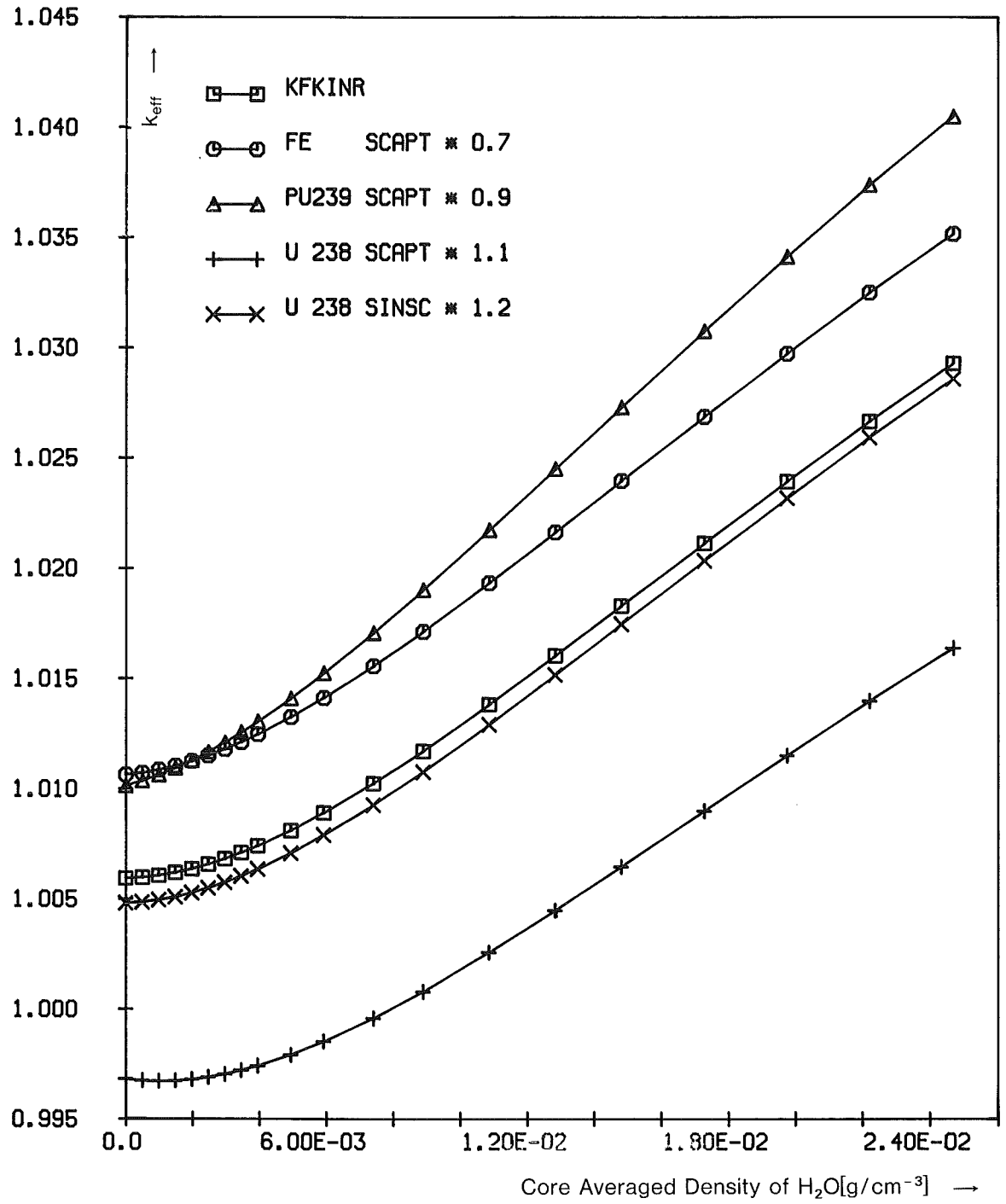

Fig. B2: Influence of cross-section changes on k_{eff} (ρ_{H_2O}) for GCFR Benchmark B1: Size: ≙ 300 MWe; Fiss. Prod.: yes; B^{10}: no; T_{fuel}: 1500 K; Pu: less dirty

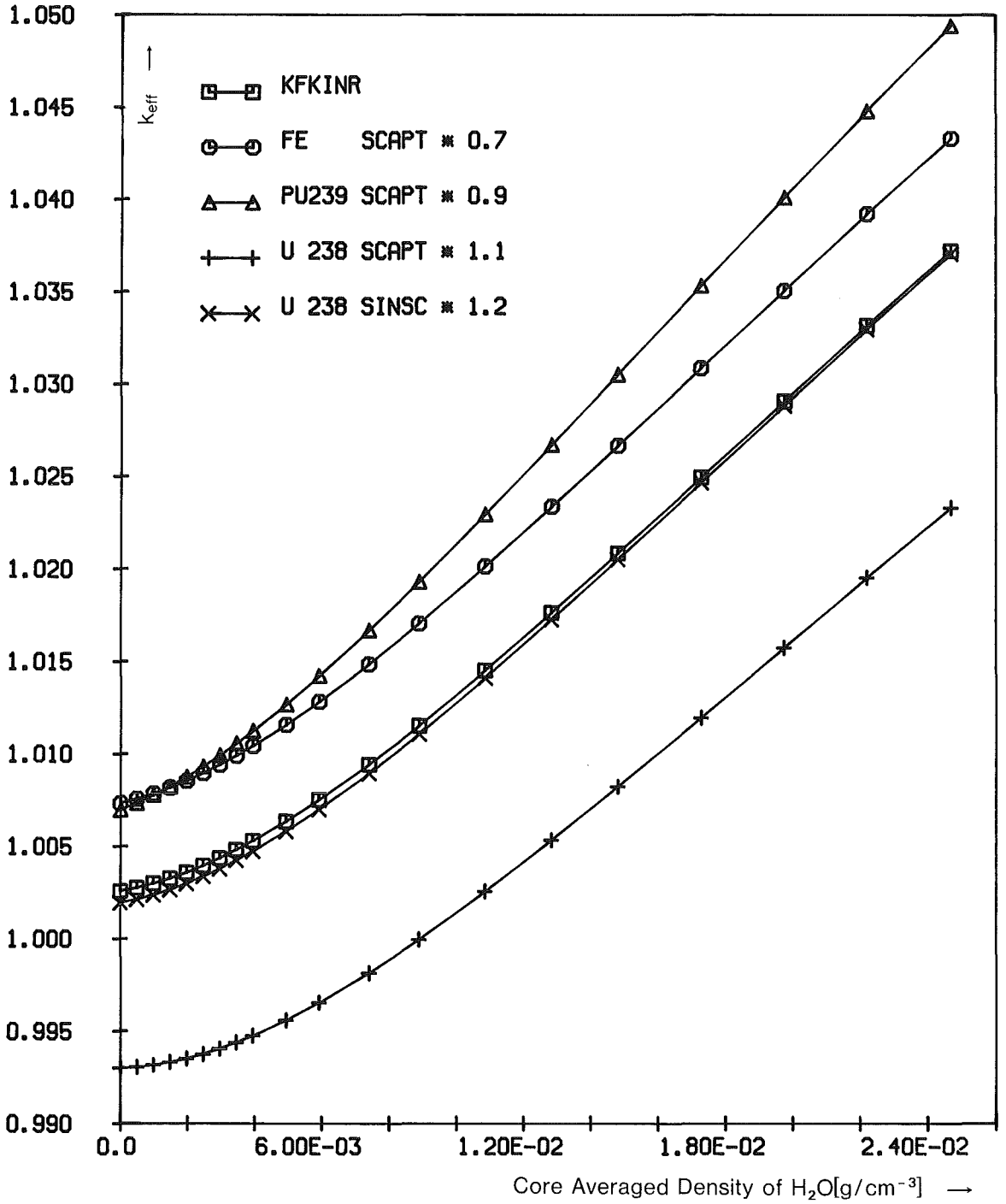

Fig. B3: Influence of cross-section changes on k_{eff} (ρ_{H_2O}) for GCFR Benchmark B2:
Size: ≙ 300 MWe; Fiss. Prod.: yes; B^{10}: no; T_{fuel}: 1500 K; Pu: clean Pu239

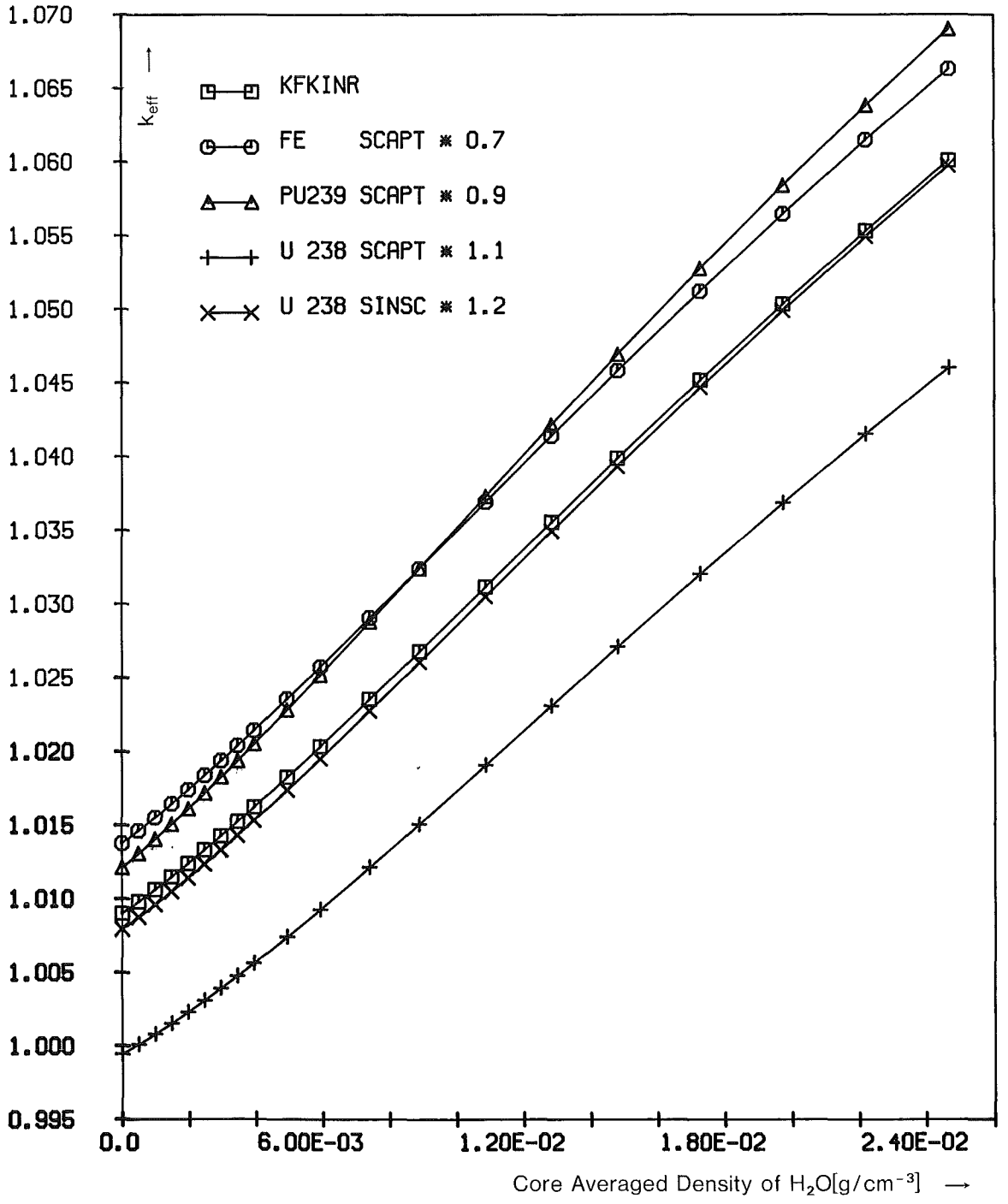

Fig. B4: Influence of cross-section changes on k_{eff} (ρ_{H_2O}) for GCFR Benchmark B3:
Size: ≙ 300 MWe; Fiss. Prod.: no; B^{10}: yes; T_{fuel}: 1500 K; Pu: dirty

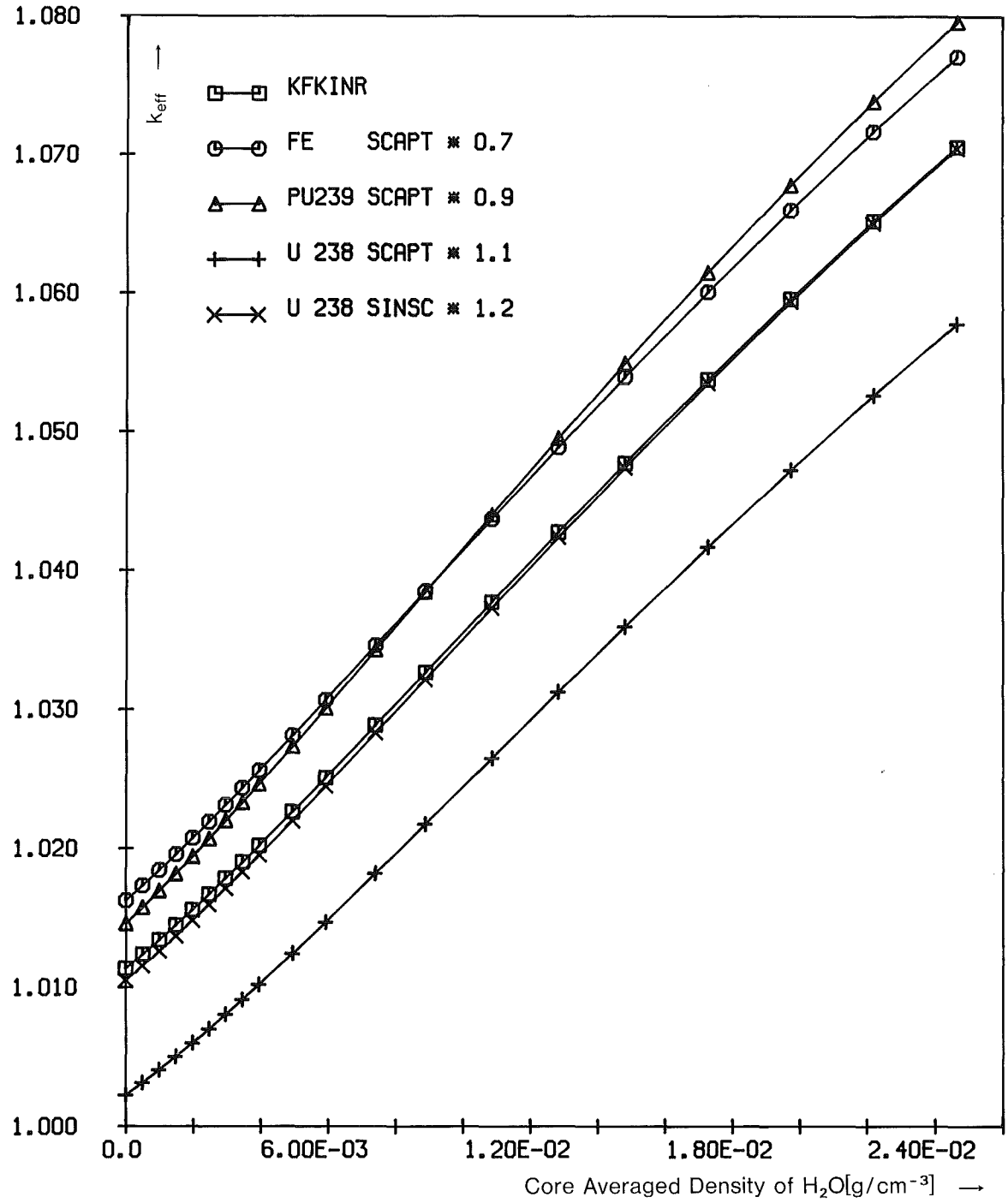

Fig. B5: Influence of cross-section changes on k_{eff} (ρ_{H_2O}) for GCFR Benchmark B4: Size: ≙ 300 MWe; Fiss. Prod.: yes; B^{10}: no; T_{fuel}: 300 K; Pu: dirty

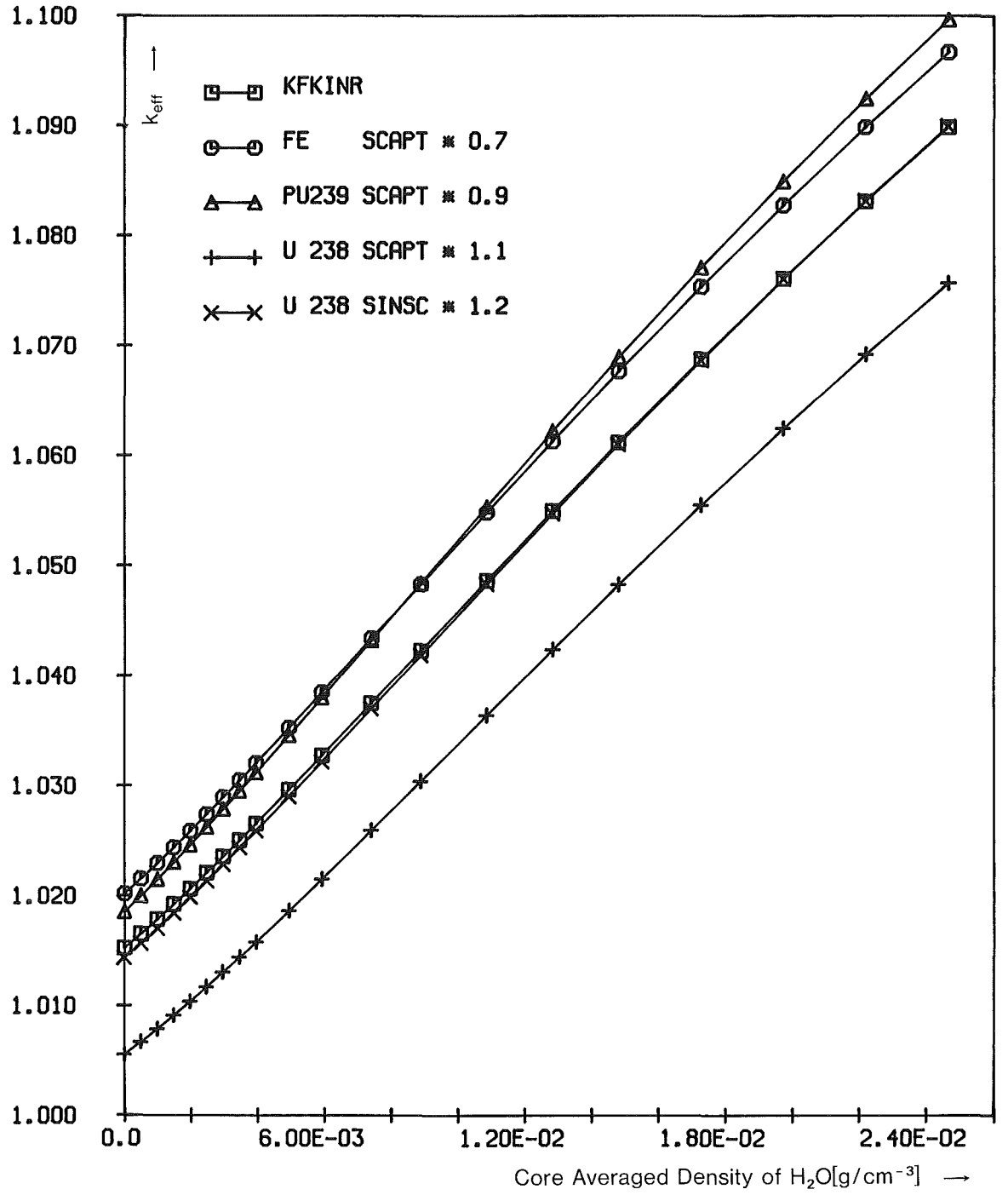

Fig. B6: Influence of cross-section changes on k_{eff} (ρ_{H_2O}) for GCFR Benchmark B5: Size: ≙ 300 MWe; Fiss. Prod.: no; B^{10}: no; T_{fuel}: 300 K; Pu: dirty

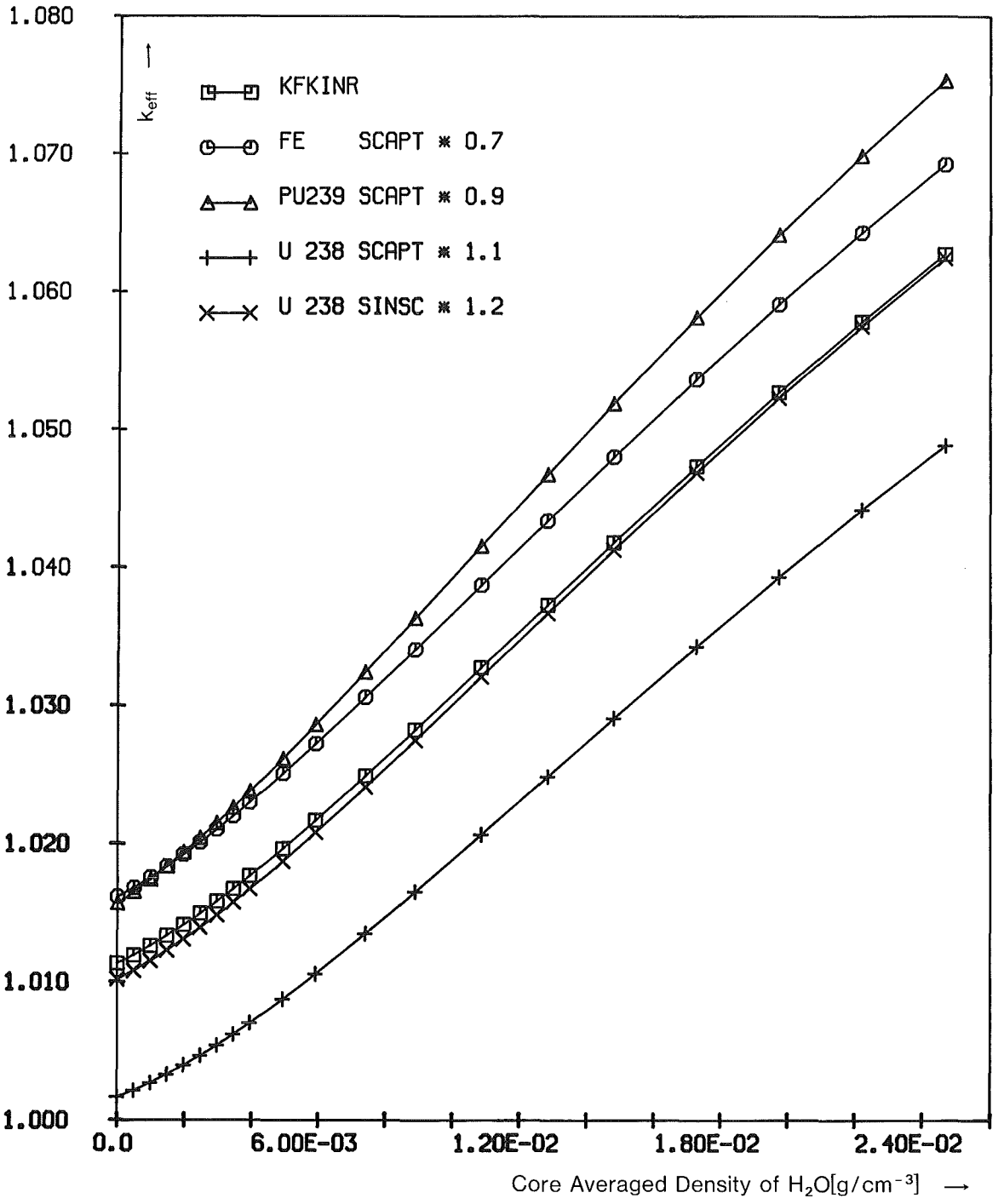

Fig. B7: Influence of cross-section changes on k_{eff} (ρ_{H_2O}) for GCFR Benchmark B6: Size: ≙ 300 MWe; Fiss. Prod.: no; B^{10}: no; T_{fuel}: 300 K; Pu: less dirty

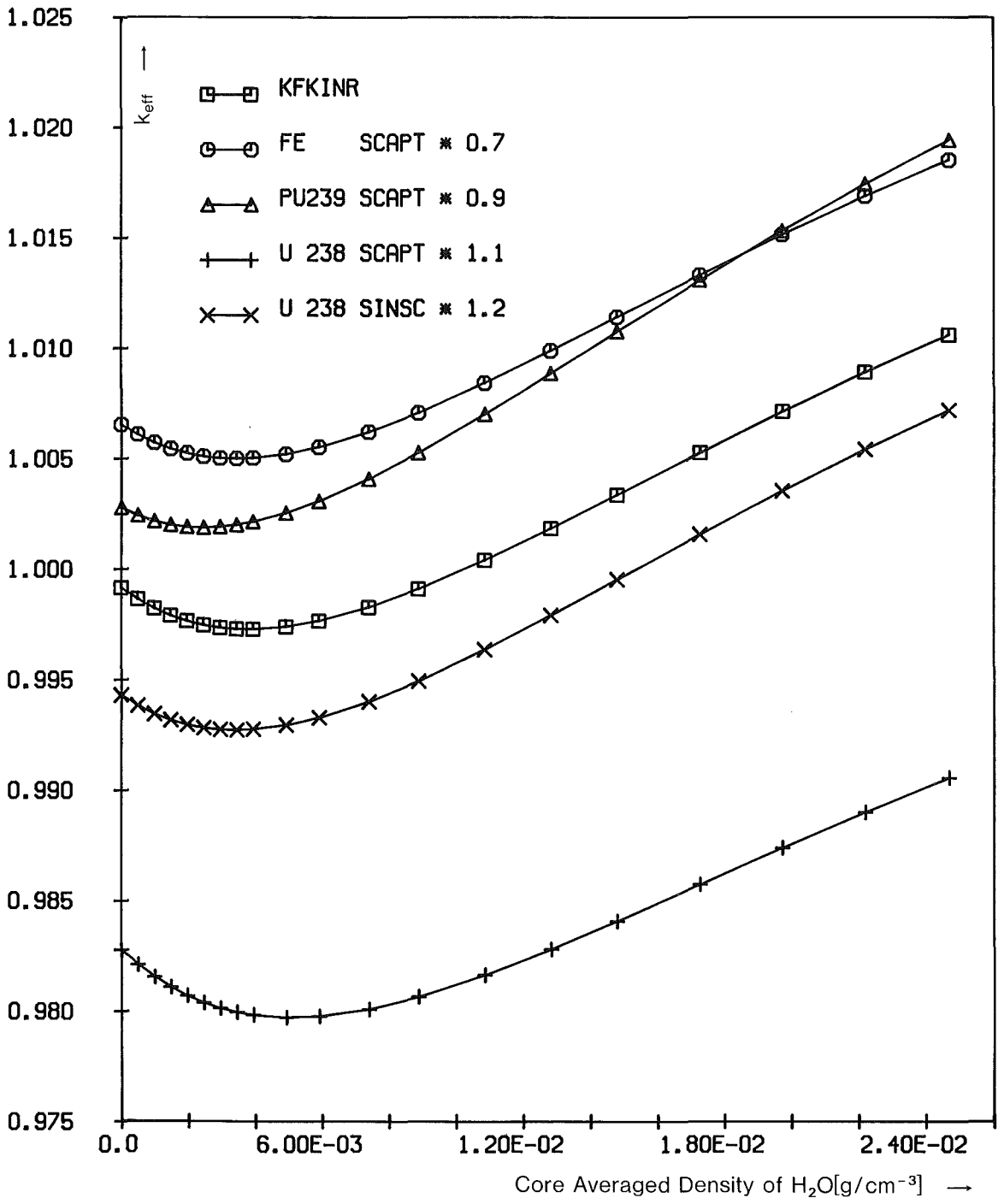

Fig. B8: Influence of cross-section changes on k_{eff} (ρ_{H_2O}) for GCFR Benchmark B7:
Size: ≙ 1000 MWe; Fiss. Prod.: yes; B^{10}: no; T_{fuel}: 1500 K; Pu: dirty

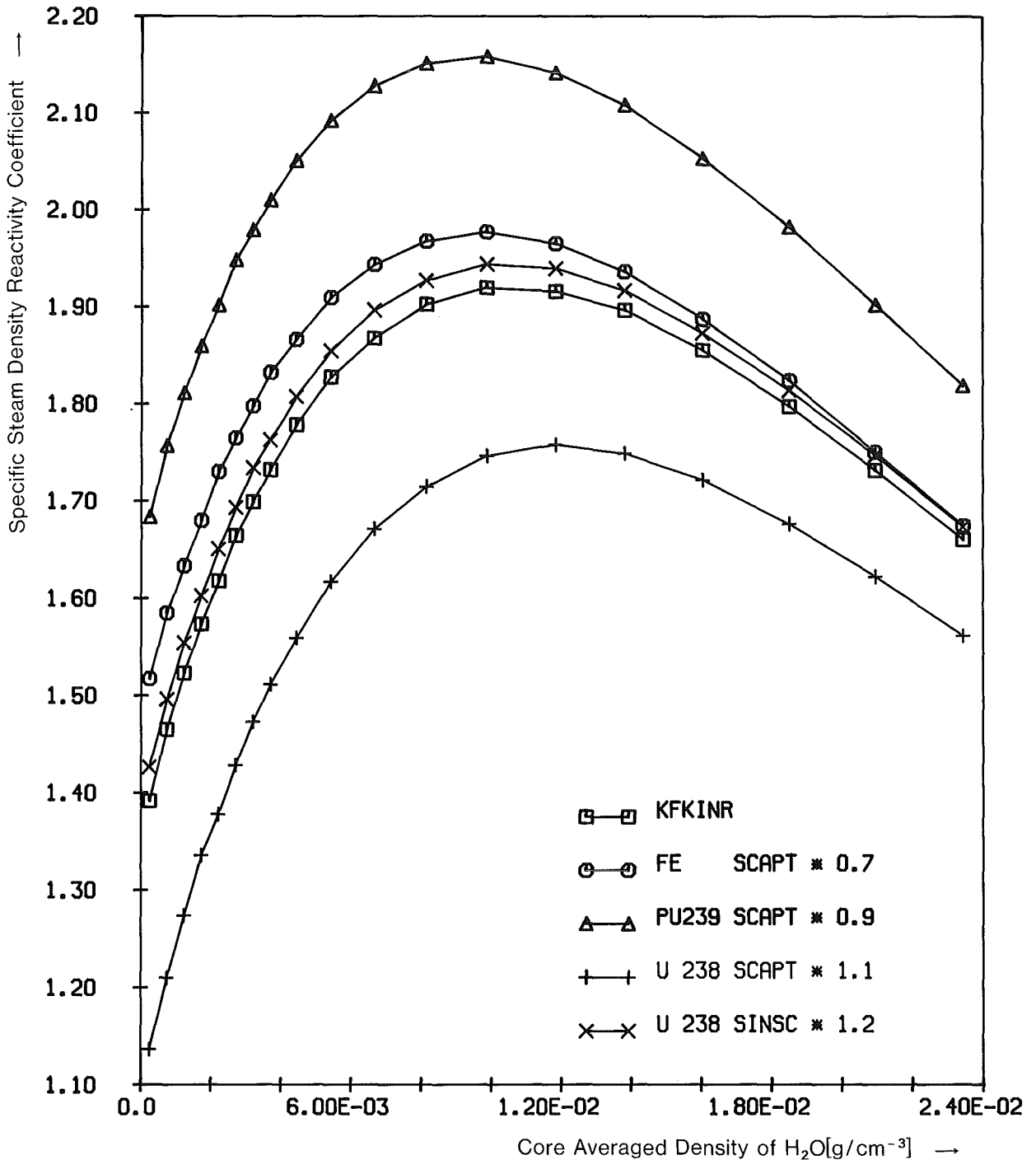

Fig. B9: Influence of cross-section changes on SSDRC(ρ_{H_2O}) for GCFR Benchmark Bo: Size: ≙ 300 MWe; Fiss. Prod.: yes; B^{10}: no; T_{fuel}: 1500 K; Pu: dirty

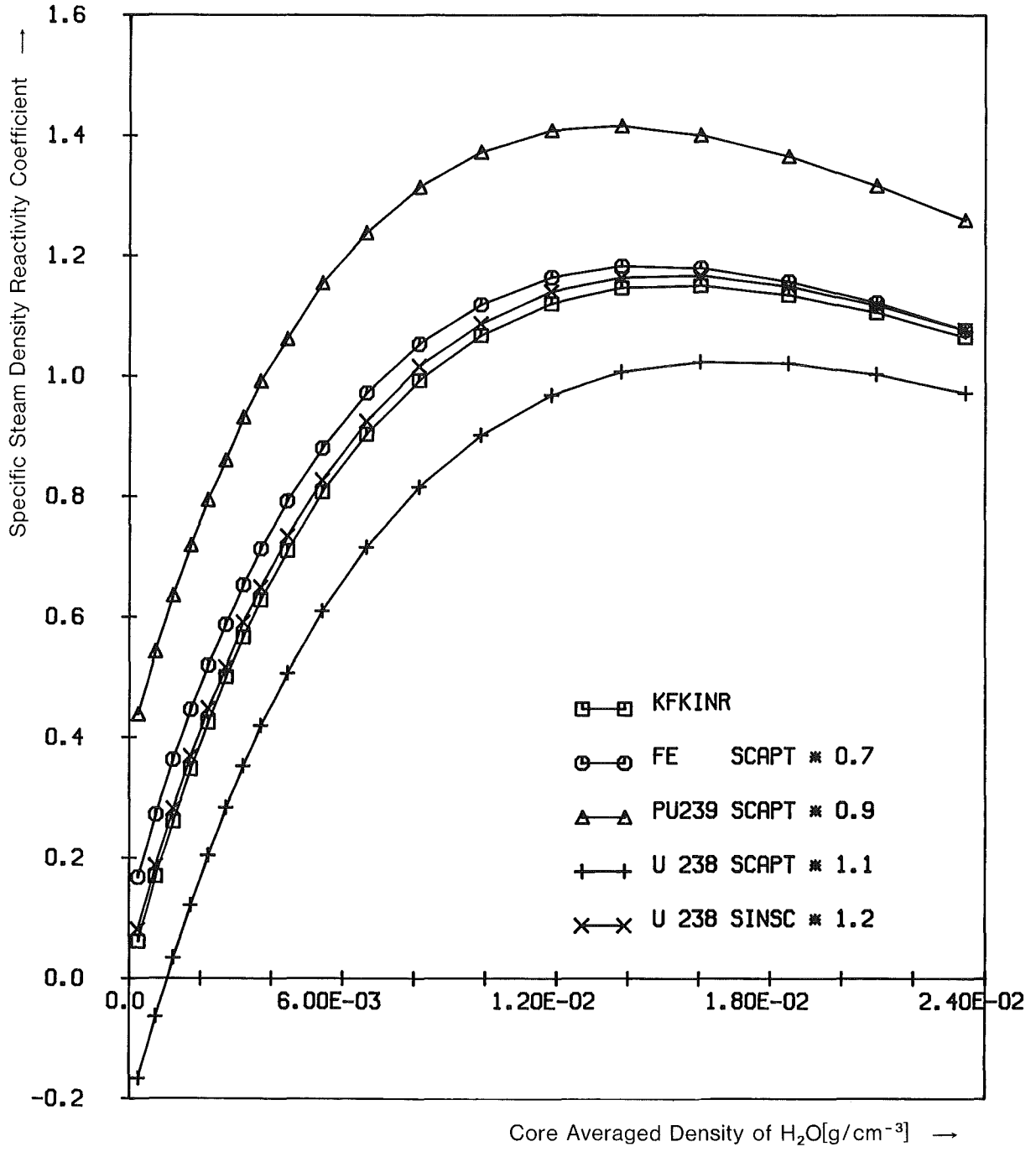

Fig. B10: Influence of cross-section changes on SSDRC(ρ_{H_2O}) for GCFR Benchmark B1: Size: ≙ 300 MWe; Fiss. Prod.: yes; B^{10}: no; T_{fuel}: 1500 K; Pu: less dirty

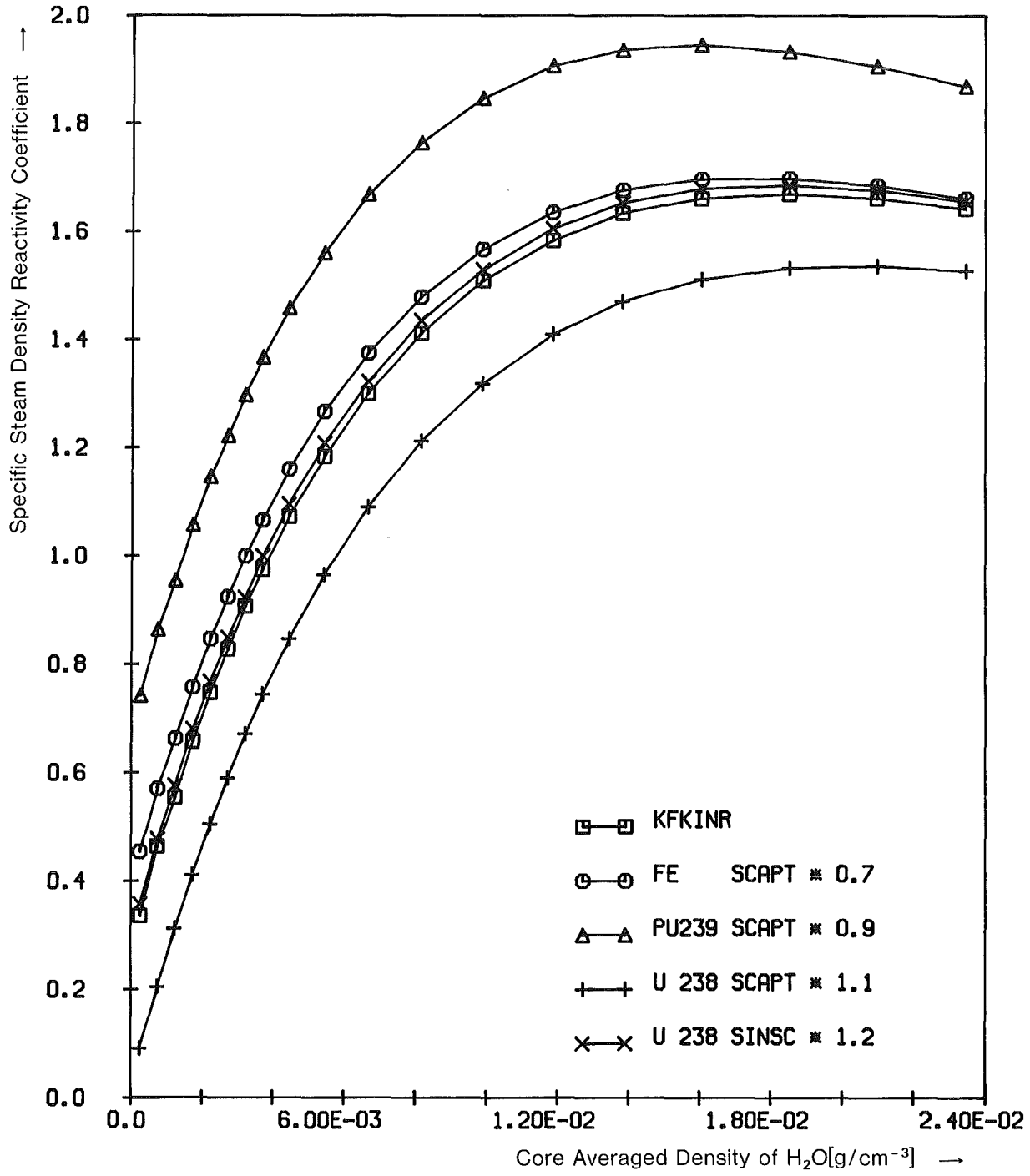

Fig. B11: Influence of cross-section changes on SSDRC(ρ_{H_2O}) for GCFR Benchmark B2: Size: ≙ 300 MWe; Fiss. Prod.: yes; B^{10}: no; T_{fuel}: 1500 K; Pu: clean Pu239

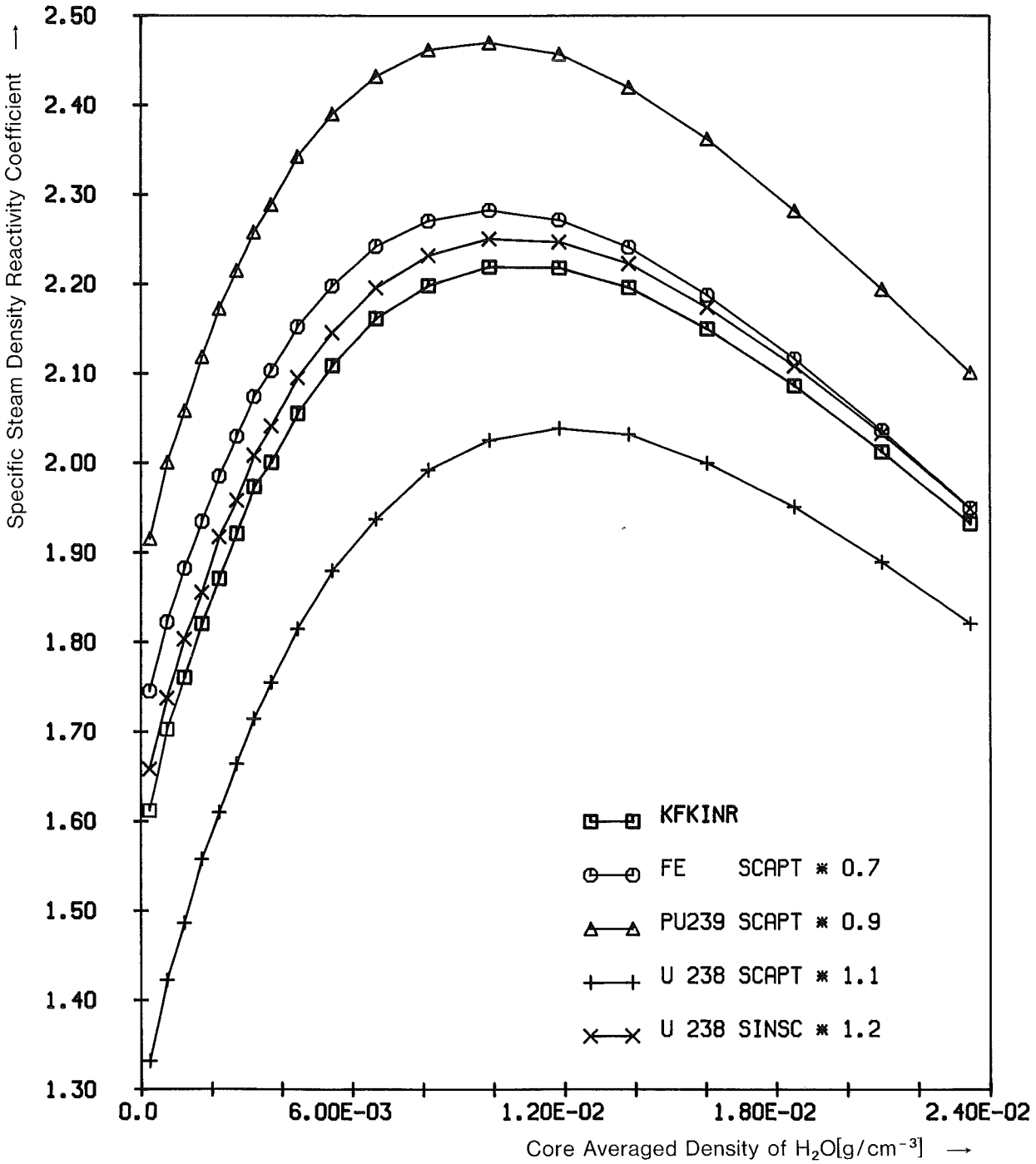

Fig. B12: Influence of cross-section changes on SSDRC(ρ_{H_2O}) for GCFR Benchmark B3:
Size: ≙ 300 MWe; Fiss. Prod.: no; B^{10}: yes; T_{fuel}: 1500 K; Pu: dirty

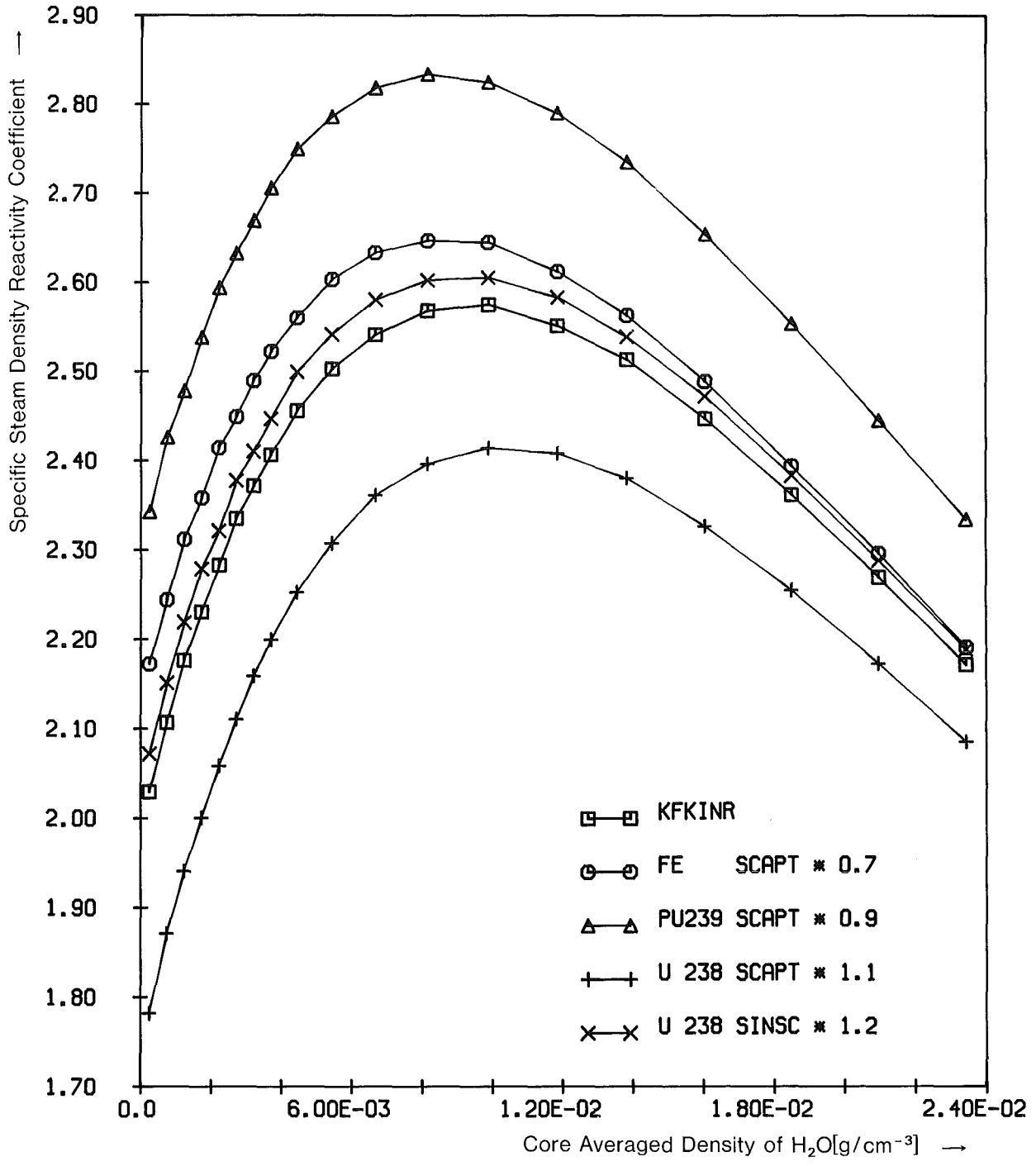

Fig. B13: Influence of cross-section changes on SSDRC(ρ_{H_2O}) for GCFR Benchmark B4: Size: ≙ 300 MWe; Fiss. Prod.: yes; B^{10}: no; T_{fuel}: 300 K; Pu: dirty

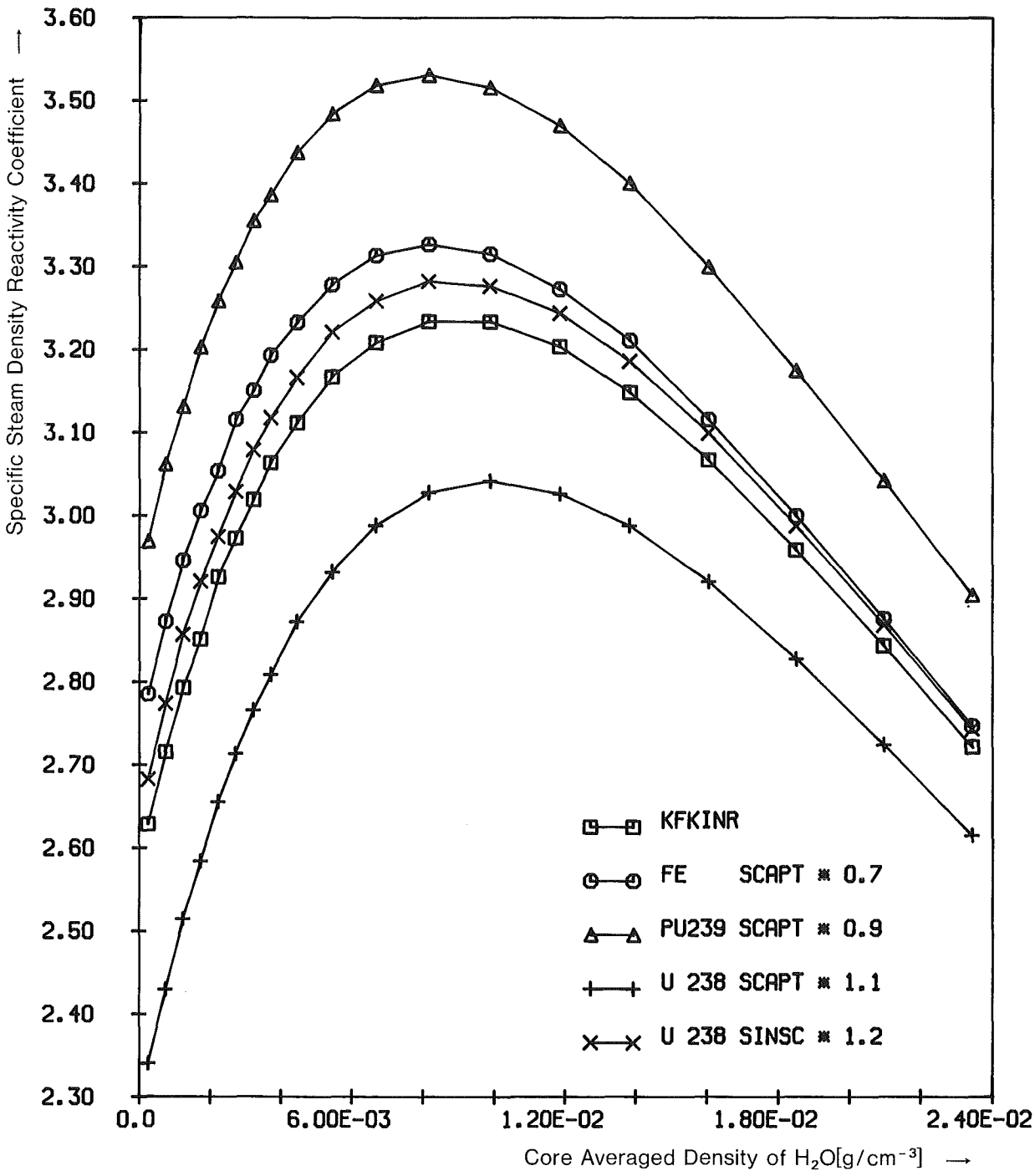

Fig. B14: Influence of cross-section changes on SSDRC(ρ_{H_2O}) for GCFR Benchmark B5:
Size: ≙ 300 MWe; Fiss. Prod.: no; B^{10}: no; T_{fuel}: 300 K; Pu: dirty

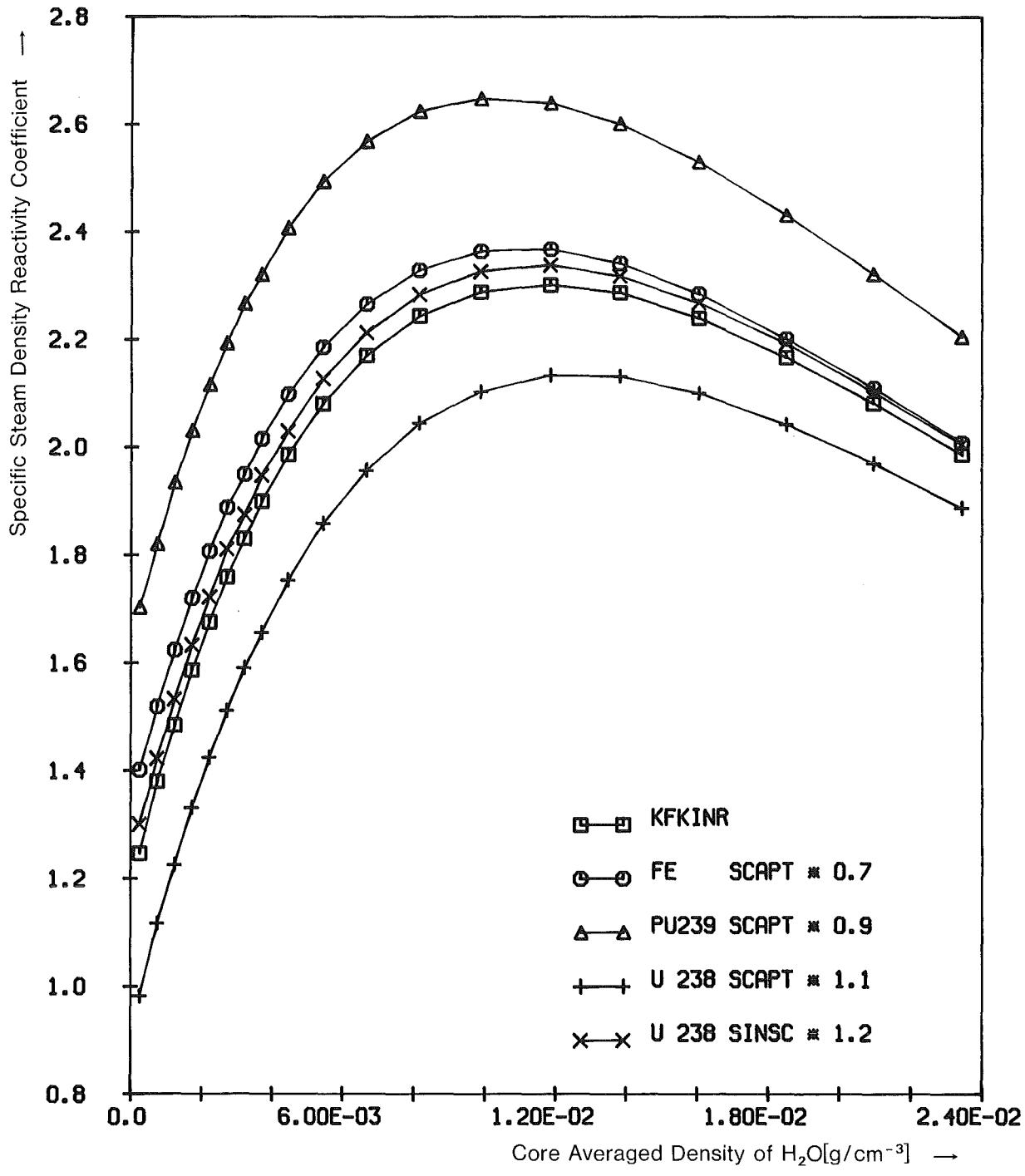

Fig. B15: Influence of cross-section changes on SSDRC(ρ_{H_2O}) for GCFR Benchmark B6:
Size: ≙ 300 MWe; Fiss. Prod.: no; B^{10}: no; T_{fuel}: 300 K; Pu: less dirty

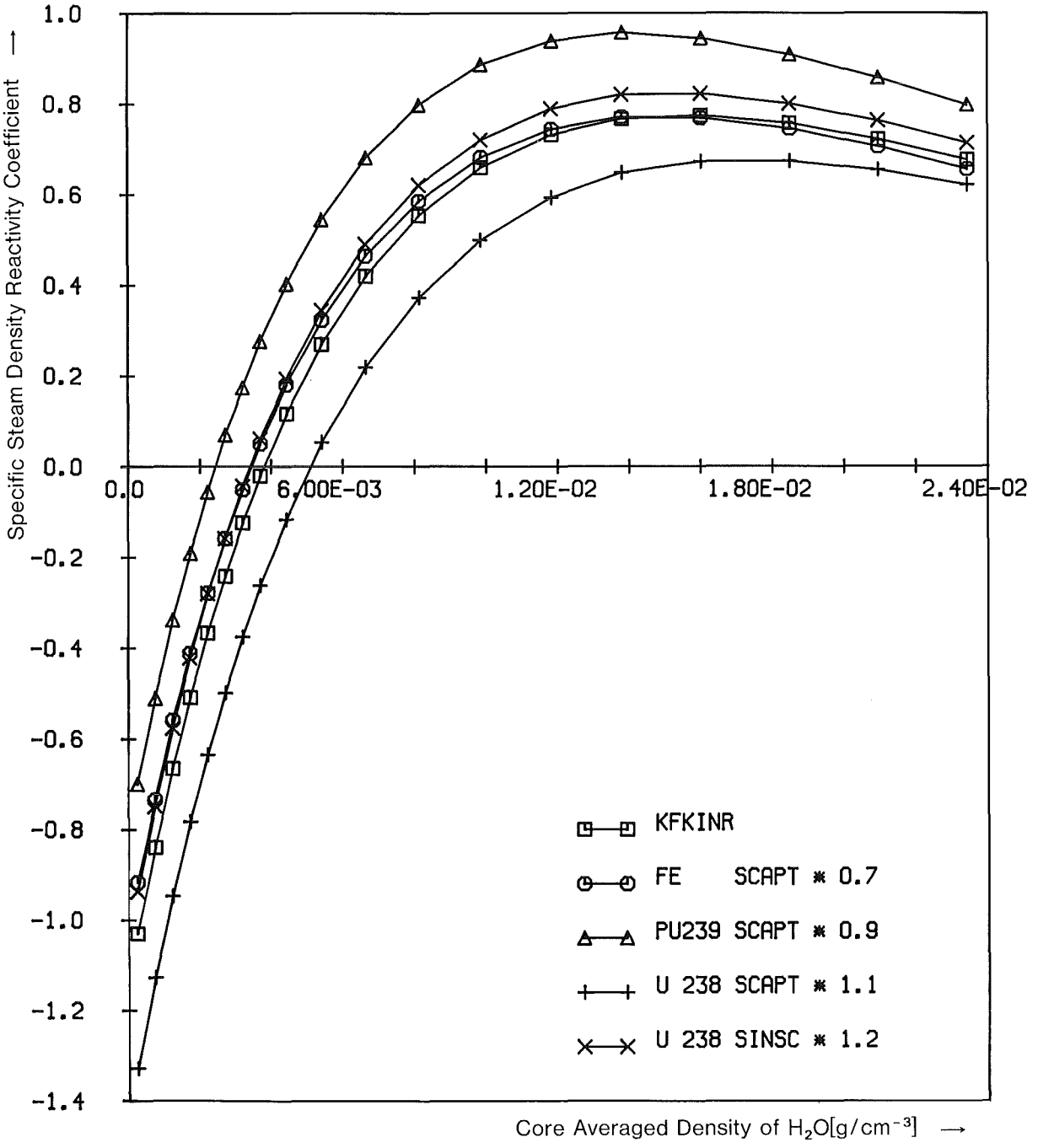

Fig. B16: Influence of cross-section changes on SSDRC(ρ_{H_2O}) for GCFR Benchmark B7:
Size: ≙ 1000 MWe; Fiss. Prod.: yes; B^{10}: no; T_{fuel}: 1500 K; Pu: dirty